CONTEMPORANEOUS GLACIAL FOLDING IN THE TABLE MOUNTAIN GROUP, WESTERN CAPE

H.J. BLIGNAULT

THESIS SUBMITTED IN PARTIAL FULFILMENT OF THE REQUIREMENTS FOR THE DEGREE OF M. Sc. IN GEOLOGY

UNIVERSITY OF STELLENBOSCH

MAY, 1970

C O N T E N T S

1 OUTLINE

1.1 STATEMENT OF PROBLEM

The contemporaneous nature of the interformational folding in the Table Mountain Group is well established by its stratigraphic setting. The zone of deformation which constitutes a distinctive stratigraphic horizon, is widespread throughout the Western Cape. Its unusual stratigraphic width attracts special interest and has resulted in differing opinions as to the mode of deformation. A glacial origin has been widely accepted.

1.2 OBJECT

The object of this study is

(i) to document the internal and external geometry of the Fold Zone,

(ii) to determine the relation between the interformational folds and the overlying Pakhuis diamictites and

(iii) to construct a hypothesis regarding the mode of deformation.

1.3 METHOD

1.3.1 Selection of areas ⁂

Ideal areas for field investigation are limited by the north-south trending tectonic folds which control the development of a rugged mountainous landscape.

The areas selected for fieldwork are located on the broad, subhorizontal hinge zone of the Cedarberg anticline, its wavelength being of the order of tens of miles. The culmination point is situated at Sneeukop (Eselbank) from where the axis plunges gently north and south.

⁂ Refer to locality Map 1.

1.3.2 Mapping

As a first approach, an area 2,000ft x 4,000ft (600m x 1200m) at De Trap (Map 2), was mapped by plane table and telescopic alidade. Regional stratification may attain a maximum dip of 10°, directed south-east. For orientation studies the regional attitude was assumed to be horizontal as direct field measurement proved impossible.

The variability of the fold elements was subsequently determined on a regional basis. Maps 4, 5 and 6 (cf. locality Map 1) were compiled from uncontrolled mosaics. Orientation data are corrected where tectonic tilt exceeds 5°.

1.3.3 Stereographic analysis

All three-dimensional orientation data were manipulated and compiled in the lower hemisphere of an equal-area Schmidt net as described by Turner and Weiss (1963; pp. 58-60), using the grid method for contouring. Nadirs are defined as poles to dip directions of planes. The projection of the plunging end of a line is referred to as the pole of that line.

1.3.4 Primary macrofabric analysis

The preferred orientation of clasts in the Pakhuis diamictites was determined at De Trap, using Member divisions to define sampled populations. The number of measurements depended on the availibility of suitable clasts in every Member. The sample domain is shown by the outcrop distribution of the Members (Map 2). The lower Sneeukop Member was subsampled by defining each synclinal core as a separate population.

By introducing a controlled bias, any inherent preferred orientation should be accentuated. This was accomplished by using well developed rod-like and discoidally shaped clasts to measure the attitude of A and the AB-surface respectively. The long axes of rod-like clasts varied from 2 to 28cm; care was taken to ensure that the A/B -ratio exceeded 1.5. The majority of clasts were discoids.

In the compilation of poles to discoids, rods are indicated by the pole of a hypothetical disc, of which the rod represents the line of dip on the AB -plane of the disc; this would indeed be true only for a longitudinal mode of transport of rods.

1.3.5 Microfabric analysis

The preferred orientation of the long axes of quartz grains was determined both for primary and imposed fabrics. Surfaces of maximum fabric contrast, defined by the preferred orientation of A' on any boundary surface of a layer, were investigated by a stereomicroscope, using either reflected or polarized light for best definition of grain boundaries. A circle-segmented graticule, fitted in the objective, was used for rapid grouping of

orientations in 20° classes (modulo π).

Only grains with an A'/B' -ratio exceeding 1.5, were used. By subsampling on a differential grain size basis, an attempt was made to determine whether orientation is a function of grain size. Separate counts were made of fractions with A' smaller than 0.4mm and larger than 1.0mm. Grains larger than 1.0mm in diameter were too few to warrant further subsampling on the available slabs. The number of grain counts (N) was determined by subsequent sampling; 100 - 150 counts usually sufficed.

Compass diagrams were compiled from these data. The central position of a modal class or classes constituting a mode was used to define the statistical orientation of A'. Block diagrams, depicting only the modal vectors, illustrate the essentially three-dimensional fabric pattern.

No significant experimental errors have been introduced during the preparation of orientated polished sections or slides. Determination of the depositional surface, however, is problematic. The attitude of intercalated arenite lentils in the lower Sneeukop Member indicates the orientation of ab(Sed.) for samples taken nearby. For the upper Sneeukop Member and Steenbras Member (De Trap) ab(Sed.) is assumed to be subhorizontal i.e. a maximum dip error of 10° is introduced. Where this direction of dip is subparallel to the preferred orientation A' on ab(Sed.) and the imbrication angle is 10° or less, erroneously inferred transport directions may result.

1.3.6 Radiography

Radiographs, taken by Dr. I.O. Faiman, Cape Town, of the Pakhuis diamictites revealed no internal structures. Rock slabs, parallel to ac(Sed.), were prepared 3mm thick and approximately 4cm x 5cm. Further technical details are:

film:	Cronex X-ray
exposure:	25 ma x 3 seconds
KV:	40
distance source-film:	100cm
developing time:	3 minutes

1.3.7 Terminology and notations

The terms used to describe folds are those proposed by Fleuty (1964) and the terminology for layering has been defined by Elliot (1965; pp. 198-199).

A, B & C	long, intermediate and short axes of clasts
A'	apparent long axes of clasts
a, b & c (Sed.)	orthogonal reference system for primary directional proper-

	ties of sediments (Potter and Pettijohn, 1963, p. 24) ab - principal surface of deposition a - line of movement b - sedimentary strike
a', b' & c' (Sed.)	for reference to deformed sedimentary fabrics
a, b & c (Geom.)	orthogonal reference system which denotes the monoclinic fabric of a tectonite geometrically (Whitten, 1966; p. 106) ab - most prominent foliation ac - monoclinic plane of symmetry b - normal to the monoclinic plane of symmetry, parallel to B, the fold axis.
a, b & c (Kin.)	orthogonal reference system which denotes the kinematic axes of a monoclinic tectonite fabric (Whitten, 1966; p. 107) a - line of movement b = B - axis of external rotation ac - plane of deformation ab - slip surface
S_1	surfaces bounding cross-laminae
S_2	stratification surfaces ("bedding planes")
S_3	slip surfaces bounding transposition bands (transposition bands will be referred to as S_3-bands)
S_4	surfaces bounding a set of S_3-bands (a set of S_3-bands will be referred to as S_4-bands)
L_1	intersection between S_1 and S_2
L_2	a special type of lineation, cf. section 2.3.2.1(ii)c
B	fold axis
β'	zone axis

2 COMPILATION AND ANALYSIS OF DATA

2.1 LITERATURE REVIEW

The interformational folding was first described by Haughton et al., 1925. They concluded that the folds formed transversely to the direction of ice-flow in front of the contact line between an ice mass and the underlying sand. An easterly direction of ice-flow was inferred from the fold asymmetry. "The horizontality of the main band of tillite .... above ....." the folding lead them to the view that the tillite was subaqueously deposited.

Haughton (1929) reported intraformational folding in both the Peninsula and Nardouw Formations of the Table Mountain Group, which was taken as evidence for more than one glacial advance.

Visser, (1962) regarded the tillite as a terrestrial glacier deposit; deposition took place after the advance of individual glaciers along synclinal valleys. Ice-flow was parallel to the fold axes from the north-northeast, as inferred from two petrofabric analyses as well as heavy mineral distribution and "glacial floors".*

Rust (1967), during the course of a regional survey, compiled extensive data pertaining to the orientation of the fold axes (cf. his fig. 99). He concluded that an ice-sheet advanced from north to south, parallel to the regional trend of the fold axes; the ice effected huge loadcasts which became elongated in canoe-shaped folds due to the forward motion of the ice sheet. The Sneeukop tillite represented an englacial deposit in the pod folds. Paleo-ice-flow was determined by petrofabric analysis on 13 samples from the Pakhuis tillites and 9 "glacial floors".*

2.2 LITHOLOGY OF STRATIGRAPHIC SEQUENCE

2.2.1 Stratigraphy

The lithostratigraphic sequence of the Table Mountain Group, as established by Rust (1967), is presented in table I.

---

* quotation marks by author

TABLE I (after Rust, 1967)

	FORMATIONS	MEMBERS	MAXIMUM THICKNESS
TABLE MOUNTAIN GROUP	Nardouw	(sandstone)	3,000ft
	Cedarberg	Disa Siltstone Soom Shale	450ft
	Pakhuis	Kobe tillite Steenbras Tillite Oskop Sandstone Sneeukop Tillite	400ft
	Peninsula	(sandstone)	6,000ft
	Graafwater	(purple fine sandstone)	1,400ft
	Piekenier	(conglomeratic)	3,000ft

Brachiopods from the Cedarberg Formation indicate an upper Ordovician (Ashgill) age (Cocks et al., 1969). Rust consequently estimates that the Table Mountain Group sedimentation spans the entire Ordovician and Silurian Periods.

Penecontemporaneous deformation enables the establishment of an informal time-stratigraphic sequence. The value of each time marker is dependent on the duration of the deformational event. Stages and substages can be delimited within such an undefined series (cf. table 2). Stage B, which is delimited by the first deformational phase and the Brachiopod Zone, is further subdivided by a second period of deformation into Substages B-1 and B-2. The boundaries of these time-stratigraphic sequences parallel the member and formation subdivisions on a regional scale.

2.2.2 Peninsula Formation

The lithology of the Peninsula Formation has an important bearing on the penecontemporaneous deformation in its uppermost horizon. The most important characteristic is its lithologic homogeneity. Stratification is invariably cross-laminated (planar type) and varies in thickness from 2ft to 10ft (0.6 - 3m); the

TABLE 2

Table Mountain Group	Litho-stratigraphic units		Time-stratigraphic units		Boundaries of time-stratigraphic units
	Formations	Members	Stages	Substages	
	Cedarberg	Disa	C (post-glacial)		Brachiopod Zone (Ashgill)
		Soom	B (glacial)	B-2	
	Pakhuis	Kobe			
		Steenbras			2nd Period of Deformation
		Oskop		B-1	
		Upper Sneeukop			1st Period of Deformation
		Lower Sneeukop			
	Peninsula		A (pre-glacial)		

cross-laminae vary in thickness from 0.4 to 3 inches (1 to 8cm).

Microscopic observations show that:

(i) The formation consists essentially of a medium grained (mode approx. 0.6mm) quartz arenite.

(ii) The arenite is well sorted; no matrix is present.

(iii) The sand is cemented by overgrowth quartz; the detrital cores being suspiciously well rounded.

(iv) The detrital cores are partly afloat in the cement, indicating a loose packing. Where the framework is intact most contacts are tangential.

(v) No dynamic metamorphic effects were detected at De Trap and De Bailie. This generally applies to the entire Formation in the Cedarberg area.

2.2.3 Fold Zone

The uppermost portion of the Peninsula lithosome, and the overlying lower Sneeukop Member, were folded prior to the deposition of the superposed sediments, and constitute the Fold Zone. The penecontemporaneous aspect of the folding is reflected by the environmental associations between the lower Sneeukop Member and the rest of the Pakhuis Formation.

The folding dies out downwards and commonly forms a regular décollement surface (Plates 1, 2A & 2B). The overlying sediments are unconformably related to the Fold Zone; the contact surface is regular (Plate 2B) and erosional features are evident from structural discontinuities (Plate 6E).

The areal distribution and external geometry of the Fold Zone in relation to the basin axis (it is assumed that the geometry of the basin is related to the geometry of the basin fill) are shown in fig. 1 (compiled from Rust, 1967; figs. 99 & 112); a genetic association is implied by the symmetric relationship. The Fold Zone attains a maximum thickness of 300ft (90m)

Profiles of the Fold Zone (fig. 2) illustrate the following conspicuous features:

(i) Isolated centres of no deformation.

(ii) Both abrupt and gradual decrease in Fold Zone thickness towards the isolated centres of no deformation.

(iii) Regional fluctuations of Fold Zone thickness.

Map 6 illustrates the marginal character of the Fold Zone which in section would appear like a thin (0-10ft/0-3m) discontinuous, tapering zone with sparsely distributed belts of deeper (15-40ft/4-12m) deformation (cf. Map 6; Karookop).

Microscopic comparisons between the deformed and undeformed quartz arenite of the Peninsula Formation reveal no compositional and textural differences. Structurally, though, there is a significant difference; the folded S_4-banding is conspicuously thinner (2ft/0.6m) than the undeformed cross-stratified layers immediately below the Fold Zone.

The sympathetically folded lower Sneeukop Member is described in section 2.2.4.2.

2.2.4 Pakhuis Formation

2.2.4.1 Introduction

For the sake of convenience the Sneeukop Member is informally divided into a lower and an upper part, the boundary being the upper surface of the Fold Zone. The Kobe Member should be grouped with the Cedarberg Formation because:

(i) Lithostratigraphic principals (A.C.S.N., 1961) demand lithologically alike sediments to be grouped together irrespective of genetic associations.

(ii) The Kobe Member is a facies variation of the Soom Shale Member of the Cedarberg Formation.

2.2.4.2 Lower Sneeukop Member

The lower Sneeukop Member constitutes the upper part of the Fold Zone. It typically occupies the synclinal cores which, in some instances, have become isolated due to tight overfolding (cf. Plate 1 and Map 2). Originally it was probably a blanket deposit not thicker than 20 - 40ft (6 - 12m).

The lower contact with the Peninsula arenite is usually sharp and conformable but irregular structure is also developed. Fig. 3 illustrates an unconformable contact. Some megaclasts typical of the Sneeukop diamictite are partly embedded in the bounding surface between the Peninsula Formation and the lower Sneeukop Member (Plate 2D).

The lower Sneeukop Member consists of arenaceous diamictite (Flint et al., 1960 (a) & (b) which rarely displays stratification (cf. Plate 1). No internal structures are revealed by radiographs. The rudite fraction

of the diamictite is sparsely and randomly distributed; these clasts are of variable composition but consist dominantly of quartzite. Most clasts are waterworn discoids, commonly faceted, polished and striated parallel to their AB-planes. The following features were determined microscopically:

(i) The arenite grains consist of quartz, rock fragments and accessory zircon, tourmaline and rutile.

(ii) The mode within the arenite fraction ranges from 0.3mm to 0.6mm.

(iii) The arenaceous grains are well rounded and loosely packed with tangential contacts.

(iv) The interpore space (5-10% by volume) is filled by smaller particles floating in a mass of cryptocrystalline material which represents the diagenetically recrystallized lutite fraction (authigenic sericite, biotite and pressure solution features indicate that at least the anadiagenetic stage was reached during burial).

Lenticular bodies of a fine grained arenite (modal development in the 0.2 - 0.3mm range) were found near the Peninsula Formation/Sneeukop Member contact (cf. Map 2). They vary in thickness from 2 to 5ft (0.6 to 1.5m) and continue along strike for 40 to 100ft (12 to 30m). In the only thin section prepared the lower contact with diamictite was found to be microscopically sharp. Internally the lenses consist of graded, laminated (0.1 - 0.5mm) sets (5 - 10cm) which depict normal faulting with slight displacement, penetrative within 5 - 15mm. The displacement surfaces are sharply defined. Some laminae have sagged and are slightly contorted. The accessory minerals zircon and tourmaline abound.

Fig. 4 depicts what appears to be a fossil ice-wedge at De Trap. The contact between the wedge-like small-pebble diamictite body and the surrounding diamictite is vague.

Medium to coarse grained quartz arenite lentils are sporadically interbedded in the diamictite. The lentils usually are less than 2' (0.6m) thick and have a strike-length of 5 - 40ft (1.5 - 12m). They have well-defined convex-shaped lower boundaries which were used to indicate the geopetal relation (plate 2E). The orientation of these lentils largely proves the folded nature of the lower Sneeukop Member (Map 2). The lentils rarely have an intertonguing relationship with the surrounding diamictite. The contacts commonly are graded. Microfabric analyses of two lentils indicate

flow in a direction 346° (dgm. 1) and parallel to 170° (dgm. 2, Map 3).* The two three-dimensional fabric patterns suggest altogether different modes of transport; dgm. 1, a typical example of an uncomplicated fabric pattern, depicts longitudinal transport with a low negative imbrication angle, probably typical of lamellar flow. More turbulent fluid-flow conditions are inferred from the complex pattern shown in dgm. 2:

(i) Imbrication angles are large and variable, indicating a rotational movement around b(Sed.).

(ii) The two principal modes on the ab(sed.)-plane, with a non-orthogonal relation, are evidence of a longitudinal as well as a transverse mode of transport; the grains transported in a longitudinal fashion, typical of suspended particles, had less constraint exercised upon them (therefore the non-orthogonal relationship) than those transported transversely i.e. traction.

The macrofabric patterns of diamictite exposed in two separate synclinal cores approach random distributions (dgms. 17 & 18). It was first assumed that the depositional interface was subparallel to regional stratification. This assumption is now considered to be in error and the already indicated folded nature of the lower Sneeukop Member is also inferred from the random fabric patterns.

Dgms. 3,4,5 & 6 illustrate the three-dimensional microfabric patterns established for four samples from the lower Sneeukop Member. The vectorial data are compiled on Map 3. Although size differentiated analysis does not prove different modes of transport for different size fractions, it is evident that the transport medium exerted more constraint on the orientation of the larger sized particles (cf. co. dgms. 6D & 6E). It may still be possible to prove orientation as a function of size by increasing the gap between the two size fractions. Different modes of transport have been established for different samples; the grains with longitudinal modes of transport have high (50°) or variable angles of imbrication (dgms. 5 & 6) while a larger constraint in the ac(Sed.)-plane and a low angle (10°) of imbrication is evident for transverse transport (dgm. 4). The non-orthogonal bimodal pattern on the ab(Sed.)-plane of one sample (dgm. 5) is significant in that it appears to represent critical fluid-flow conditions between that necessary for transverse (dgm. 4), and longitudinal (dgm. 6) modes of transport. Three samples thus represent fabric patterns reflecting three different flow regimes. Two samples taken within 10ft (3m) of one another (1ft/0.3m vertically) have different fabric patterns (dgms. 3 & 4), suggesting short distance variability in the flow regime. The one sample, measuring 7cm x 5cm x 3cm, does not even constitute a homogeneous domain (dgm. 3); the modes on the vertical planes do not define the mode on the ab(Sed.)-plane. This heterogeneity

* The localities with the vectorial data are shown on Map 3 by the diagram number.

can be ascribed to either

(i) variability in the flow regime, or

(ii) penetrative deformation.

2.2.4.3 Upper Sneeukop Member

The upper Sneeukop Member overlies the Fold Zone unconformably. The unconformity commonly is an undulating surface with the low areas related to underlying synclines. The upper Sneeukop Member is a blanket deposit, estimated not to exceed 40' (12m) in thickness.

The upper Sneeukop Member consists dominantly of feebly stratified (1 - 2ft/0.3 - 0.6m) arenaceous diamictite; no internal structures were revealed by radiographs. Thin (less than 0.5ft/15cm) beds of quartz arenite and pebble washes occur frequently towards the top. The upper arenaceous diamictite corresponds in all textural and compositional features with the lower Sneeukop diamictite.

The fabric pattern of the rudite fraction, representative of the mapped area (Map 3), defines flow in direction 167°. Dgm. 19, which depicts nadirs to planar and poles to linear fabric elements, illustrates a secondary mode transverse to the current direction. Using the same field data it is shown that the compilation of poles to fabric elements (dgm. 20) is not sensitive enough to identify flow characteristics.

Microfabric analysis on three samples yielded unsatisfactory results. Dgm. 7 illustrates the fabric pattern of a heterogeneous sampled domain (5cm x 5cm x 5cm) i.e. the modal vectors on the ac(Sed.)- and bc(Sed.)-planes do not define the modal vector on the ab(Sed.)-plane. This can be due to

(i) a primary heterogeneous flow regime or

(ii) deformation.

The triclinic fabric patterns (dgms. 8 & 9) are probably due to ill-defined surfaces of deposition ($\pm$ 10°). Size differentiated analysis of the bimodal pattern on the ab(Sed.)-plane (dgm. 8; cf. co. dgms. 8D & 8E) proves the preferred orientation of A' as a function of size. Under fluid-flow conditions the larger particles will tend to be transversely transported (Rusnak, 1957) and the smaller particles longitudinally; an approximately east-west line of flow can thus be inferred from dgm. 8.

2.2.4.4 Oskop Member

The Oskop Member is a conspicuous quartz arenite bed (2 - 6ft/0.6 - 2m) which overlies the Sneeukop Member discontinuously. At De Trap it consists of a single cross-stratified layer which indicates flow in direction 210° (cf. Map 3). A second period of penecontemporaneous deformation affected the Oskop Member locally, and is discussed in section 2.4.

2.2.4.5 Steenbras Member

The Steenbras Member is a discontinuous sheet of feebly stratified (1 - 2ft/0.3 - 0.6m) arenacious diamictite; no internal structures were revealed by radiographs and the compositional and textural features are similar to those of the Sneeukop diamictite. The diamictite grades upward into either the Kobe Member (lutaceous diamictite) or the Soom Shale Member.

A northerly flow is indicated by one microfabric pattern (dgm. 10: Map 3); the non-orthogonal bimodal pattern on the ab(Sed.)-plane reflects both longitudinal and transverse modes of transport. The recurrence of the non-orthogonal relation between the two principal modes on the ab(Sed.)-plane suggests that it is an inherent characteristic to the mode of transport of the diamictites; assuming fluid-flow conditions, it is proposed that the particles in longitudinal motion describe a sinuous curve i.e. the spiral motion of a vortex parallel to a(Sed.).

2.3 INTERNAL STRUCTURE OF THE FOLD ZONE

2.3.1 Flexural-slip folding *

2.3.1.1 Introduction

Folding of the Peninsula quartz arenite took place by

(i) flexuring in S_2 and S_4, and

(ii) slip on S_1, S_2, S_3 and S_4.

As slip occurred on both primary and secondary S-surfaces the definition of Whitten (1966) does not strictly apply. The movement picture, though, remains the same. Flow, by slip on S_1 and S_3, within S_2 and S_4 resulted in classical "incompetent" behaviour (Plate 6c).

Slip on S_2, either by slip between S_2-layers or by rotation-drag of S_1 on S_2, is well illustrated where the movement is obstructed by pebbles lying in S_2 (Plate 3A); this line of movement defines a(Kin.) and is situated in the ac(Geom.)-plane of the fold.

The intensity of deformation always increases upwards from the décollement surface. The transposition of S_3 occurs from bottom to top with associated change in fold style.

2.3.1.2 Folding in S_2

Flexuring in S_2 is characteristic of the lowermost part of the Fold Zone as delimited on Map 3. Concomitant slip on S_1 resulted in different internal configurations of S_2-layers:

---

* Defined by Whitten (1966; p. 131)

(i) In rare box-like folds S_1 tends to parallel S_2 on the limbs while it is perpendicular on the crests (fig. 5, Plate 2F).

(ii) A single example was observed where S_1 maintained an approximately perpendicular relation to S_2 throughout the folded S_2-layer (fig. 6).

(iii) A well exposed hinge zone at De Trap (Plate 3F) allowed a detail orientation study of S_1, S_2 and L_1. With respect to the fold elements, the hinge zone constitutes a homogeneous domain. All possible attitudes of S_1, S_2 and L_1 were measured, and compiled on a Schmidt net (dgm. 21). The following features are evident:

(a) The orientation of S_1 remains unchanged throughout the fold.

(b) The distribution of L_1 is such that it could be described by either a great circle or a small circle. These two possibilities are mutually exclusive, except for the special case where B_{S_2} is parallel to S_1, which in this particular case is not so. It is concluded that L_1 lies on a great circle because

(i) The pole to this great circle (P) coïncides with the locus of S_1 poles and

(ii) S_1 has a constant orientation.

(c) The locus of S_1-poles lies on the axial plane (S_5), meaning that S_1 is constantly orientated normal to S_5.

The fold is illustrated in Fig. 7.

2.3.1.3 Transposition of S_1

Cross-laminae were transposed to S_3-bands by progressive slip on, and rotation of cross-laminae. Sets of parallel S_3-bands are bounded by S_4-surfaces which probably represent the original stratification surfaces (Plate 2G). Pure strain rendered the S_3-bands thinner (0.1 - 3cm) than the original S_1-layers (1 - 7cm).

A single outcrop at De Trap (locality 22, Map 3) displays the transposition of S_1-layers to S_3-bands parallel to the original stratification, S_2 (Plate2H).

Progressive increased transposition of S_1-layers is first associated with a thickening of the S_2-layer as the S_1-layers are rotated subperpendicular to S_2. S_1-layers become curviplanar due to drag; the increase in curvature towards the bottom suggests that most movement due to slip on S_2 occurred on the lower S_2-surface while the upper part remained relatively passive (fig. 8). Dgm. 22 is a stereographic representation of the transposition, compiled from measurements taken representatively over the section. The poles plot along a small circle indicating homoaxial rotation. This axis of internal rotation approximately corresponds to B when assuming the limb to be part of a horizontal fold (the limb actually is a divergent part of a horizontal syncline). The slip on S_2, parallel to the dip of the fold limb, defines a(Kin.) while the (internal) rotation axis defines b(Kin.)= B (cf. dgm. 22).

It is thus concluded that transposition is effected by differential slip on S_2; the mode of rotation reflects the effect of increased friction due to normal stress.

2.3.1.4 Imposed fabric

A microfabric study of samples taken at different stages of S_1-transposition (sample locations are indicated on Plate 2H as 1, 2 & 3 which also denote the transposition stages)reflects a continuous change in fabric to ultimately result in the imposed fabric of the S_3-bands.

The first stage is represented by a S_1-layer in an initial state of deformation but before rotation through the vertical. The three-dimensional fabric pattern is shown on dgm. 11:

(i) The modal vector on a'b'(Sed.) is not symmetrically related to the dip direction but tends to be transversely orientated.

(ii) The large "imbrication" angle on a'c'(Sed.) and its direction of dip suggest some rotation around b'(Sed.)

(iii) The low variance modes possibly indicate an imposed constraint on the rearrangement of grains.

Such a deformed fabric pattern is thought to be due to

(a) bodily movement of S_1-layers and/or

(b) pure strain of S_1-layers and/or

(c) rearrangement of individual grains (to a lesser extent during the first stage of transposition)due to slip on S_1.

The second stage is represented by an inverted S_1-layer after its rotation through the vertical. The three-dimensional fabric pattern (dgm. 12) differs significantly from that of the first stage:

(i) The modal vector on a'b'(Sed.) parallels the dip direction.

(ii) The modal vector on a'c'(Sed.) now makes a small (20°) angle with the S_1-surface.

(iii) A lower modal spread on all three planes of maximum fabric contrast is evident by comparing the relevant compass diagrams with those of the first stage.

The final transposed stage is represented by an orientated sample taken from a S_3-band 2ft (0.6m) from the arenite/diamictite contact (3rd stage, Plate 2H) and does not necessarily represent the same cross-stratified layer referred to above. The three-dimensional fabric pattern has essentially orthorhombic symmetry (dgm. 13)

(i) The modal vector on the S_3-surface makes a 10° angle with the dip direction i.e. subparallel.

(ii) The modal vector on a'c'(Sed.) is parallel to S_3.

(iii) The modal spread on the S_3-surface is significantly larger than those of stages 1 and 2.

The mode of fabric imposition is functionally related to the large constraint exerted on movement and to the movement picture of mean strain as described by the three stages above:

(i) The preferred direction of A attains an orientation subparallel to dip of S_3. This direction has previously been defined as a(Kin.) by differential slip on S_2 (section 2.3.1.3).

(ii) The componental movement of grains on a'b'(Sed.) and a'c'(Sed.) appears to be rotational. Such movement probably requires a significant normal stress component along with slip parallel to a(Kin.).

The shearing and normal stresses on S_1 during transposition to S_3 resulted in dilatation of S_1-layers by means of considerable flow along a(Kin.). It is proposed therefore that the degree of fabric imposition is a function of the change in thickness of S_1-layers.

Ill-defined S-surfaces, approximately 5cm apart, are sporadically present in the diamictite within 5' (1.3m) from the contact with the Peninsula Formation (Plate 3B). These S-surfaces are always parallel to S_3. The microfabric pattern (dgm. 14) of these S-layers has a near-orthorhombic symmetry, suggesting an imposed fabric. It is concluded that these S-surfaces are essentially S_3-surfaces developed in the lower Sneeukop Member. The preferred orientation of A on S_3, defining a(Kin.) differs significantly from the dip direction of the fold limb, and apparently is unrelated to the micro-fold elements (Map 3); this locality (14, Map 3) is situated in a domain of crossfolding.

2.3.2 Geometric analysis

2.3.2.1 Small structures

(i) Folds. Minor folding in S_4-bands is rare and always congruous. More common are congruous minor similar folds in S_3-bands within S_4-bands:

(a) Some are parasitic to folding in S_4-bands (Plate 3C & D).

(b) Others probably formed by differential slip on S_3(Plate 3E).

(c) A single outcrop depicts a fold which consists of one fold form and probably originated by parallel slip on both bounding surfaces of the S_2-layer during transposition (Plate 2G).

(d) Buckling of S_3-bands on the crest of an anticline in the lower part of the Fold Zone probably indicates compression within the S_4-band (fig. 9).

(ii) Lineations.

(a) Fold mullions (Whitten, 1966; p. 315) are rare and formed by tight folding in S_3-bands; the enveloping surface of the hinge zones being S_4 (Plate 3D). The mullions are aligned parallel to B.

(b) S_1/S_2 intersections (L_1) yield:

1. b(Geom.)-lineations on the crests of box-like folds (Map 3, domain 4; cf. Map 2).
2. lineations unrelated to the fold elements (Plate 3F; cf. section 2.3.1.2 (iii)).

(c) The most abundant lineation, L_2, is difficult to define but apparently is an S_3/S_4 intersection. It commonly resembles a linear parting of S_3-bands and also occurs as alternating "grooves" and "ridges" (Plates 3C, 3G & 3H). It rarely is curvilinear on a mesoscopic scale (Plate 3G) and macroscopically defines B (dgms. 23 & 25)

(iii) Structures due to rupture are rare and were observed to cluster at two widely separated localities, situated in the upper limits of the Fold Zone.

(a) The Pup: Small scale faulting and the apparent bodily translation of a set of S_3-bands were observed (Plate 4A & B).

(b) De Trap: Faulting has been preceded by plastic behaviour as shown by the sympathetic folding of S_3-bands (fig. 10).

(iv) Sedimentary dikes (Plate 4D) are common in the lower Sneeukop Member i.e. in the synclinal cores (Map 2):

(a) The dikes vary in width from 1 to 14 inches (2 to 35cm) and are from 5 to 100ft (1.5 to 30m) long.

(b) They are slightly curvilinear, frequently bifurcate and usually taper out; a single example of abrupt termination against the Peninsula arenite was observed.

(c) The dikes are always orientated normal to the synclinal axis.

(d) Grading along strike was observed; the coarser part of the dike being away from the Peninsula arenite contact.

(e) Grading across strike is common and was also observed microscopically within the sand-sized fraction. The coarser material is concentrated in the middle portion of the dikes, and commonly contains odd pebbles and grit.

(f) The contact between a dike and the surrounding diamictite is sharp.

(g) The compositional and textural features of the dike material are similar to those of the diamictite of the lower Sneeukop Member described

in section 2.2.4.2; euhedral pyrite, though, is much more common in the dikes.

The perfect orthorhombic microfabric symmetry of one dike (dgm. 15) is thought to be characteristic for quasi-liquid (Elliot, 1965; p. 195) flow parallel to the dike walls. Assuming (after Bhattacharyya, 1966) parallel arrangement of linear grains with flow, a(Kin.) is defined as shown on dgm. 15, fig. 11 and Map 3.

A second dike yielded a triclinic fabric pattern (dgm. 16) which is probably due to flow, obliquely aligned with respect to the dike walls. Net flow, parallel to the dike walls, apparently was horizontal. Such flow can be ascribed to a variance in the viscosity of the flow medium or to obstacles.

(v) Detached and semi-detached bands of Peninsula arenite are commonly situated in the lower Sneeukop diamictites at or near the contact. The arenite bands are easily recognized as of Peninsula origin by their transposition features. The bands range in length from 1 to 40ft (0.3 to 12m) and are generally only 6 inches (15cm) thick (exceptionally 3ft/1m). Where abundant, the contact is rendered irregular by the mixing of the two components (Plate 4E). Map 2 shows that the bands are concentrated on the western contacts and culminations of the diamictite-containing synclines; the bands are generally aligned parallel to or tangential to the structural trend. Folding and buckling of detached arenite bands are shown on Plate 4F and fig. 16. The detachment is thought to take place by splaying (an initial splaying process is illustrated in Plate 4G), and by parting along S_3-surfaces of the Peninsula arenite.

2.3.2.2 Fold dimensions

(i) Amplitude. The amplitude (2A) is expressed by a value which is the shortest distance between the enveloping surfaces of a folded surface. 2A, for the different folded surfaces, varies from top to bottom in the Fold Zone and commonly increases stratigraphically upwards (Plate 2A & 6E). 2A for synclines, especially in the

intensely deformed areas, closely corresponds to the Fold Zone thickness (Plate 1); a maximum value for 2A thus inferred is 200 - 250ft (60 - 80m). The areal variation of 2A will therefore also parallel the trend of the Fold Zone thickness (Maps 4 & 5).

(ii) Wavelength, λ is approximated by the crestal distance (λ') between adjoining anticlines (or synclines) parallel to the enveloping surface of the Fold Zone. Areally, λ' varies considerably, ranging from 35 to 350ft (10 - 100m). At De Trap (Map 3) λ' is fairly constant, generally varying from 100 to 200ft (30 - 60m) (cf. fig. 11). A scatter diagram (fig. 17) shows no relation between Fold Zone depth and λ'.

(iii) Fold Dihedral angle (θ). θ increases downwards for successively folded surfaces (Plate 2A). Very typical is the difference between θ for anticlines and θ for synclines; θ(anticlines) varies from close (30° - 70°) to tight (0° - 30°) while θ(synclines)is always open (70° - 120°) (cf. Plates 6E & 4H). Isoclinal folding ($\theta = 0$) is rare and occurs mostly in the uppermost folded surfaces of anticlines (Plate 6D) and some recumbent folds. Elasticas-like($\theta < 0$) (Ramsay, 1967, pp. 349, 387-388) synclines were observed at De Bailie (Plate 1). θ(anticlines) tends to equal θ(synclines) where the Fold Zone is less than 50ft (15m) thick.

(iv) Continuation along fold axis. The detailed mapping at De Trap discloses that some individual synclines or anticlines continue for at least 2,000ft (600m) along their axes. The pod folds which have definite closures normal to their axes, have the following long dimensions:

Karookop - 200ft (60m), 400ft (120m), 600ft (180m) & 1,000ft (300m)

Donkerkloof - 200ft (60m), 300ft (90m)

2.3.2.3 Fold style

" ....., folds of a given generation in a given rock type usually can be recognized and correlated by identity of style more than by any other character." (Turner and Weiss, 1963; p. 112).

(i) Shape of folds in three dimensions. The classification of a fold according to the character of its axis and axial surface (Turner and Weiss, 1963; p. 110) is largely dependent on scale. Macroscopically, many folds may be regarded as plane or nonplane cylindrical; the fold axis being statistically rectilinear. Mesoscopically the folds are commonly nonplane, noncylindrical, nonplane or plane cylindrical (cf. Map 3 & figs. 11 & 15). The plane cylindrical shape becomes more common (macroscopically and mesoscopically) from Patryskop northwards i.e. in the direction of the Fold Zone margin.

Pod Folds are plane noncylindrical synclines, dominantly doubly plunging (Plate 5A & B and fig. 18). They are common towards the marginal areas of the Fold Zone e.g. at Karookop and Bakleikraal.

Map 2 illustrates two conical folds with subvertical axes. They have resulted from superposed folding.

(ii) The shape of folds in profile is shown on cross sections from Map 3 (figs. 11 - 15), fig. 18, Plates 1, 2A, 6E & 4H. These profiles are typical of disharmonic folding as defined by Whitten (1966; p. 606), Badgley (1965; p. 55) and De Sitter (1956; p. 213) and also correspond to Ramsay's Class 3 (1967; p. 366). Diagnostic features are listed below:

(a) The radius of curvature increases downwards to a horizon of no deformation, which commonly is a detachment zone. Note that the opposite is true for parallel folds.

(b) S_4-bands are markedly thickened in the cores of anticlines.

(c) Hinge zones are never angular, which is a reflection of competency.

(d) Second or higher order folds on the limbs of major folds are uncommon.

(e) The contrasting profile of anticlines and synclines is the most striking aspect of style; the small tightly folded anticlines are situated between the wide open folded synclines, which commonly bulge downwards where overfolded.

2.3.2.4 Fold attitude and symmetry

Regarding cylindrical domains, most folds are rendered asymmetric by overfolding and have therefore monoclinic symmetry. Exceptions are rare; folds with orthorhombic symmetry (mm) were observed at Langkloof (Plate 6E). Orthorhombic symmetry is more common towards the marginal areas of the Fold Zone; folds with monoclinic symmetry are, however, always dominant.

Horizontal to gently plunging inclined and recumbent folds (Plate 5C & D) are more typical than plunging upright folds (Map 3 & figs. 11 - 15); overfolding becomes scarcer and upright folds more common towards the marginal Fold Zone areas. The lower part of the Fold Zone usually consists of upright folded surfaces (Maps 2 & 3).

2.3.2.5 Fold Zone fabric

(i) Small scale (De Trap). The configuration of fold elements in a small portion of the Fold Zone is presented on Map 3. The area is divided into four domains of least heterogeneity; inspection reveals the impracticability of subdivision into homogeneous domains.

Domain 1 represents the lower portion of the Fold Zone, which is also the domain of least heterogeneity; the S_2-pole girdle (dgm. 26) is ill-defined and indicates low-dipping fold limbs. The subhorizontally plunging mesoscopic fold axes are scattered about β. The S_2-pole girdle maximum and β define the preferred upright orientation of the axial surfaces.

Domain 2 is typical of an overfolded upper part of the Fold Zone. The distribution of S_3-poles has a large spread (dgm. 25). β forms the locus of the linear element distribution; statistically L_2 is orientated parallel to the mesoscopic fold axes. Taken in conjunction with field data (figs. 12 & 13) the position of the maximum within the girdle indicates overfolding; the great circle through the minimum and β dips 40° west and defines the preferred orientation of axial surfaces in domain 2. The axial trace thus inferred corresponds with the trend on Map 3.

Domain 3 comprises an area of more complex folding in the upper part of the Fold Zone. The stereographic compilation of (S_3-poles) (dgm. 24) indicates superposed folding. The π-circle is the best fit locus

to the S_3-pole girdle which combines a continuous spread of divergent S_3-poles. β, the preferred orientation of B, coincides with the locus of the linear elements (dgm. 23). The primary mode of the L_2 and mesoscopic fold axes distribution has a large spread, which is significantly skew anticlockwise. A notable secondary mode developed approximately normal to the primary mode is further indication of superposed folding. Overfolding is less dominant; axial surfaces preferably dip 70° west.

By comparison of domains 1 and 2 (dgms. 25 & 26), it is evident that from bottom to top in the Fold Zone, upright folding gives way to overfolding. The mode of deformation effected more constraint on the attitude of folds lower down in the Fold Zone.

By inspection of Map 3 it appears as if the east-west crossfolding is superposed on the major north-south trend (domain 3), and would therefore constitute the "younger" event. This virtually coeval event is expressed by the tendency of the north-south trend to become tangentially related to the cross trend (cf. domain 4); this is supported by the skew distribution of linear elements in domain 3 (dgm. 23).

Dgms. 24 & 25 show that all linear elements (including B) have a constant preferred orientation i.e. a 5° - 10° plunge in the direction 343°; the axial surfaces, though, have variable dip components.

(ii) Regional scale. The traces of fold axes and axial surfaces are compiled on Maps 4, 5 & 6 while the inferred trends are shown on Map 1. The following characteristics are noted:

(a) The stereographic compilation of fold elements on Map 4 (dgm. 27 on Map 4) shows that:

1. The axial surfaces, having different dip components, are preferentially arranged round a zone axis, β', which forms the locus of the fold axes. β' plunges 5° in a direction 321° and the axial surfaces preferentially dip towards the southwest.

2. Axial surfaces of anticlines which are commonly upright, have a more variable trend than those of the synclines (the poles along the primitive are mainly those of anticlinal axial surfaces).

(b) Dgm. 28 (on Map 5) which is a composite of data on Maps 5 & 6, indicates a preferential dip of axial surfaces towards the east-northeast.

(c) The areal configuration of axial traces in the south apparently describes an arc with the convex side pointing towards the east-northeast (Maps 1 & 4), while the data on Maps 5 & 6 seem to describe an arc with the convex side pointing towards the west (Map 1). The isolated centres of no deformation at De Trap and De Bailie (Map 4) appear to be related to the associated divergent structural trends.

2.4 SECOND PERIOD OF PENECONTEMPORANEOUS DEFORMATION

2.4.1 Introduction

Small scale folding, well typified by magnitude and style, documents a second period of deformation. These phenomena were observed at De Trap, Groenberg and at Karookop (Map 6) where Visser (1962, 1965) followed by Rust (1967), described these structures as glacial grooves and striae.

At De Trap the deformation has affected the Oskop Member. Two stratigraphic horizons are similarly deformed at Karookop:

(i) The upper surface of the Peninsula Formation (or Oskop Member after Rust, 1967; p. 43) which locally has an intertongueing relationship with overlying arenaceous diamictite.

(ii) An arenite lentil 6ft (1.8m) higher up in arenaceous diamictite (Kobe Member after Rust, 1967; p. 46).

2.4.2 Structure

Low irregular undulations (Plate 5E) in cross-stratified layers (λ' = 20 - 30ft/6 - 9m, 2A = 4 - 10ft/1.2 - 3m) locally give way to cylindrical folding, notable for its regular spacing (λ' = 2ft/0.6m, 2A = 1ft/0.3m) and rectilinear parallel trend of fold axes (Plate 5F). Symmetric forms predominate (cf. Plates 6A & 5G).

A notable feature of these folds is a periodical distribution of folded

forms which transgresses all size classes (Plates 5H & 6A). b(Geom.)-wrinkles are found only in the troughs of synclines.

At Karookop the depth of fold penetration in the cross-stratified layers is not known but the effect of folding on the cross-laminae is clearly illustrated by their sigmoidal posture on an eroded surface (Plate 6B). At De Trap where the Oskop Member consists of sets of layers, both folding and wrinkling are penetrative within at least the upper 2ft (0.6m).

The structural trends of the two periods of penecontemporaneous deformation corresponds (cf. Map 6).

At Groenberg, on the upper surface of the Peninsula Formation, the same small scale folding is present in association with a grounded ice-block cast; Plate 4C illustrates the ice-thrusted ridge (fold) which developed in front of the ice-block. Drag effects below the block are documented by linear drag marks and tools (first described by Rust 1967; p. 76). Ripple marks can be seen beyond the ridge. The movement direction of the ice block (probably caused by tidal currents) parallels the long axis of the small folds (Map 6), but is transversely related to the ice-thrust ridge.

3 DISCUSSION AND CONCLUSIONS

3.1 DEPOSITIONAL ENVIRONMENT OF THE DIAMICTITES

Following Harland et al. (1966), the arenaceous diamictites of the Pakhuis Formation are considered to be tillites. A glacial origin, although "distant" is well founded on the common occurrence of facetted, striated and polished clasts.

The blanket shape of the diamictite lithosomes, stratification, intercalation of sorted arenite lentils etc. indicate subaqueous deposition. Microfabric analysis largely substantiates this view:

(i) Differential constraint was imposed on the orientation of grains of different size fractions.

(ii) A variable mode of particle transport has been established, indicating different flow regimes.

(iii) The variability of the flow medium is indicated by a variance in fabric pattern within and between samples.

Pulsatory turbulent flow is implied.

The paleocurrent data (Map 3) indicate flow in a south-southeasterly direction which corresponds with the paleocurrent trend for the Table Mountain Group (Rust, 1967).

The lower Sneeukop, upper Sneeukop and Steenbras diamictites represent discrete episodes of like diamictite deposition intermitted by two periods of superficial deformation. The badly sorted nature of the diamictite and turbulent character of the transport medium indicate high density and fast flowing currents of short duration. The fallacy of inferring ice-flow directions from fabric analysis of the Pakhuis tillites is well borne out (Visser, 1962; Rust, 1967).

3.2 RHEOLOGY OF THE DEFORMED SEDIMENTS

3.2.1 Peninsula Arenite

The absence of erosional features such as unconformaties, channels, fossil soil profiles (Rust, 1967) at the arenite/diamictite interface indi-

cates that deposition of the Peninsula sand was followed uninterruptedly by the deposition of the Sneeukop diamictites. An unconsolidated condition for the Peninsula sand during deformation is implied.

The mode of transposition and conservation of structure during folding imply hydroplastic (Elliot, 1965) behaviour of the sand. Sparse examples of rupture indicate solid or quasi-solid (Elliot, 1965) behaviour, which was effective after hydroplastic transposition. Apparently the hydroplastic strain limit was exceeded under local conditions of tensional stress (fig. 10).

3.2.2 Lower Sneeukop Diamictites

Microfabric analysis on samples taken approximately in the central part of the Member, reveals typical primary textures (dgms. 4 - 6). The preservation of primary textures rules out the possibility of liquid or quasi-liquid (Elliot, 1965) behaviour for at least the central part of the Member.

The sedimentary dikes always lie in the ac(Geom.)-plane of the synclines, indicating that the dike formation was contemporaneous with, and controlled by the deformation. Solid tensional fracturing preceded injection of the dike material. The implication is that a large, apparently the upper, part of the lower Sneeukop Member behaved as a solid while portions of the lower part, source of the injected diamict, was in a quasi-liquid state. Quasi-liquid behaviour of the diamict in the dikes is indicated by grading within the dikes; the central part of the dike constituted the more competent flow regime.

S_3-surfaces, infrequently found at or near the diamictite/ Peninsula arenite contact, represent discrete slip surfaces which are more likely to be formed in a hydroplastic than quasi-liquid sediment.

Solid/quasi-solid behaviour of the basal part of the diamict is ruled out by the occurrence therein of detached bands of Peninsula arenite. During an "advanced" stage of deformation (i.e. after transposition took place) S_3- and/or S_4-bands became parted from the Peninsula sand contact by a splaying mechanism. Progressive deformation, in some instances, further folded and buckled these S_3- and/or S_4-bands. Whereas both the Peninsula sand and the diamict near the contact are considered to have been in a hydroplastic state, their relative competency is clearly illustrated by this phenomenon: the sand behaved as an entity while the diamict flowed in a more unconstrained manner.

The same relation is illustrated where clasts are partly embedded in the Peninsula arenite (Plate 2D). Some amount of relative slip during flexural-slip folding is expected on the contact surface. As no relative movement between the clasts and arenite is evident, it is inferred that the

flowing diamict exercised little force on the obstructive clasts.

The external morphology of the coarse-grained arenite lentils, intercalated throughout the lower Sneeukop Member, does not show any deformation. The fine-grained arenite lentils, situated at the base, have undergone solid/quasi-solid deformation by small scale penetrative normal faulting. This phenomenon is an anomaly within the rheological and deformational pattern; it is proposed after Shotton (1965; p. 422 - 425) that this structure has resulted from shrinkage of frozen ground prior to deformation and immediately after deposition of the lentil during subaerial exposure.

3.2.3 Discussion

The behaviour of unconsolidated sediments under stress can largely be inferred from the Mohr-Coulomb law (Mathews and MacKay, 1960; Williams, 1960; Viete, 1960; De Sitter, 1956):

$$\tau(\text{crit}) = \tau_o + (\sigma - p) \tan \phi$$

where the critical shear stress (τcrit.) is a function of the

(i) cohesion of the sediment (τ_o),

(ii) total normal stress (σ),

(iii) hydrostatic pore pressure (p) and

(iv) the angle of internal friction (ϕ).

Cohesion, pore pressure and internal friction (shearing resistance) are functions of grain size and grain size distribution. Cohesion increases with a decrease in grain size and approaches zero for sand. The angle of internal friction is ca. zero for saturated clays and 30° - 35° for sand (Spencer, 1969). The angle of internal friction is also dependent on packing and/or porosity and is, according to Van Schalkwyk (1967), ca. 32° at failure for the critical porosity of ca. 0.41. Pore pressure controls effective stress (σ - p) which is partly dependent on the density of the sediment in relation to its critical density (De Sitter). The effect of pore pressure is largely dependent on permeability and rate of stress application; a clay, thus would more easily be liquified than a sand.

The sedimentary environment of the Table Mountain Group suggests a water saturated condition of the sediments prior to deformation. Theoretical considerations indicate that the Peninsula sand would have required a large critical shearing stress. This appreciable shearing stress would be reduced by increased pore pressure and by adjustment along potential slip surfaces, such as S_1 and S_2. In this manner laminar hydroplastic flow may develop in the sand under stress. The total absence of thrust faulting is significant (by comparison with similarly deformed sediments - section 4.2) and ex-

presses this unique mode of stress accommodation. The permeability of the sand, coupled with a not too rapid application of stress, would have inhibited the local development of high pore pressures which facilitate thrust faulting.

A low critical shearing stress for the lower Sneeukop diamict can be inferred from its bad sorting (low permeability) and notable clay content. The homogeneity of the diamictite lithosome contrasts sharply with its inferred variable rheologic behaviour during deformation. The upper part of the diamict acted as a solid while the lower part behaved more unconstrained under stress. It is therefore postulated that the more solid diamict was rendered thus by ground-ice, say to a depth of 20' or so. Ground-ice increases the critical shearing stress appreciably by elimination of the hydrostatic pore pressure and increase in the cohesion factor; effective stress becomes equal to total normal stress. A blanket of frozen ground explains the solid behaviour while the partial liquefaction of the underlying diamict is due to the blanketing effect which increases pore pressure under load. At the diamict/sand interface, the larger permeability of the Peninsula sand drained off pore water in the diamict, thereby increasing its critical shearing stress and S_3-slip surfaces developed in it.

In places where the overlying cover of diamict was thin or absent, ground ice might have been developed in the Peninsula sand. During deformation the frozen sand would have resisted transposition and might have yielded by rupture. Such effects of solid behaviour were observed at the Pup (Plates 4A & B) in the upper reaches of the Fold Zone.

3.3 INTERPRETATION OF THE STRUCTURE

3.3.1 External geometry of the Fold Zone

The functional relation between the basin axis and external geometry of the Fold Zone, especially the gradual decrease in Fold Zone thickness towards its margins, indicates a homogeneously and regionally operating force markedly affected by the basin shape.

The isolated centres of no deformation from where the Fold Zone thickness gradually increases, probably represent more competent areas rendered such by frozen ground.

The regular lower décollement surface is due to relative slip on stratification surfaces.

3.3.2 Flexural-slip folding

The cusp and caries style of folding is typical of penecontemporaneous deformational features e.g. convolute laminae, load folds, slump struc-

tures etc. 'The "anticlines" tend to be narrow and sharp, whereas the "synclines" tend to be wide and flat-bottomed. Features with this geometry are diagnostic of décollement; in reality the "synclines" are but passive features that are outlined by the rising "anticlines" as adjustment takes place along a gliding or slipping surface below.' (Sanders, 1960; 416).

Ramsay (1967; pp. 382 - 386) considers this style of folding to be typical of structures developed by lateral compressive stress on a contact surface between materials of different composition. The sharp-crested antiforms will point towards the higher density (viscosity) material.

Arguments are considered below which show that folding was dominantly caused by vertical stress conditions i.e. a load pressure which resulted in a lithostatic stress environment. (The deviatoric stress component is discussed in section 3.3.3).

(i) Appreciable load is necessary for the liquefaction and intrusion mechanism of the diamict.

(ii) Complete transposition is thought to be effected under more severe stress than that necessary to overcome the initial slip resistance. This overstress condition was homogeneously distributed in the upper part of the Fold Zone as documented by the presence of S_3-bands. By implication, it is inferred that appreciable load stress operated on the upper surface of the Fold Zone.

(iii) Laminar flow within S_4-bands took place from the "passive" synclines to the "active" anticlines; this is well illustrated by the relative attenuation of bands in the synclines and thickening in the anticlinal cores. The resulting movement picture necessitates a vertical stress system (fig. 19) to correspond with mean strain. No lateral shortening took place.

The movement picture (fig. 19) is composed of:

(i) Mean strain which is inferred by considering S_4-bands as passive markers.

(ii) a(Kin.) within homogeneous domains (fold limbs *) as inferred from pure strain of S_4-bands.

a(Kin.) inferred from slip on S_2 (section 2.3.1.1 and 2.3.1.3) and microfabric patterns (section 2.3.1.4) have the same orientation, within respective fold limbs, approximately normal to β. a(Kin.) depicts the componental move-

---

* The homotactic fabrics of the fold limbs have orthorhombic symmetry.

ments of mean strain.

3.3.3 Fold Zone fabric

The alignment of the sedimentary dikes parallel to ac(Geom.) of the synclines, allows the conventional orientation of the strain ellipsoid with its long axis parallel to B. Mean strain, in the diamictite is therefore perpendicularly orientated with respect to mean strain of the fold system (cf. fig. 19).

The asymmetry of the fold system renders the total fabric monoclinic. The plane of symmetry is ac(Geom.). The internal axis of rotation defines b(Kin.) and parallels B (section 2.3.1.3), which again corresponds with the external axis of rotation (fig. 20) as defined by the zone axis, β' (section 2.3.2.5 (ii)). The sense of rotation around the internal and external axis of rotation need not be the same. The external axis of rotation, β', indicates a stress couple (fig. 20) which constitutes a deviatoric (Turner & Weiss, 1963; p. 261)component of the earlier deduced lithostatic stress system. The stratigraphic position of the Fold Zone indicates that this stress couple operated along the horizontal i.e. parallel to the depositional interface.

The stress couple consisted of an active stress deviator operating in the direction of asymmetry, and a passive resistive stress. Where the two opposing stresses approached each other in magnitude a movement picture with orthorhombic symmetry should have resulted. Folds with orthorhombic symmetry were frequently observed towards the marginal areas of the Fold Zone.

The preferred orientation of B, as well as that of the zone axis, β', plunges from 5° to 10° in a direction 330° (Map 4). This anomalous orientation of B has undoubtedly not been effected by later tectonic tilting, and remains problematic.

Pod folding developed towards the marginal areas of the Fold Zone is ascribed to discontinuous stress environments.

The regional configuration of the stress deviator is depicted on Maps 1, 4 & 5, i.e. normal to the fold axes and opposite to the dip direction of the axial surfaces. Note that the sense of direction tends to be towards the basin axis.

4 HYPOTHESIS

4.1 INTRODUCTION

Penecontemporaneous superficial folding on this grand scale can be accounted for by only two known processes:

(i) Gravitational sliding of the sediment under its own weight.

(ii) Overriding by ice sheets or glaciers.

Gravitational gliding is discarded on the following grounds:

(i) It does not provide the necessary stress configuration.

(ii) No significant lateral translation occurred on the décollement surface.

(iii) The marginal areas of the Fold Zone could not have been deformed under their own weight, especially as a natural gliding surface was lacking.

(iv) As a model it fails to explain many features of the Fold Zone.

The glacial model is accepted as a working hypothesis because:

(i) Sediments of glacial origin are associated with the Fold Zone.

(ii) Certain phenomena can only be explained by the presence of ground ice.

(iii) Similar structures have been formed by the Pleistocene ice sheet in the Northern Hemisphere.

(iv) As a model it successfully explains most of the observed features.

4.2 GLACIAL MODEL

The deformation of unconsolidated substrata by overriding ice-sheets and glaciers of Pleistocene age, has been described by Fuller (1914), Slater (1926, 1927), Byers (1959), Viete (1960), Kupsch (1962), Rutten (1960, 1965), Mathews and MacKay (1960, 1964, 1965), and Dellwig and Baldwin (1965).

The main features are listed below.

(i) Mainly compressional structures develope while tensional forms are rare. The larger structures usually are folds and thrust faults. Folds with a vertical extent of 500 - 600ft and thrust faults with dip-slip components of 150 - 200ft have been reported. Ice-thrust ridges are characteristically sharp crested; the bevelling of the folds may be due to the flowing ice. Synclines generally are much wider, their axes being 50 - 100m apart. Fold axes commonly converge along strike and thrust planes show slickensides and grooves. Allochtonous rafts (locally a few km across), while being incorporated as englacial material, have undergone deformation in the same manner as the glacial ice itself; some have been broken into fragments and deposited with an imbricate structure.

(ii) The following small structures have been described:

(a) Minor folds.

(b) Sedimentary dikes which tend to be sub-parallel with the normal to the ice-front.

(c) Irregular intrusions i.e. mutual flow effects between beds; mixing of rotated slabs of material from the lower bed with the overlying material.

(d) Fuller (1914; fig. 140) shows an irregular contact, the bottom material being splayed along bedding planes.

(iii) Deformational zones, characterized by different types of structures, can be related to distance behind the ice-front; imbricate thrust blocks form closest to the terminus while flat lying folds farther back, originated by frictional drag underneath the ice mass.

(iv) The folds form transversely to the direction of ice-flow. Axial planes and thrust faults usually dip in a direction opposite to ice-flow. The plunge of individual fold axes may range from 20° to 35° in opposing directions; thus several culminations and depressions appear on strike within the same fold.

Structural features typically define an arcuate pattern in plan, with the convex side pointing in the direction of ice-flow.

(v) The relation between the deformed structures and the overlying till is well described by Kupsch: "The ablation till lies disconformably on the bevelled bedrock structures, but the basal till constitutes a conformable part of the deformations."

(vi) The absence of inverted fold limbs in association with thrust faults indicates superficial folding (De Sitter, 1956; p. 405) and disproves gravitational gliding (De Sitter, 1964; p. 255).

(vii) Controlling factors of deformation are firstly the nature of the overridden sediment and secondly the static and dynamic pressures exerted by the ice-load. These are functions mainly of ice thickness, velocity of flow and topography.

(a) Kupsch estimated that ice thicknesses of 450 - 900ft formed ice-thrust ridges with 200' vertical dimension. According to Viete (from Kupsch): ".... the static pressure exerted by a glacier 200m thick varies between 18kg/cm^2 for clean ice to as high as 36kg/cm^2 for ice choked in debris." Huizinga (1944; from Kupsch) pointed out that a minimal lateral push of ca. 300kg/cm^2 is necessary to form ice-thrust ridges. Kamb (1964) regards the shearing stress at the bottom of glaciers to be roughly constant at 1kg/cm^2. "..., there is considerable evidence to support the view that deformation commonly occurred near the margin of an actively moving lobe" (Mathews and MacKay, 1960). Kupsch explains: "It has been observed in existing glaciers that thrusting in ice is best developed near its margin, where the rigid upper surface of the glacier, which further upstream overlies plastic ice, extends to the base ...."

(b) Pre-glacial topography is an important controlling factor; the maximum development of structures is along slopes facing the direction of

ice-flow and along borders of pre-glacial valleys. Mathews and MacKay (1964) do not consider an opposing slope a necessary condition for ice-thrusting.

(c) Controversial opinions have been expressed by Kupsch and Mathews and MacKay (amongst others) on the effect of ground-ice on ice-thrusting. Mathews and MacKay (1960) conclude that:

1. The shear strength of sediments usually exceeds the shear stress applied by a glacier on its substratum (1kg/cm^2). "Abnormal circumstances such as unusually high shear stress beneath the ice, unusually low shear strength of soils, or unusually high pore pressures seem, however, to have permitted shear failure in many widely separated localities."

2. The development of interstitial ground-ice is not a necessary condition to transmit stress as loading by the overlying ice would render the sediments sufficiently competent.

(viii) Various modes of deformation by the overriding ice have been postulated:

(a) Incorporation of substratal material by the glacial ice will result in a glacial pseudomorph structure of such material.

(b) Ice-push in front of the ice sheet.

(c) Frictional drag beneath the ice-sheet by means of a basal slip mechanism.

(d) A permafrost substratal layer in essence constitutes part of the glacier and becomes deformed by glacier tectonics.

4.3 PENECONTEMPORANEOUS DEFORMATIONAL ENVIRONMENT

The Table Mountain embayment in the Western Cape was affected by at least two ice sheat transgressions. Small advances of short duration along the marginal areas are indicated. The first transgression was preceded by a retreat of the water, to such an extent that a thin veneer of ground-ice was sporadically formed under permafrost conditions; locally the ground-ice

penetrated deeply and formed a bulwark against subsequent deformation. The preglacial topography could at the most have been slightly undulating and controlled local development of ground-ice. Deformation took place predominantly by frictional drag underneath the ice-sheet. The ice advanced from the south-west as well as from the north-east towards the basin axis. The thin active frontal surges reached the basin axis where the deepest deformation is recorded. Superposed structures are ascribed to coalescing piedmont ice sheets and to the radial expansion advance mechanism of ice-sheets. The second ice advance took place after an increase in water depth in the basin. The predominantly floating ice sheets sporadically touched down to form peculiar structures of small magnitude.

The lower Sneeukop Member represents proglacial drift dispersed subaquously during the first and major retreat of the water level. Following the first period of deformation the upper Sneeukop Member was deposited during the interglacial period while the embayment became flooded again. A second glacial period set in during or shortly after deposition of the upper Sneeukop Member. The water level steadily lowered and permitted redistribution and sorting of the upper part of the diamict. This resulted in the formation of the Oskop sand. The deformation of the Oskop Member documents the culmination of the second glacial period together with the associated increase in water depth. The Steenbras Member was deposited during the first stage of the waning ice-age. Thereafter the water deepened progressively during the formation of the Kobe Member; this lutaceous diamictite laterally (towards the basin axis) and vertically grades into the Soom Shale Member which marks the maximum water depth attained in the embayment and discontinuation of the glacial environment.

5 REFERENCES

AMERICAN COMMISSION ON STRATIGRAPHIC NOMENCLATURE, 1961. Code of stratigraphic nomenclature. Am. Assoc. Petr. Geol. Bull., 45, 645 - 665.

BADGLEY, P.C., 1965. Structural and Tectonic Principles. Harper & Row.

BHATTACHARYYA, D.S., 1966. Orientation of mineral lineation along the flow direction in rocks. Tectonophysics, 3, 29 - 33.

BYERS, A.R., 1959. Deformation of the Whitemud and Eastend Formations near Claybank, Saskatchewan. Royal Soc. Canada Trans., V.53, ser. 3, sec. 4, 1 - 11.

COCKS, L.R.M., C.H.C. BRUNTON, A.J. ROWELL and I.C. RUST, 1969. The first Lower Palaeozoic Fauna proved from South Africa. Q.Jl. Geol. Soc. London, 125.

DELLWIG, L.F. and A.D. BALDWIN, 1965. Ice-push Deformation in Northeastern Kansas. Bulletin Kansas, State Geol. Survey, 175 (2).

DE SITTER, L.U., 1956. Structural Geology. McGraw-Hill.

_____, 1964. Structural Geology. McGraw-Hill.

ELLIOT, R.E., 1965. A classification of subaqueous sedimentary structures based on rheological and kinematical parameters. Sedimentology, 5, 193 - 209.

FLEUTY, M.J., 1964. The description of folds. Proc. Geol. Assoc., 75, 461 - 492.

FLINT, R.F., J.E. SANDERS and J. RODGERS, 1960a. Symmictite: a name for nonsorted terrigenous sedimentary rocks that contain a wide range of particle sizes. Bull. Geol. Soc. Am., 71, 507 - 510.

_____, 1960b. Diamictite: a substitute term for symmictite. Bull. Geol. Soc. Am., 71, 1809 - 1810.

FULLER, M.L., 1914. The Geology of Long Island, New York. U.S. Geol. Survey Prof. Paper 82.

HARLAND, W.B., K.N. HEROD and D.H. KRINSLEY, 1966. The definition and identification of tills and tillites. Earth-Sci. Rev., 2, 225 - 256.

HAUGHTON, S.H., 1929. The glacial beds in the Table Mountain Series. Compte Rendu, XV Session, Int. Congress, Volume II, 85 - 89.

HAUGHTON, S.H., L.J. KRIGE and A.V. KRIGE, 1925. On intraformational folding connected with the glacial bed in Table Mountain Sandstone. Proc. Geol. Soc. S. Afr., 28, 19 - 25.

HUIZINGA, T.K., 1944. Geologie en grondmechanica: Geol. Mijnbouwk. Genootschap Nederland en Koloniën, Geol. Ser., v. 14, p. 259 - 275.

KAMB, B., 1964. Glacier Geophysics. Science, 146.

KUPSCH, W.O., 1962. Ice-thrust ridges in Western Canada. Jour. Geol., 70, 582 - 594.

MATHEWS, W.H. and J.R. MACKAY, 1960. Deformation of soils by glacier ice and the influence of pore pressures and permafrost. Roy. Soc. Canada Trans., v. 54, ser. 3, sec. 4, pp. 27 - 36.

_____, 1964. Discussion: Role of permafrost in ice-thrusting. Jour. Geol., 72, 378 - 380.

_____, 1965. Discussion: Ice-pushed ridges, permafrost and drainage. Jour. Geol., 73, 896.

POTTER, P.E. and F.J. PETTIJON, 1963. Paleocurrents and basin analysis. Springer-Verlag.

RAMSAY, J.G., 1967. Folding and fracturing of rocks. McGaw-Hill.

RUSNAK, G.A., 1957. The orientation of sand grains under conditions of "Unidirectional" fluid flow. 1. Theory and experiment. Jour. Geol., 65, 384 - 409.

RUST, I.C., 1967. On the sedimentation of the Table Mountain Group in the Western Cape Province. Unpub. doctorate thesis, University of Stellenbosch, Stellenbosch.

RUTTEN, M.G., 1960. Ice-pushed ridges, permafrost and drainage. Am. Jour. Sience, 258, 293 - 297.

_____, 1965. Discussion: Ice-pushed ridges, permafrost and drainage. Jour. Geol., 73, 895 - 896.

SANDERS, J.E., 1960. Origin of convoluted laminae. Geol. Mag., 97, 409 - 421.

SHOTTON, F.W., 1965. Normal faulting in British Pleistocene deposits. Quart. J. Geol. Soc. Lond., 121, 419 - 434.

SLATER, G., 1926. Glacial tectonics as reflected in disturbed drift deposits. Proc. of the Geol. Assoc., 37, 392 - 400.

_____, 1927. Part I. The structure of the disturbed deposits in the lower part of the Gipping Valley near Ipswich. Proc. of the Geol. Assoc., 38, 157 - 182.

_____, 1927. Par II. The structure of the disturbed deposits of the Hadleigh Road area, Ipswich. Proc. of the Geol. Assoc., 38, 183 - 216.

_____, 1927. The structure of the Mud Buttes and Tit Hills in Alberta. Geol. Soc. Am. Bull., 38, 721 - 730.

SPENCER, E.W., 1969. Introduction to the structure of the earth. McGraw-Hill.

TURNER, F.J. and L.E. WEISS, 1963. Structural analysis of metamorphic tectonites. McGraw-Hill.

VIETE, G., 1960. Zur Entstehung der glazigenen Lagerungs-störungen unter besonderer Berücksichtigung der Flözdeformationen im mitteldeutschen Raum: Freiberger Forschungshefte c78, Berlin, Akademie Verlag.

VISSER, J.N.J., 1962. Die voorkoms en oorsprong van die tillietband in die Serie Tafelberg. Ongepubliseerde M.Sc.-tesis, Universiteit Oranje Vrystaat, Bloemfontein.

_____, 1965. Gletservloer in die Pakhuisberge, Distrik Clanwilliam. Annals of the Geol. Survey, Dept. Mines, Vol. 4.

WHITTEN, E.H.T., 1966. Structural geology of folded rocks. Rand McNally.

WILLIAMS, E., 1960. Intra-stratal flow and convolute folding. Geol. Mag., 97, 208 - 214.

6. A C K N O W L E D G E M E N T S

The writer is grateful to the following persons and institutions for guidance and assistance:

1. Prof. I.C. Rust who initiated this study.
2. Prof. A.P.G. Söhnge.
3. Geological Survey, in person Mr. J.N. Theron.
4. Personnel of the Geological Department, University of Stellenbosch.

7 A P P E N D I X

PLATES	-	nos. 1 - 6 (Plate 1 - Frontispiece)
FIGURES	-	nos. 1 - 20
DIAGRAMS (dgms.)	-	nos. 1 - 28
COMPASS DIAGRAMS	-	nos. 1A - 16C
MAPS	-	nos. 1 - 6 (Maps 2 & 3 in folder).

PLATE 2

A and B — The Fold Zone at De Bailie and Donkerkloof respectively. Note the regular bounding surfaces.

C — See Plate 6E.

D — Megaclasts from the lower Sneeukop diamictite are partly embedded in the upper surface (vertical face) of the folded Peninsula arenite. The lineation, L_2, is well developed. The observer stands on diamictite (Platberg).

E — An example of the arenite lentils which are intercalated throughout the lower Sneeukop Member (De Trap).

F — Cross-laminae (S_1-layers) are perpendicular to stratification (S_2) on the "saddle" of a box-like fold (Peninsula arenite, De Trap).

G — The transposed cross-laminae (S_3-bands) are shown to be bounded by S_4-surfaces in Peninsula arenite. The arrows indicate the relative movement (slip on S_4) which caused the folding in S_3 (De Trap).

H — The different stages of transposition within a single cross-stratified layer are illustrated; the final transposed stage i.e. where S_1 is parallel to S_2, has been attained between 2 and 3. The clipboard is 15" long (Peninsula arenite, De Trap).

PLATE 1

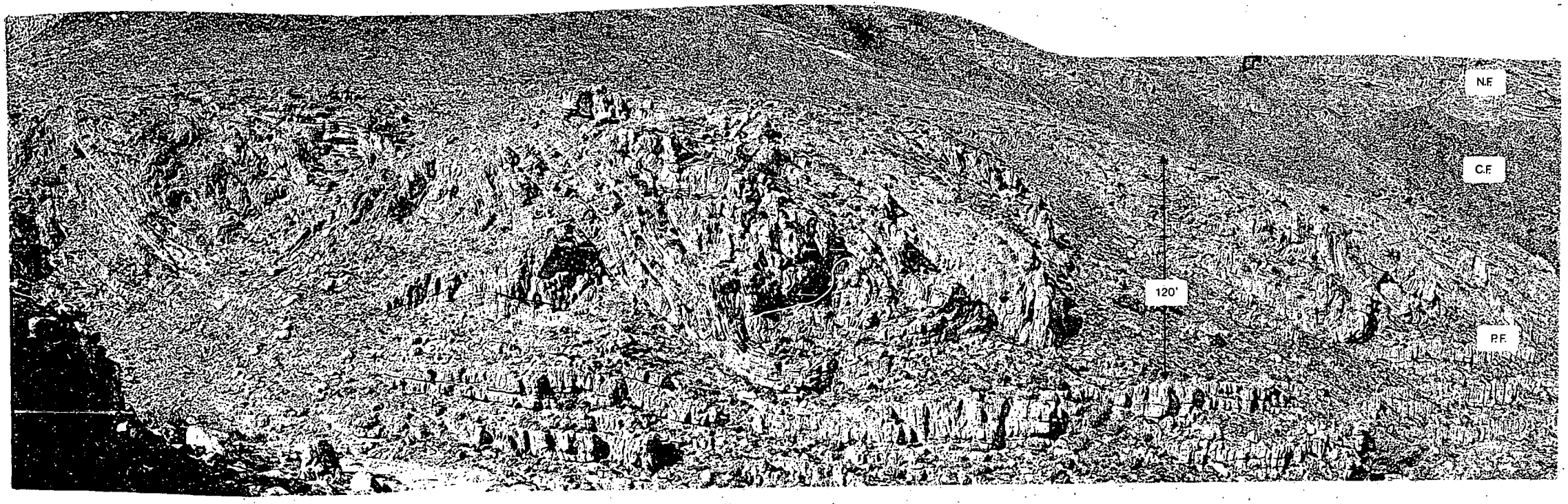

THE FOLD ZONE

(at De Bailie)

NARDOUW FORMATION – N.F.

CEDARBERG FORMATION – C.F.

PAKHUIS FORMATION – outlined

PENINSULA FORMATION – P.F.

PLATE 2

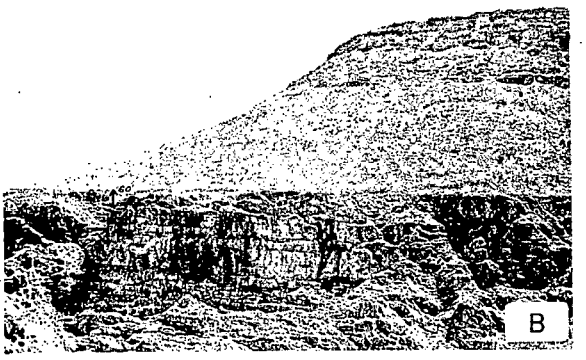

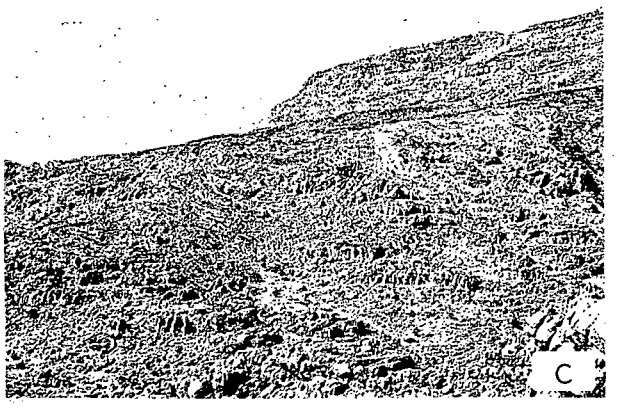

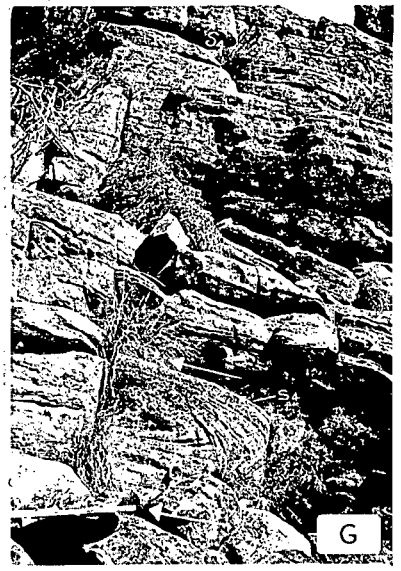

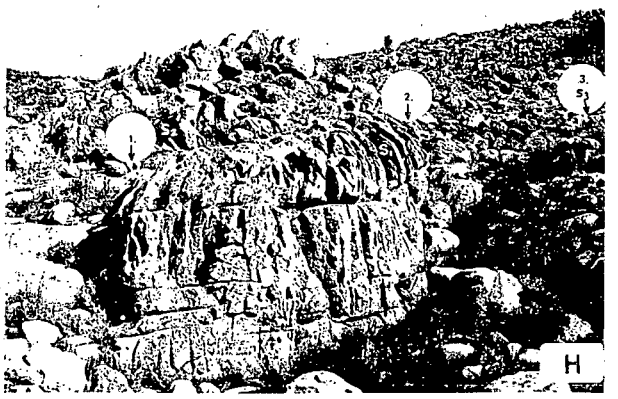

PLATE 3

A The drag feature is caused either by slip between S_2- layers (cross-stratified layers) or by slip between the S_1-layers (cross-laminae) and the S_2- surface, facing reader (Peninsula arenite, De Trap).

B The S_3-surfaces demarcate S_3-bands in the diamictite of the lower Sneeukop Member (De Trap).

C Folding in S_3 parasitic to folding in S_4 (Peninsula arenite, De Trap).

D Fold mullions; their enveloping surface constitutes a S_4-surface. (Peninsula arenite, De Trap).

E Similar folding due to differential slip on S_3 (Peninsula arenite, De Trap).

F The hinge zone of an anticline in the lower part of the Fold Zone. The folded surface is S_2 (De Trap).

G and H The lineation, L_2, developed in transposed structures (Peninsula arenite, Langkloof and Sneeukop (Bo-Rozendal)).

PLATE 3

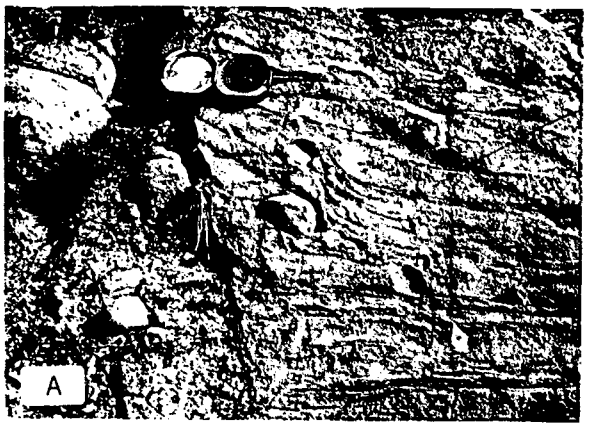

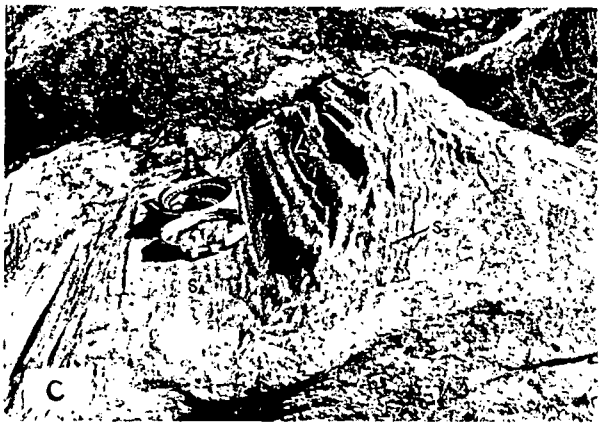

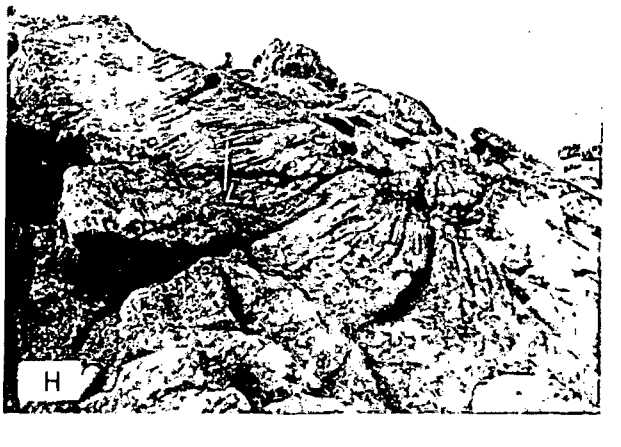

PLATE 4

A Penecontemporaneous faulting in the upper horizons of the Fold Zone (Peninsula arenite, The Pup).

B The enigmatic posture of S_3-bands within a S_4-band (Peninsula arenite, The Pup).

C The cast of a grounded ice block on the upper surface of the Peninsula Formation; note the drag marks below and the ice-thrusted ridge in front (Groenberg).

D A sedimentary dike in the lower Sneeukop diamictite (De Trap).

E Detached bands of arenite situated in diamictite (lower Sneeukop, De Trap).

F The band of arenite, situated in the diamictite, has been folded after detachment from the Peninsula contact (De Trap).

G An initial stage in the "stoping" or "splaying" process by which bands of arenite became detached from the upper Peninsula surface (De Trap).

H The sharp isoclinal crestal form of the anticline is typical; note the attenuation of S_4-bands in the crest and thickening in the core (Sneeukop, Nuweberg).

PLATE 4

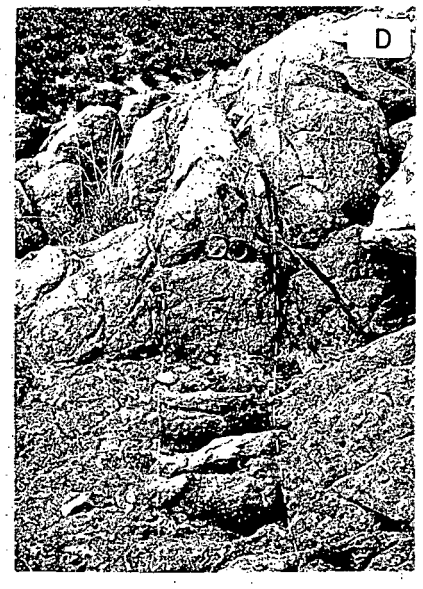

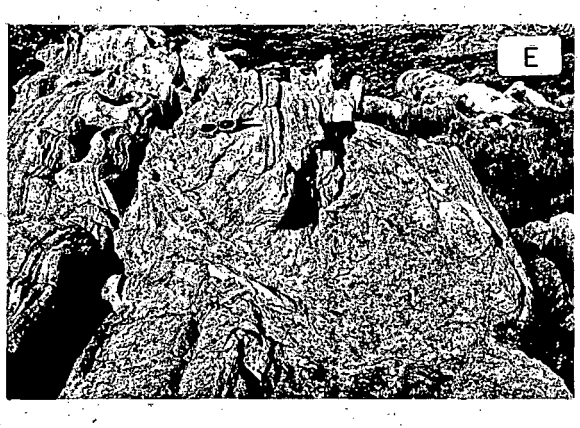

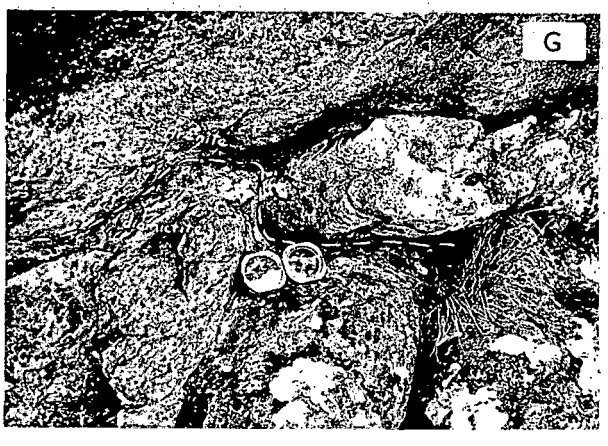

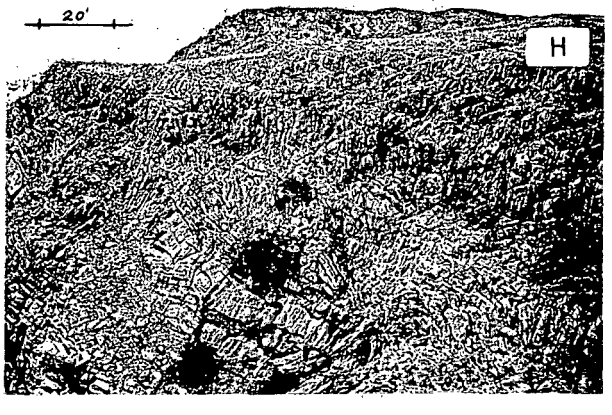

PLATE 5

A The end-on closure of a pod fold (Donkerkloof).

B An asymmetric pod fold (Karookop).

C The hinge zone in the core of a recumbent fold (De Trap).

D A recumbent fold; the upper limb forms the top of the Fold Zone (Patryskop).

E Irregular undulations in the upper surface of the Peninsula Formation (Karookop).

F A local occurrence of small rectilinear folds in the upper surface of the Peninsula Formation; note the regular spacing and parallelism (Karookop).

G An asymmetric form of the folds described above.

H The b-wrinkles in the troughs of folds (Plate 6A) reflect the same periodicity and style of folding as the larger folds (Karookop).

PLATE 5

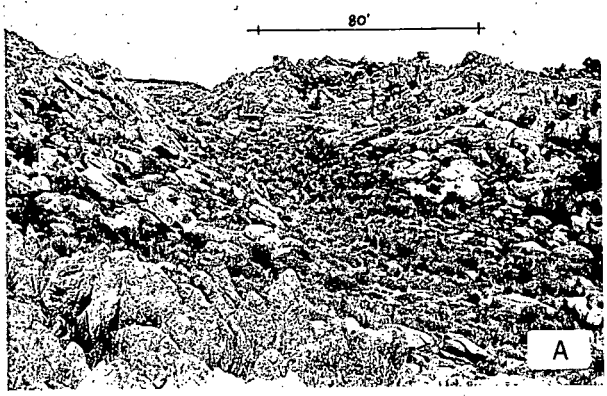

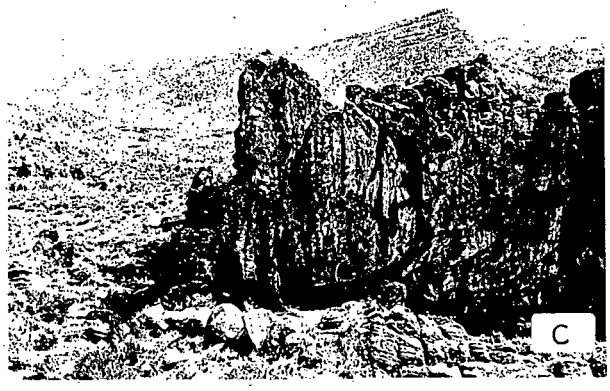

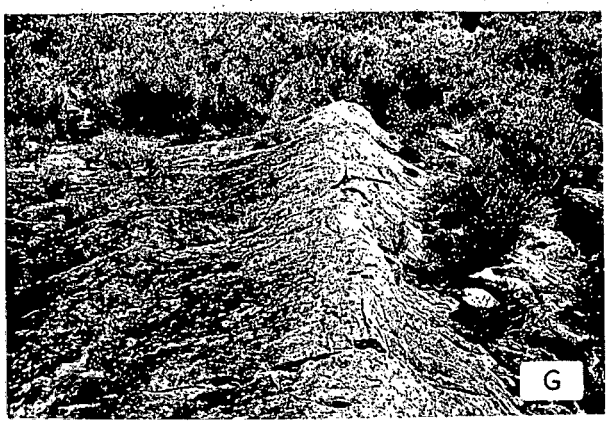

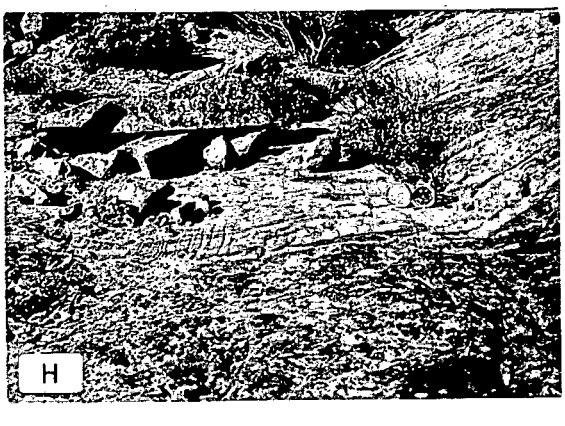

PLATE 6

A The folded surface of an arenite lentil in diamictite, ca. 6 feet above the upper surface of the Peninsula Formation. Note the periodicity and style of folding (cf. fig. 19) (Karookop).

B The sigmoidal curve illustrates the deformed nature of the cross-laminae where the folded upper part of the cross-stratified layer has been eroded away. The photo was taken in the lower right corner of Plate 5F (Karookop).

C The incompetent behaviour of the Peninsula arenite is reflected by the variable thickness of the S_4-band (De Trap).

D The isoclinal crestal part of an anticline in the uppermost part of the Fold Zone. Note the nonplane cylindrical form of the fold (De Bailie).

E A rare occurrence of upright folding in the southern part of the area investigated. The broad synclines and narrow cuspate anticlines are characteristic. The structural discontinuity at the upper surface of the Fold Zone implies post-deformational erosion (Langkloof).

PLATE 6

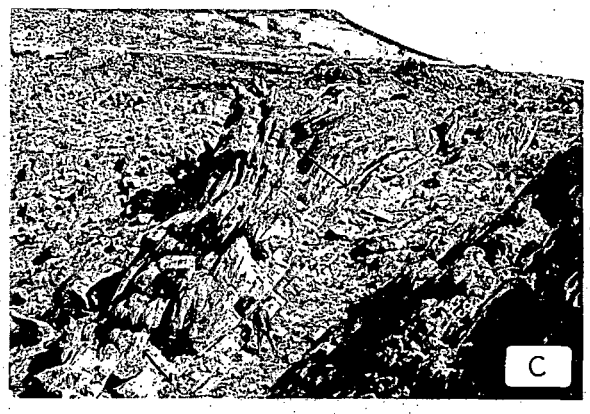

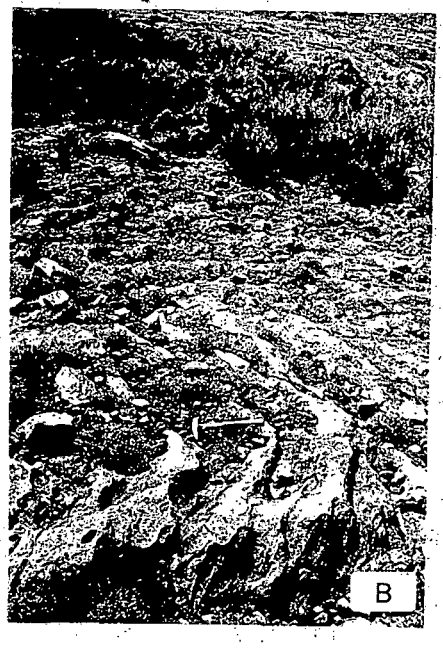

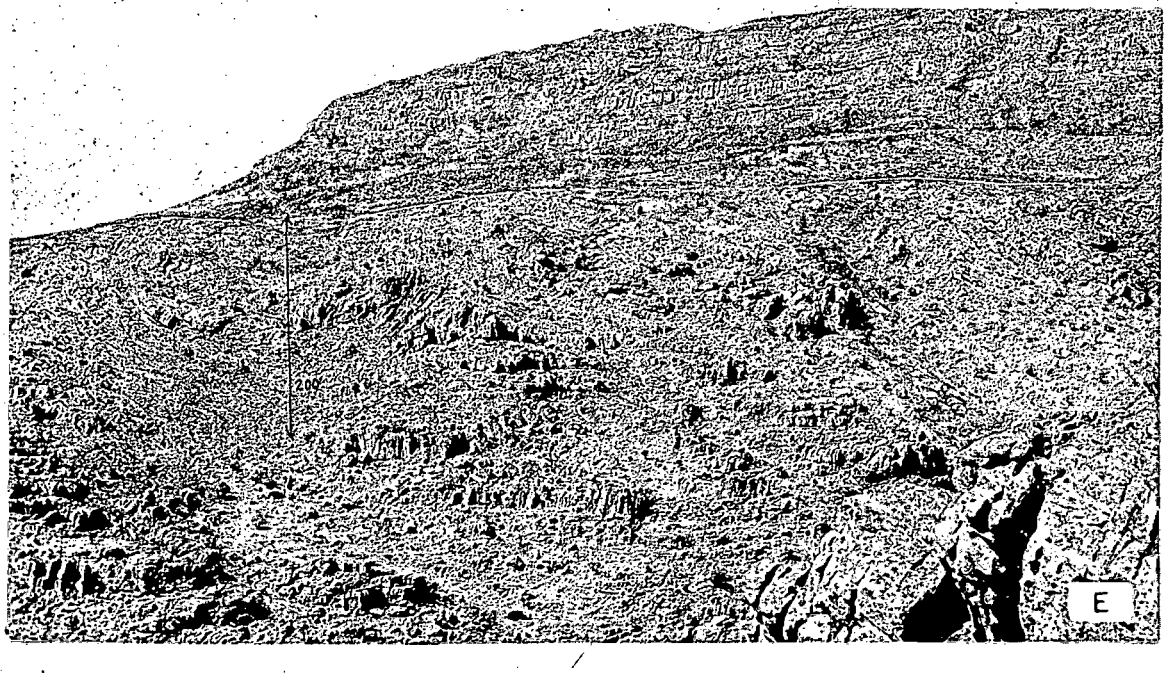

FIGURE 1

(compiled from Rust, 1967; figs. 99 & 112)

The broken lines show the variation in Fold Zone thickness with respect to the basin axis

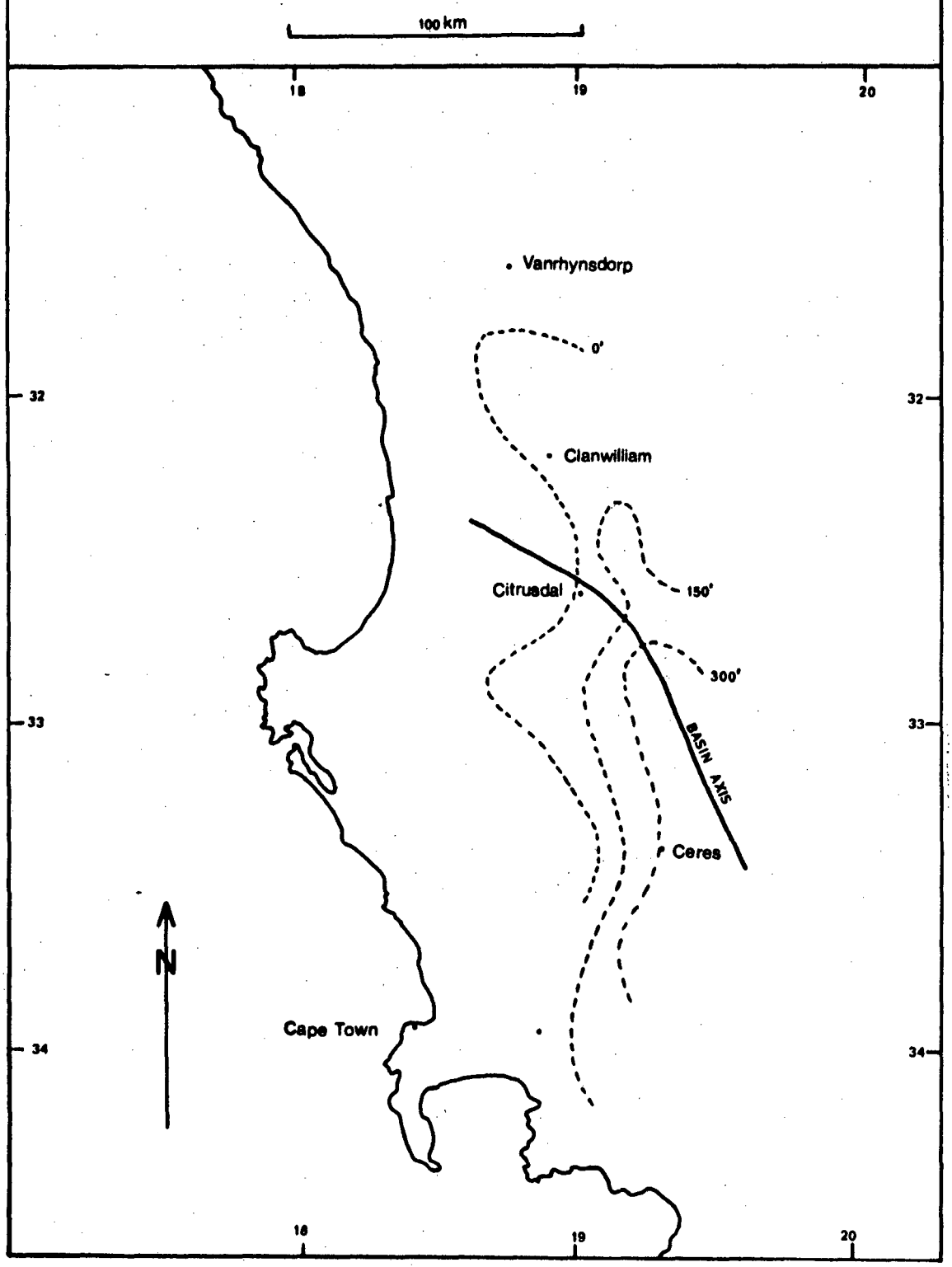

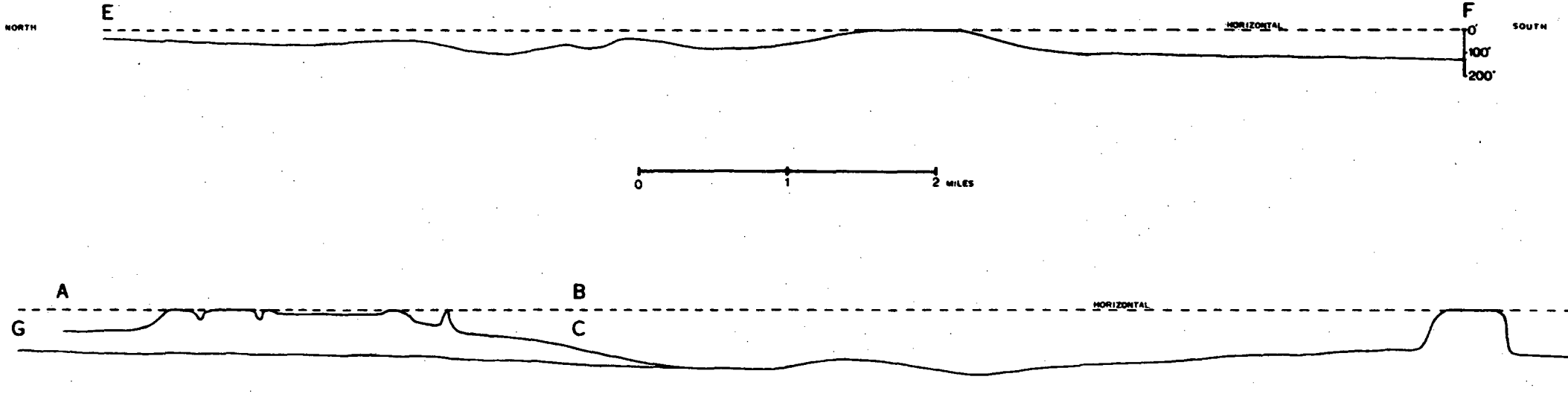

The lower limit of the Fold Zone is shown relative to the horizontal which represents the upper boundary. The section lines are given on Maps 4 & 5

FIGURE 2

FIGURES

3

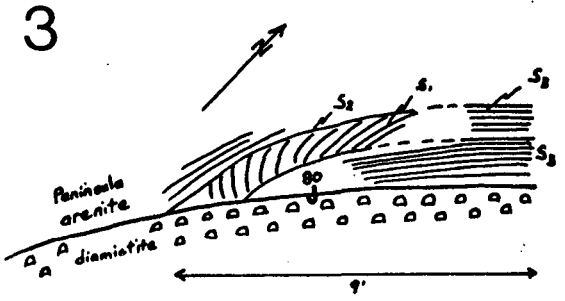

4

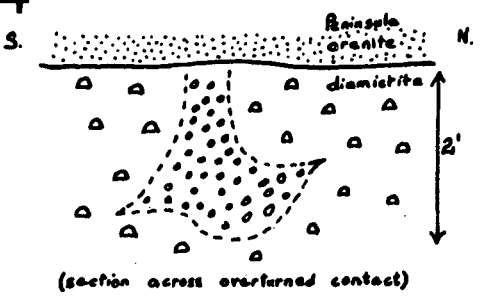

(section across overturned contact)

5

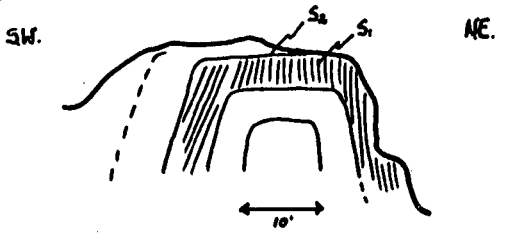

6

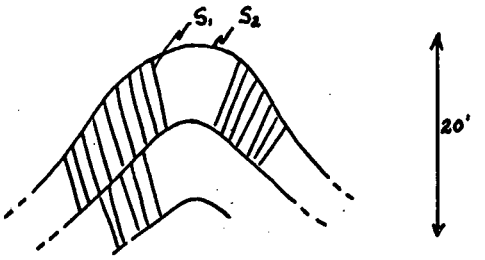

7

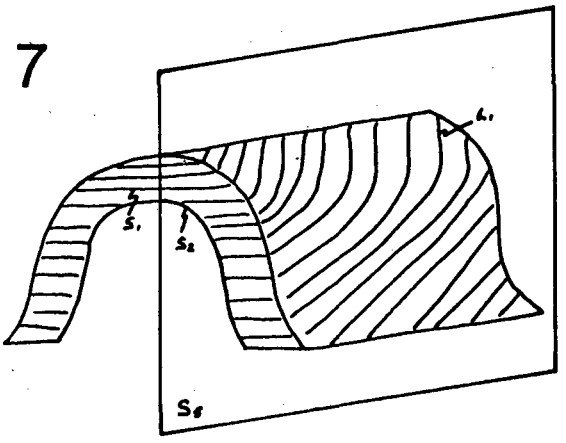

8

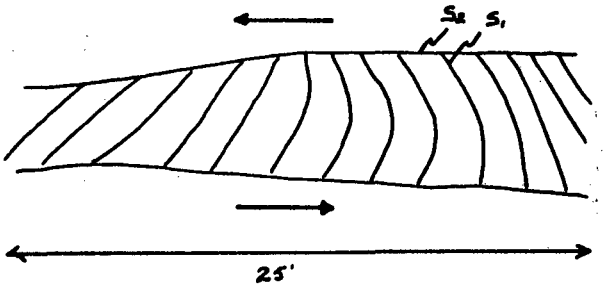

9

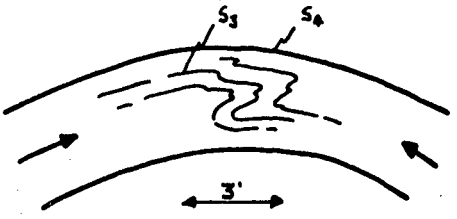

10

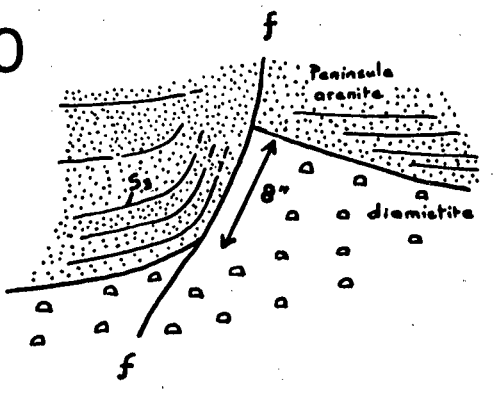

(section across overturned contact)

SECTION EFABCD, MAP 3

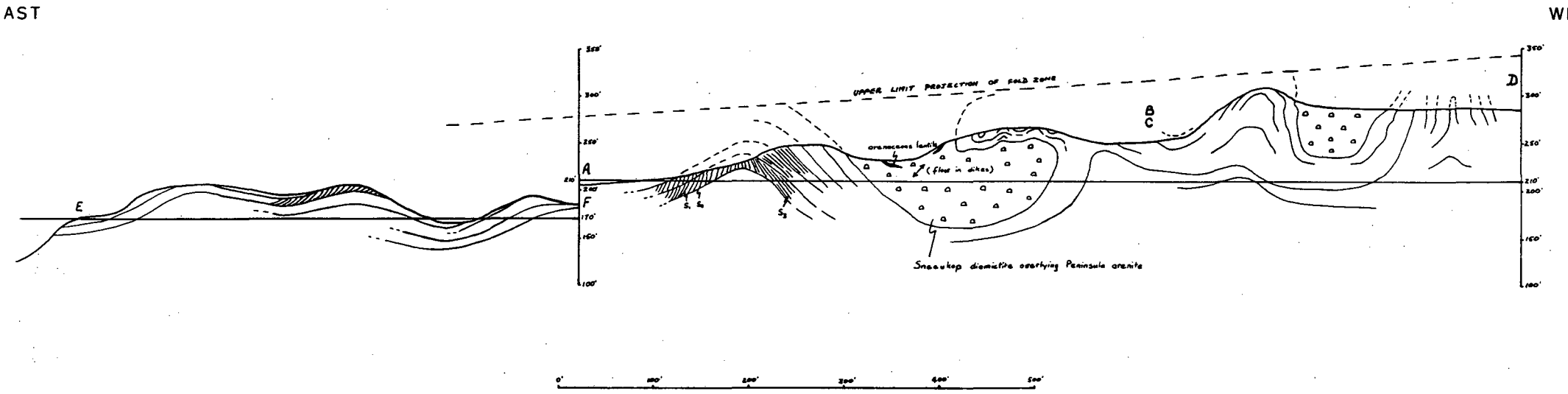

FIGURE 11

12

SECTION NO. MAP 3

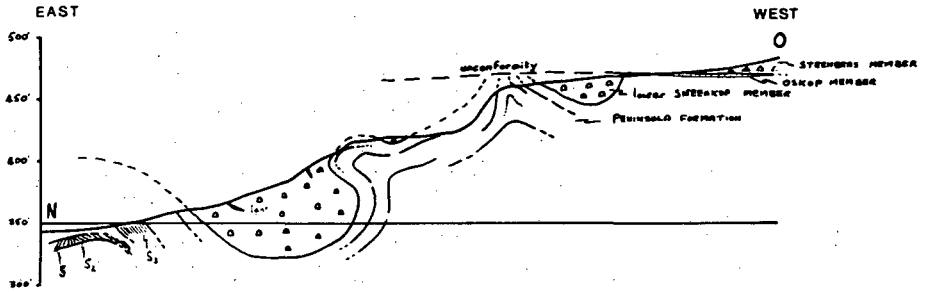

13

SECTION PQ. MAP 3

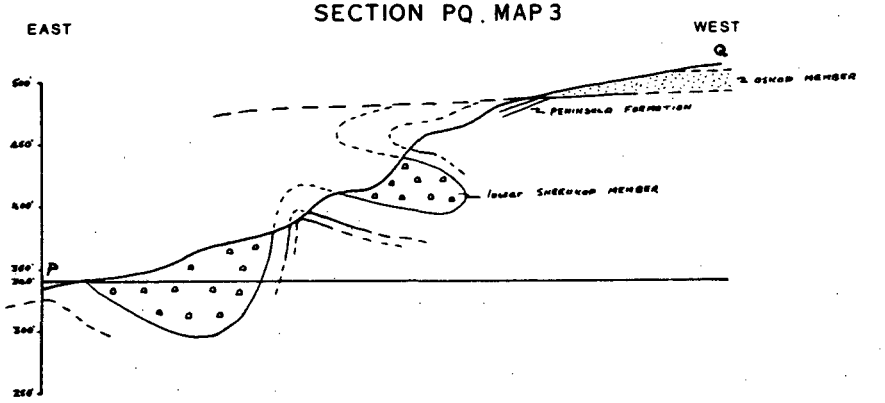

14

SECTION RST. MAP 3

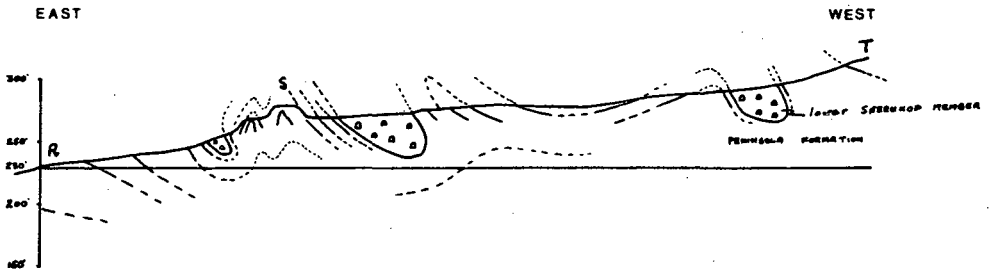

FIGURES 12,13&14

SECTION JJKLM. MAP 3

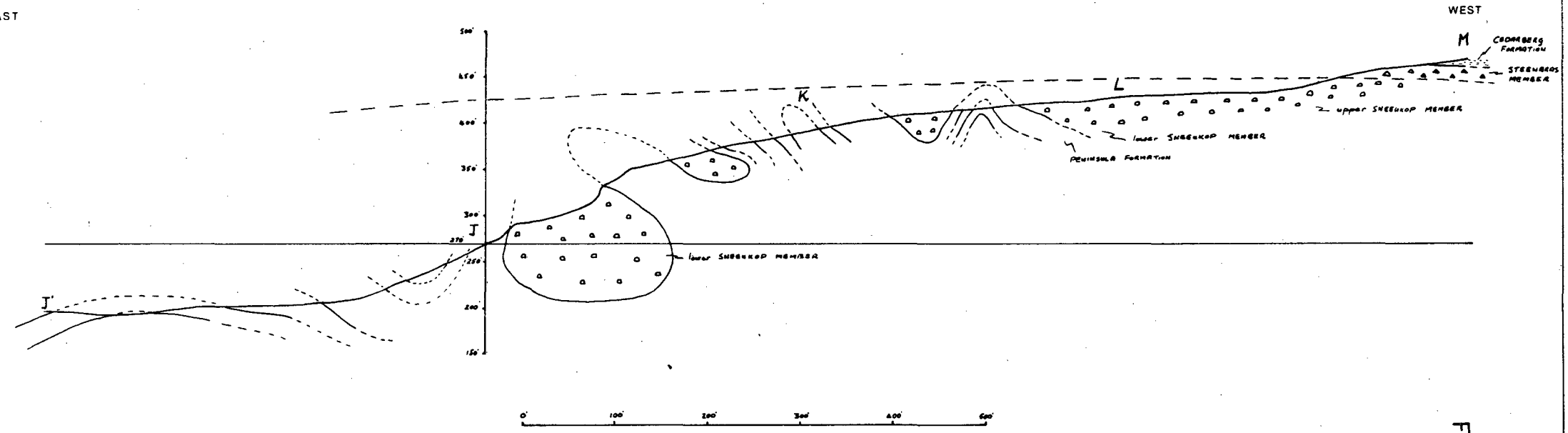

FIGURE 15

FIGURES

16

17

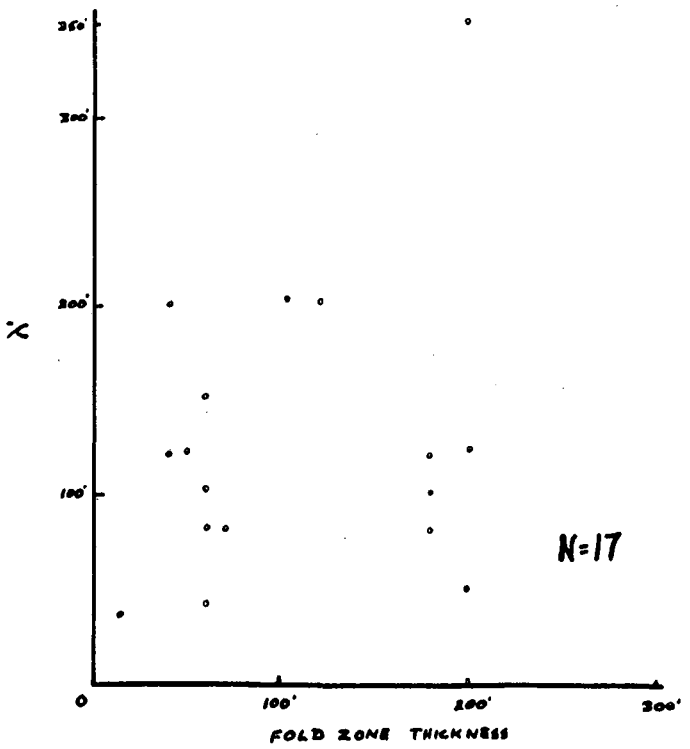

18

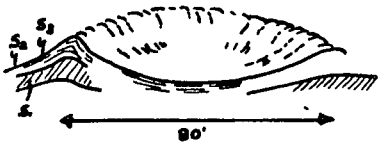

19

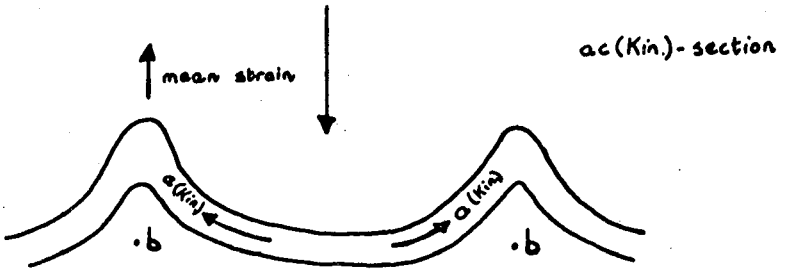

20

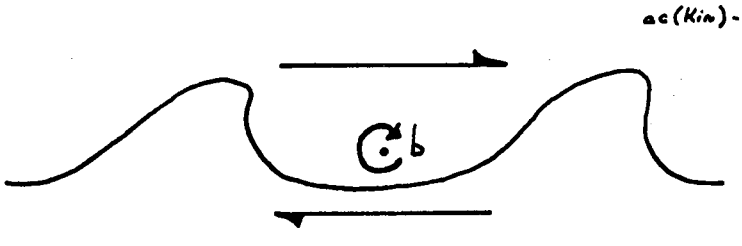

DIAGRAMS

1. Diagrams 1 - 16:

   (a) The block diagrams illustrate the three-dimensional fabric pattern of quartz grains.

   (b) The sample positions are indicated on Map 3 by the diagram number.

   (c) The modal vectors as inferred from the relevant compass diagrams (co.dgms.) are depicted on each face of maximum fabric contrast:

Primary modal vector

Secondary modal vector

Random distribution

   (d) All azimuthal notations refer to true north i.e.

      (i) the geographic attitude of the main bounding surface; 12345 means that the surface dips 45° towards the right hand side when looking in the direction 123°,

      (ii) the zero position of the orientation circle on the main bounding surface is referred to true north either by a strike or dip direction or by the projection there-on of true north,

      (iii) where the direction of a (Sed.) is indicated, it has been corrected for tilt if necessary.

   (e) Lines on planes perpendicular to the main bounding surface and parallel to it are defined by the zero position (000).

2. Diagrams 17 - 28 :

   (a) Dgms. 27 & 28 are on Maps 4 & 5.

   (b) All stereographic plots are in the lower hemisphere.

   (c) The localities are indicated on Map 3 by the diagram number.

DIAGRAMS

The preferred orientation of quartz grains

1

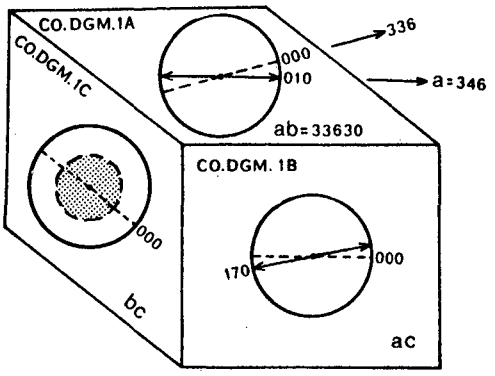

arenite lentil, lower Sneeukop Member (De Trap)

2

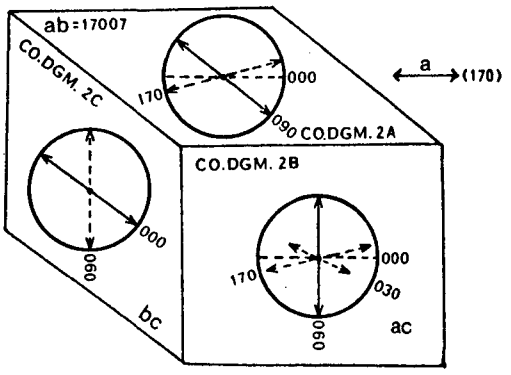

arenite lentil, lower Sneeukop Member (De Trap)

3

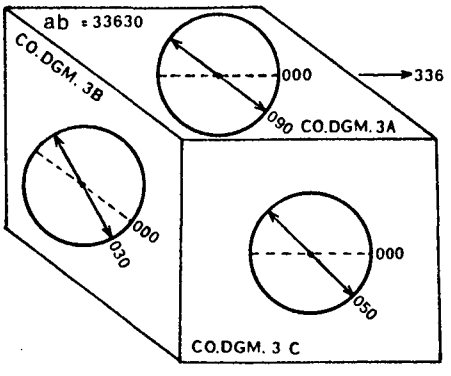

diamictite, lower Sneeukop Member (De Trap)

4

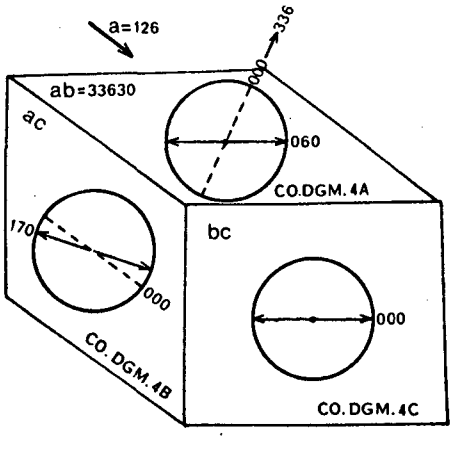

diamictite, lower Sneeukop Member (De Trap)

DIAGRAMS

The preferred orientation of quartz grains

5

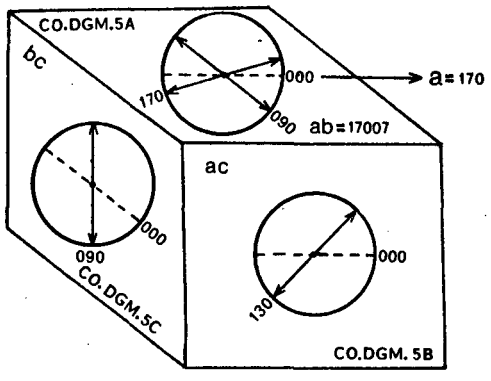

diamictite, lower Sneeukop Member (De Trap)

6

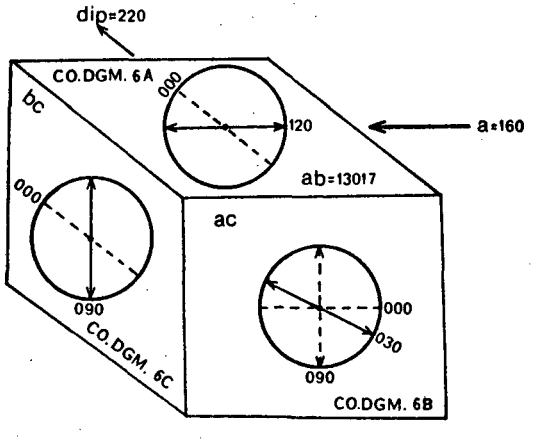

diamictite, lower Sneeukop Member (De Bailie)

7

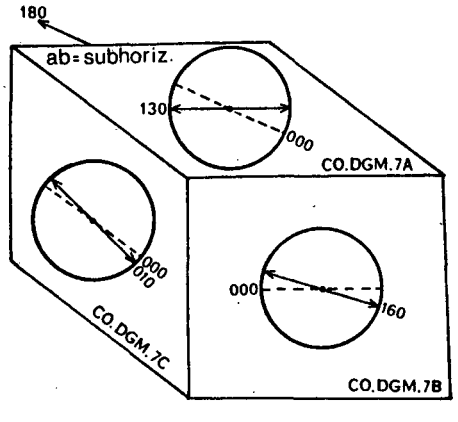

diamictite, upper Sneeukop Member (De Trap)

8

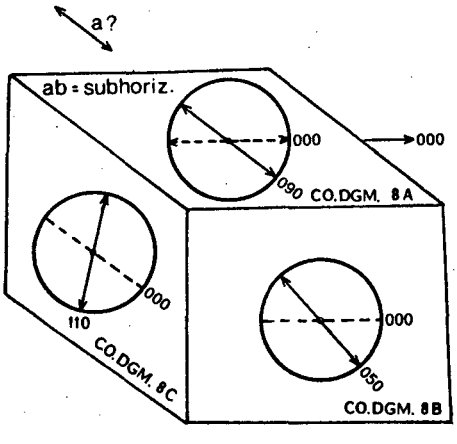

diamictite, upper Sneeukop Member (De Trap)

DIAGRAMS

The preferred orientation of quartz grains

9

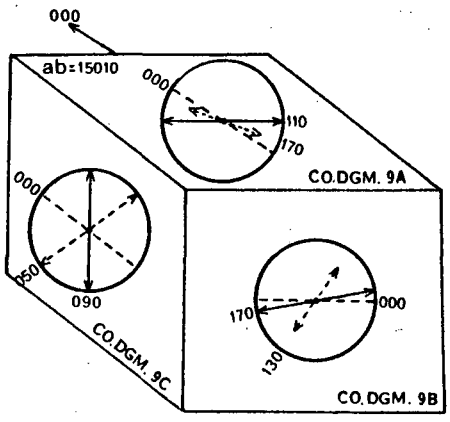

diamictite, upper Sneeukop Member (De Bailie)

10

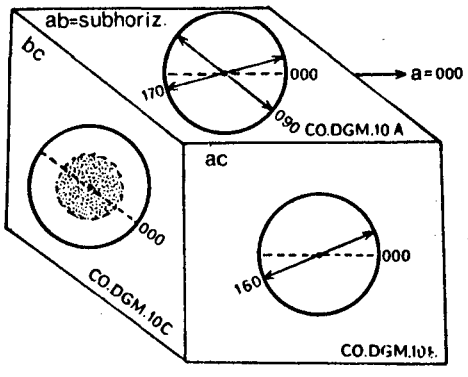

diamictite, Steenbras Member (De Trap)

11

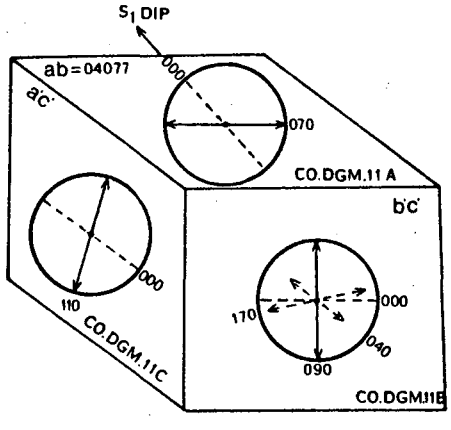

deformed arenaceous cross-lamina, Peninsula Formation (De Trap)

12

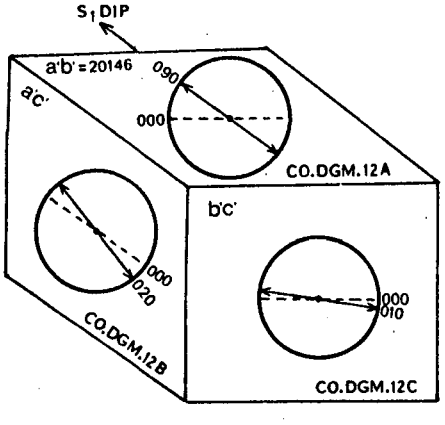

deformed arenaceous cross-lamina, Peninsula Formation (De Trap)

DIAGRAMS

The preferred orientation of quartz grains

13

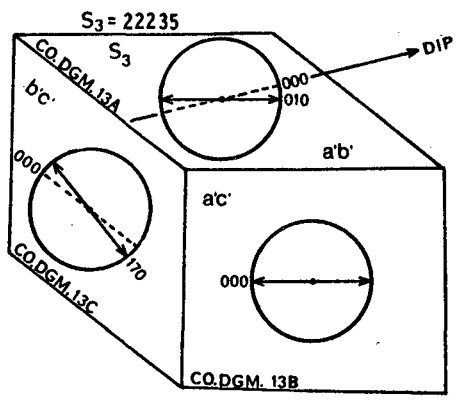

S3-band, Peninsula Formation (De Trap)

14

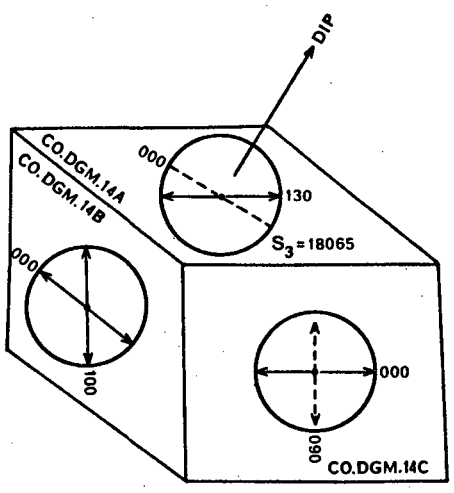

S3-band, lower Sneeukop diamictite (De Trap)

DIAGRAMS

(Preferred orientation of quartz grains in sedimentary dikes, lower Sneeukop Member - De Trap)

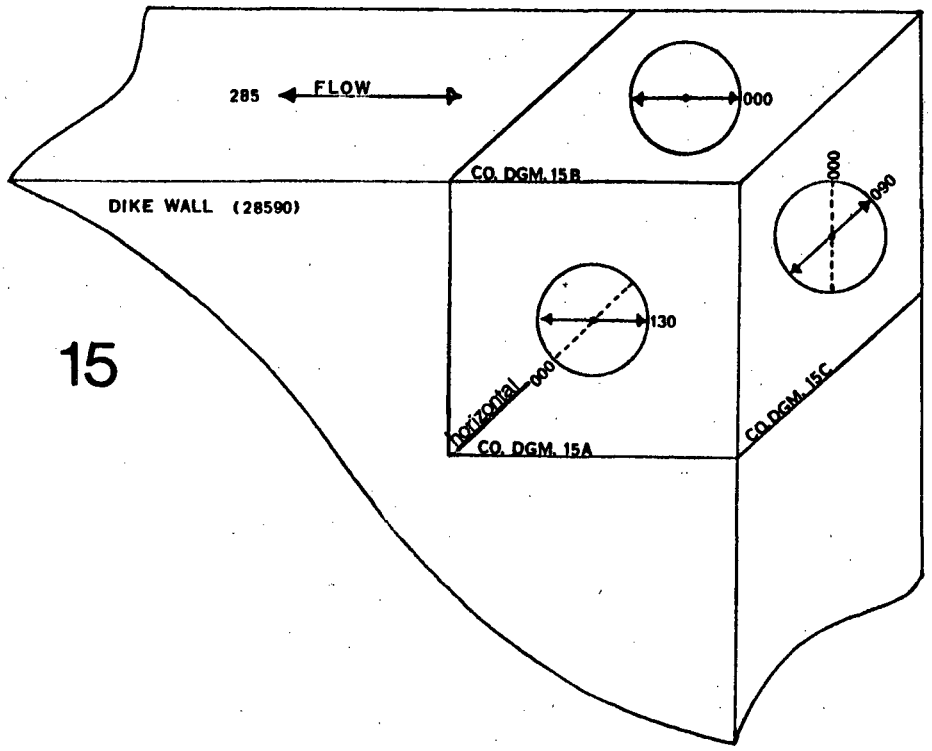

15

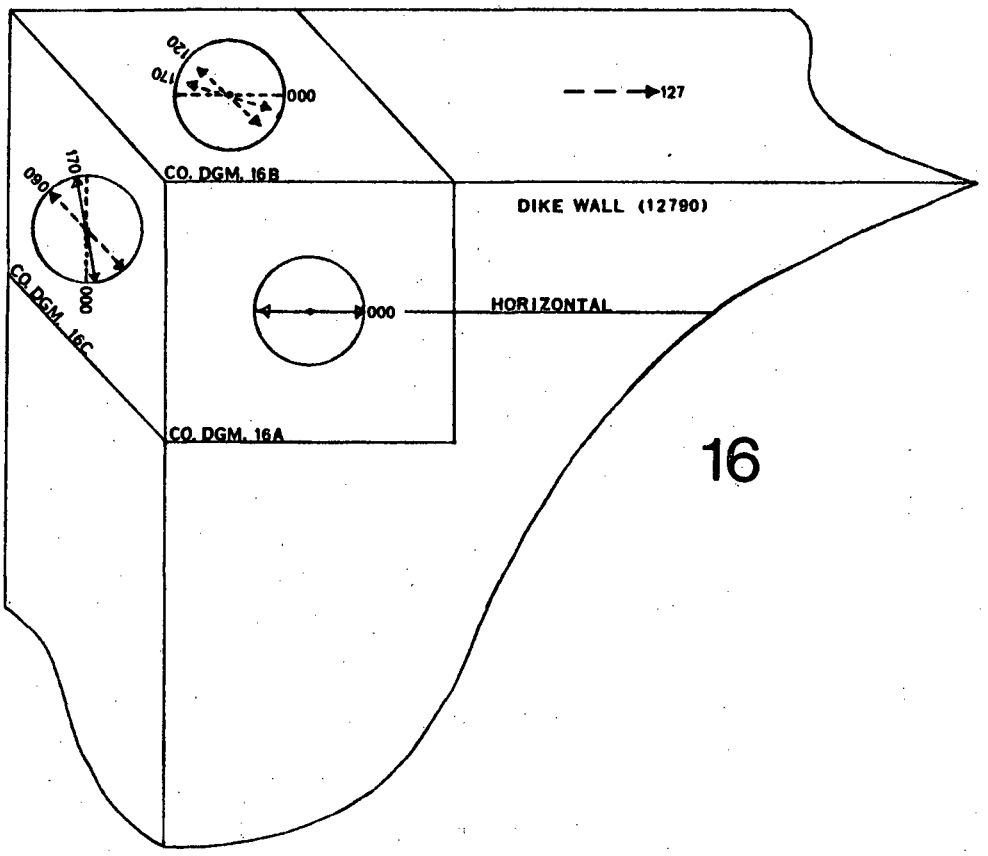

16

DIAGRAMS

17

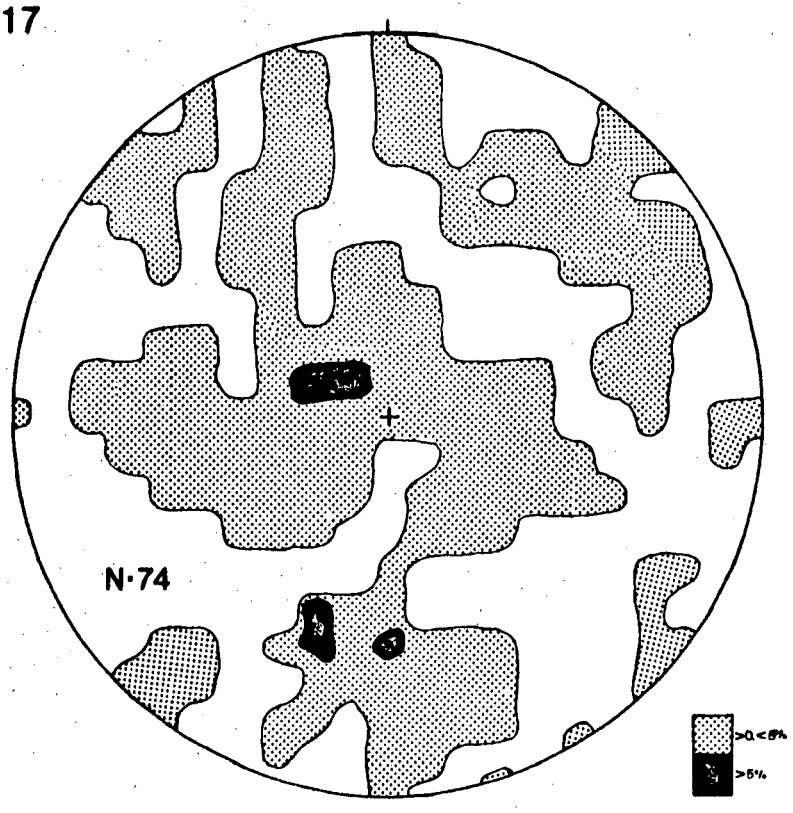

Poles to rudaceous clasts in the lower Sneeukop Member showing a random distribution (De Trap).

18

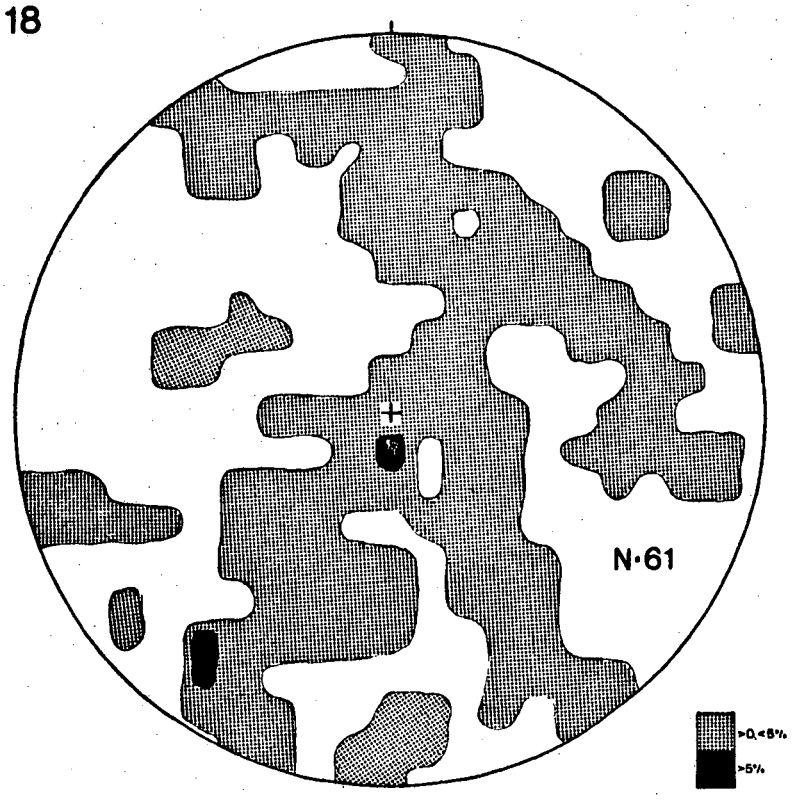

Poles to rudaceous clasts in the lower Sneeukop Member showing a random distribution (De Trap).

19

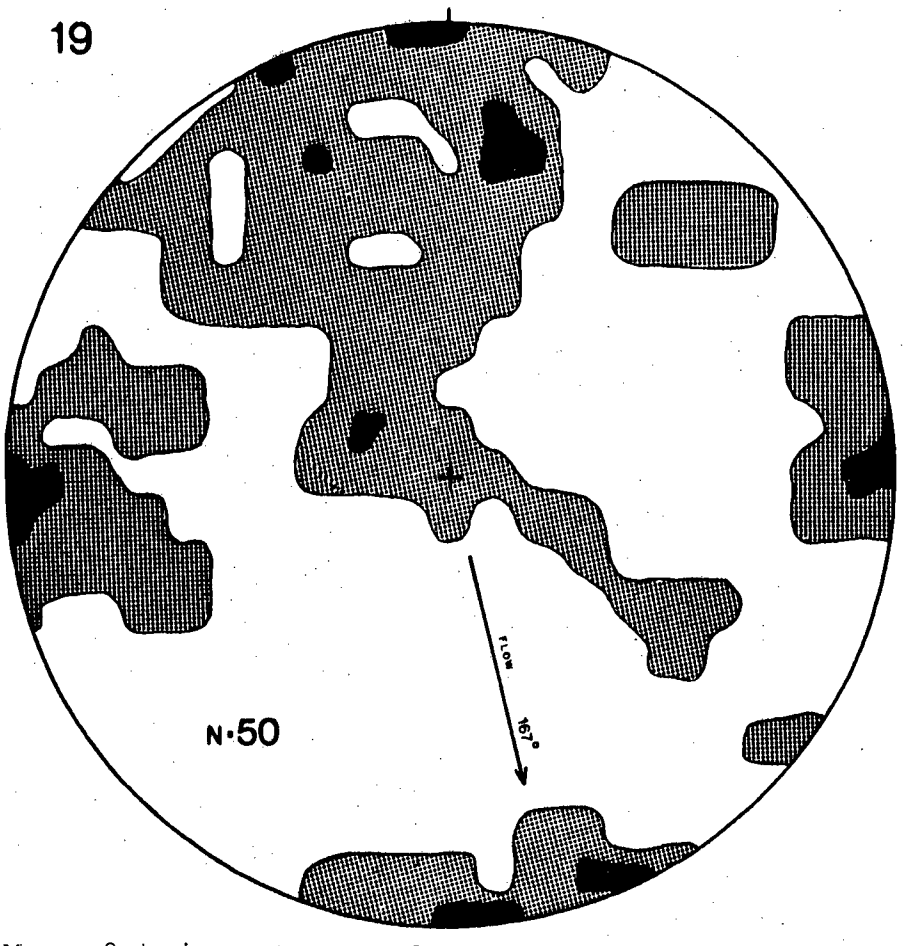

Macrofabric pattern of the upper Sneeukop Member as depicted by nadirs to planar and poles to linear clasts (De Trap). Contours at 0% and 6%.

20

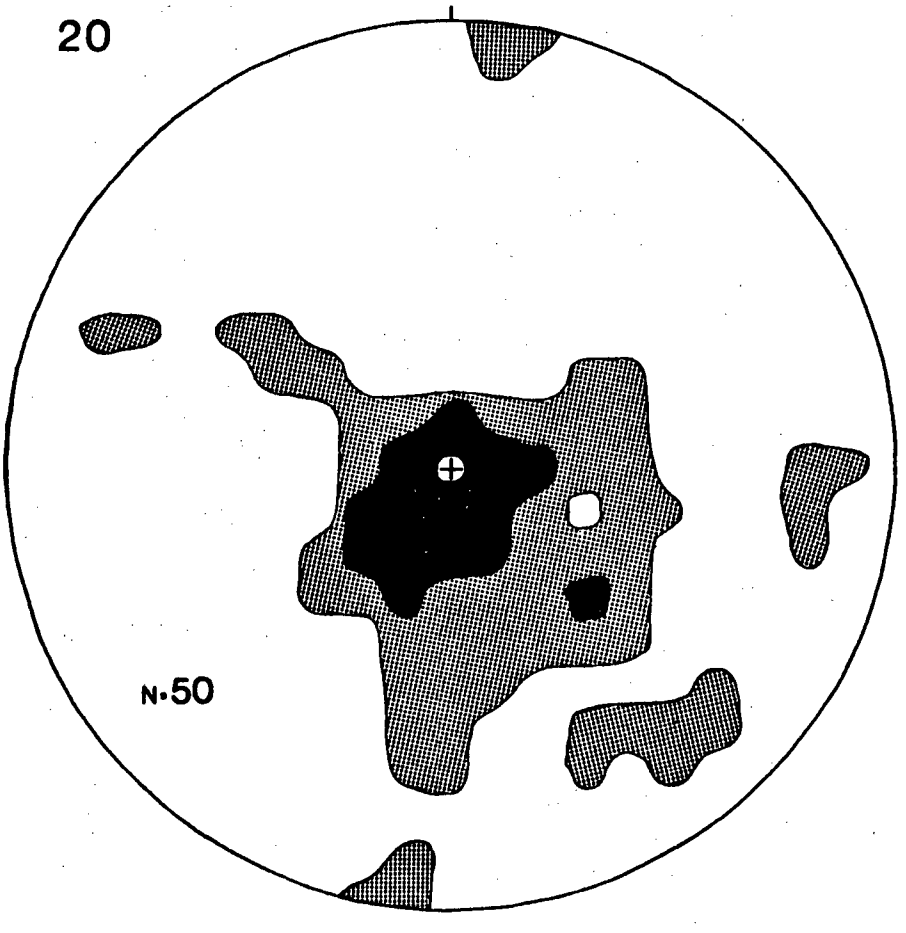

Macrofabric pattern of the upper Sneeukop Member as depicted by poles to clasts (De Trap). Contours at 0% and 6%.

21

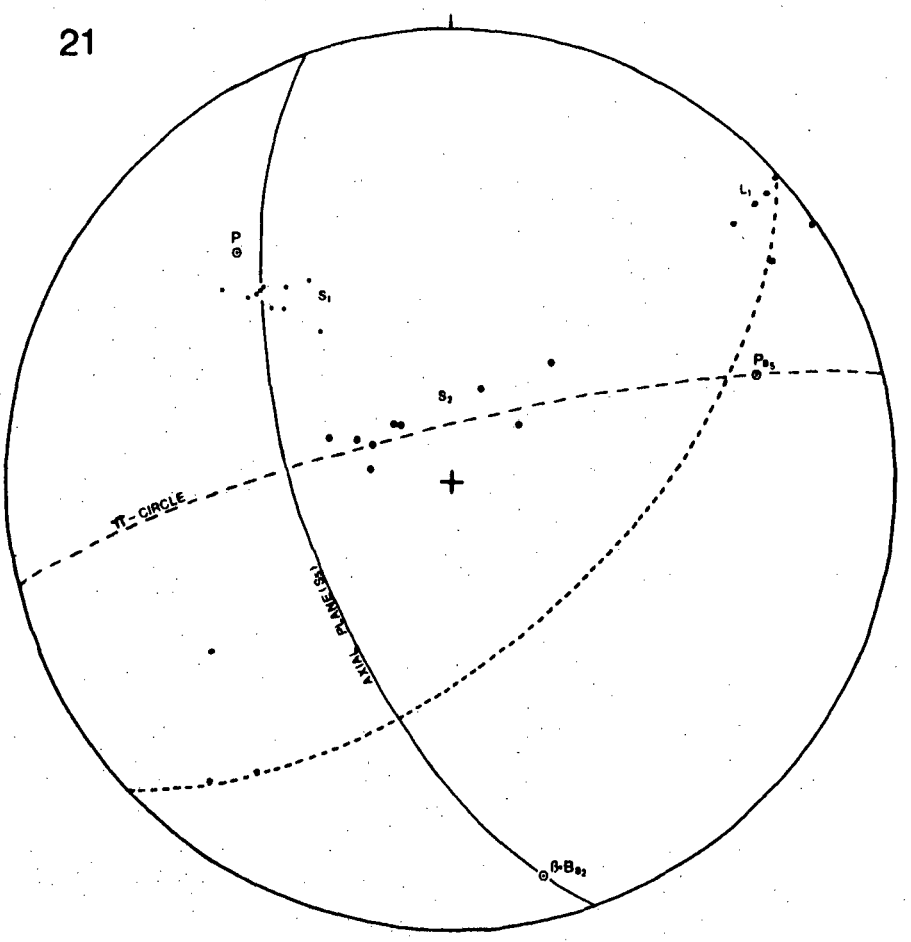

Stereographic compilation of S_1, S_2 and L_1 of an anticline in the lower part of the Fold Zone(De Trap).

22

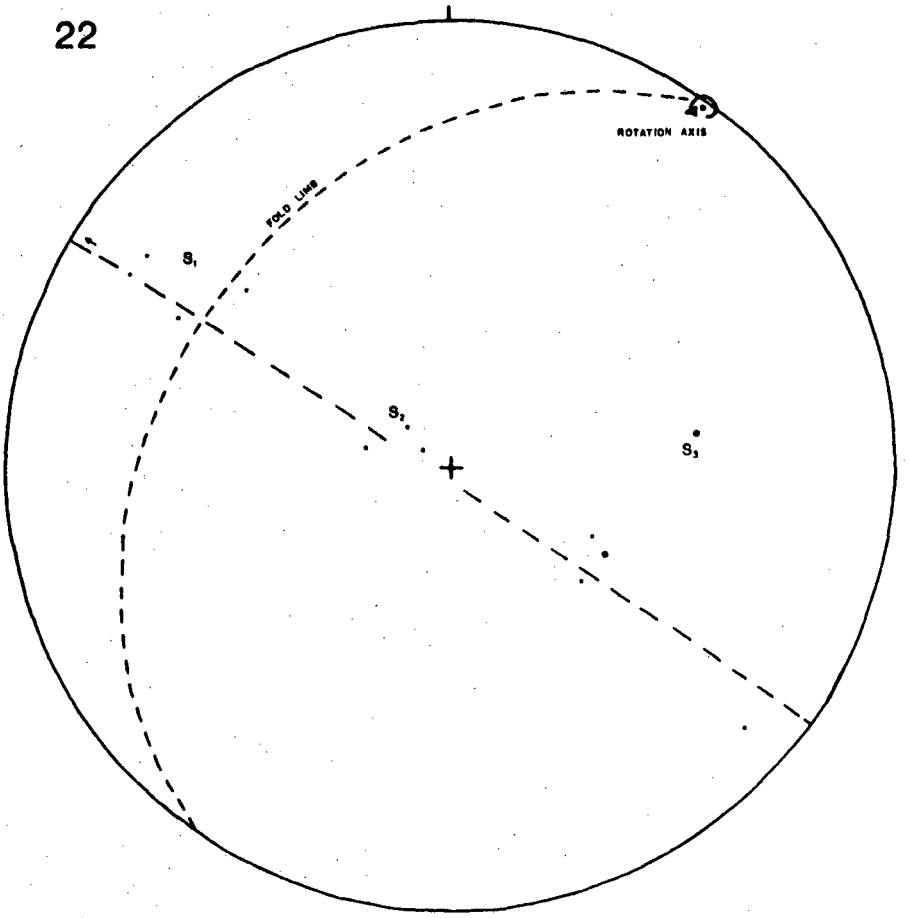

Stereographic representation of the transposition of S_1 to S_3 (De Trap).

23

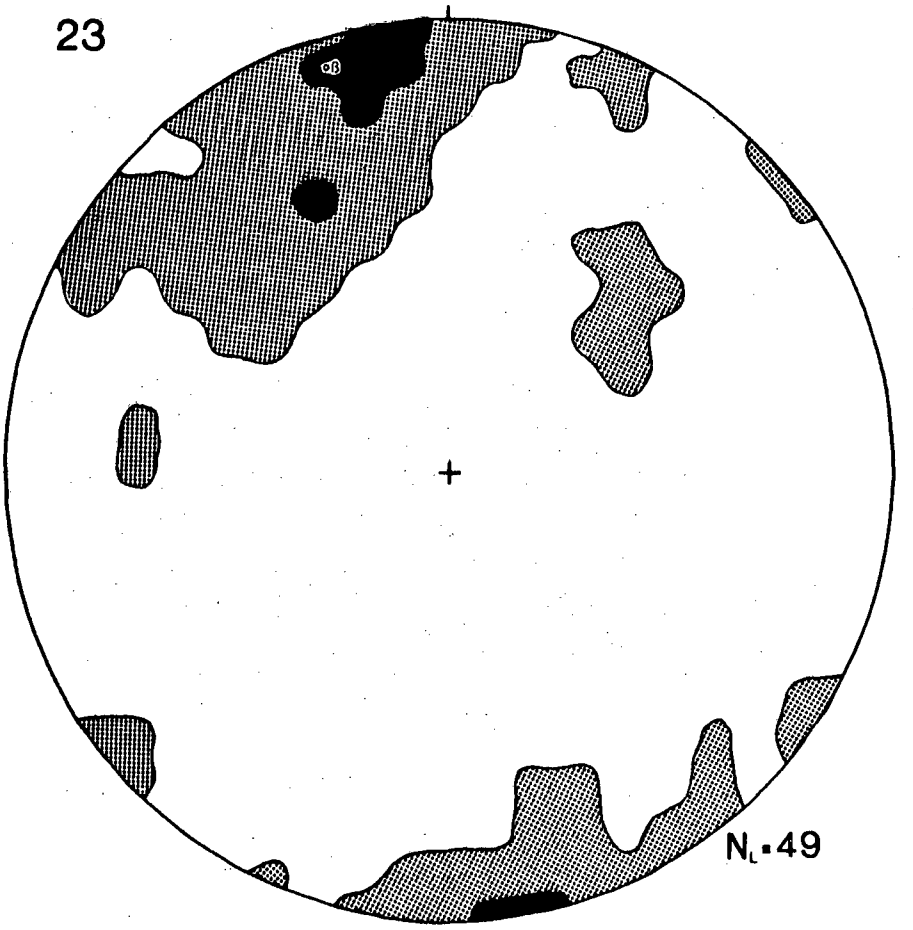

Compilation of linear elements (mesoscopic fold axes and L_2) in domain 3, Map 3 (De Trap). is derived from dgm. 24. Contours at 0% and 10%.

24

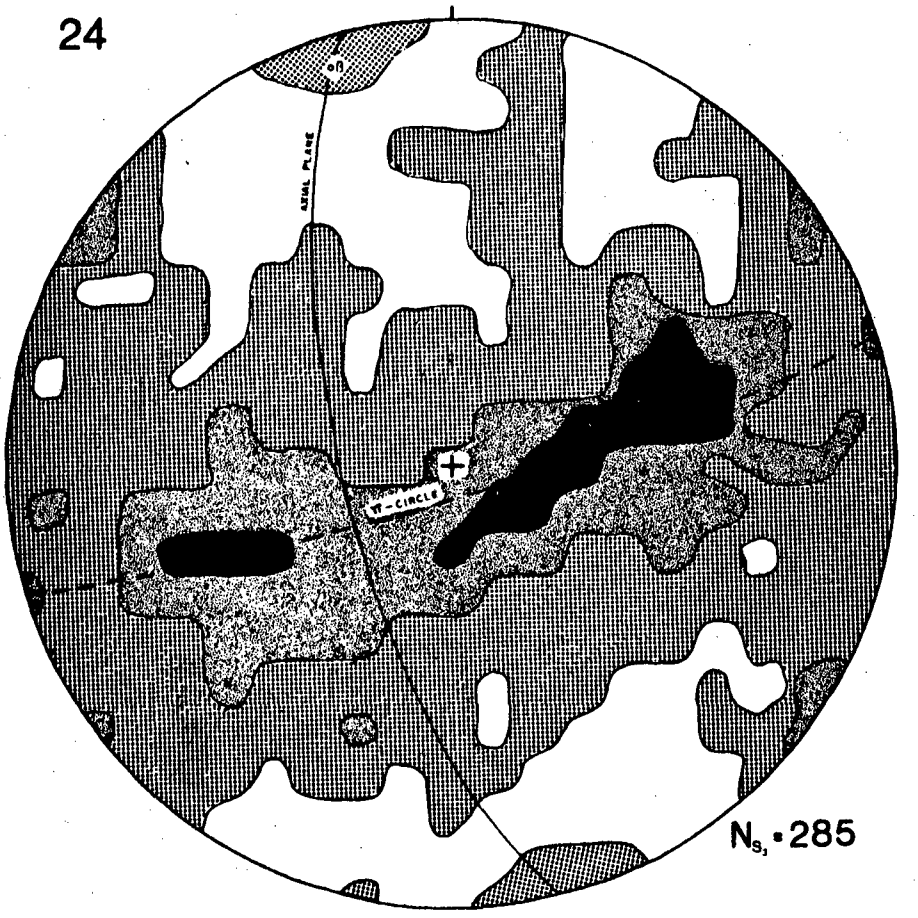

S3-pole diagram, domain 3 (Map 3, De Trap). Contours at 0%, 2% and 4%.

DIAGRAMS

25

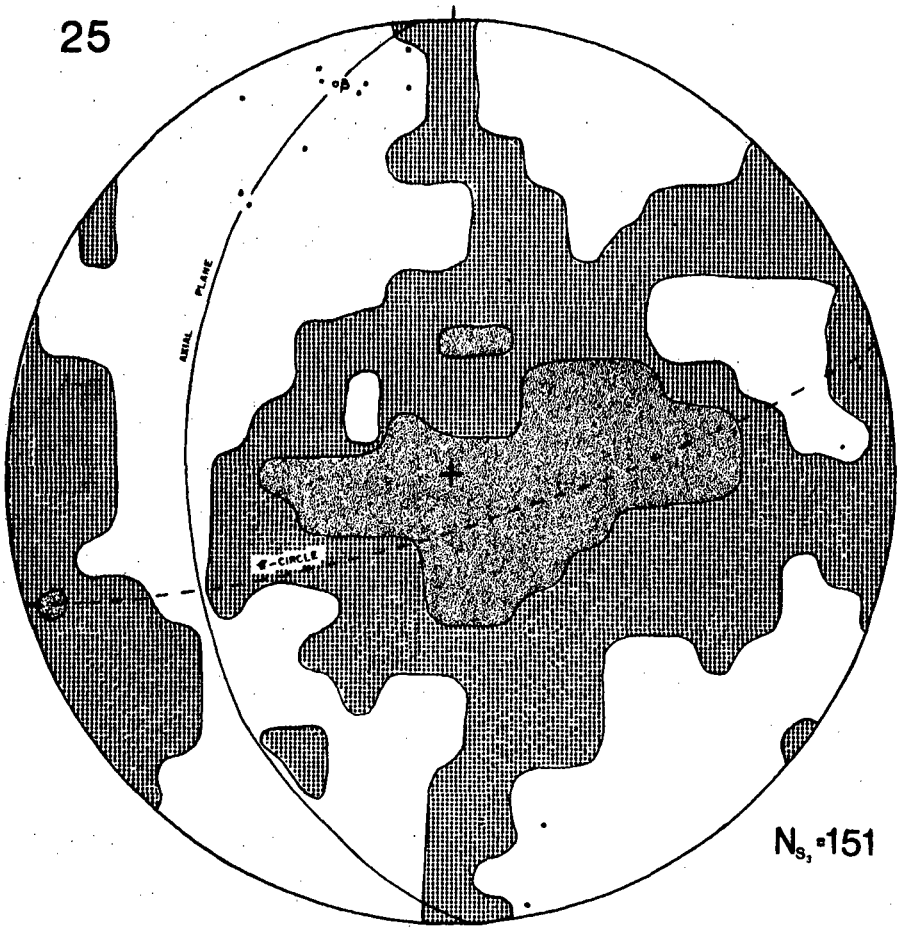

Compilation of subfabrics (S_3-poles, mesoscopic fold axes and L_2), domain 2 (Map 3, De Trap). Contours at 0% and 3%.

26

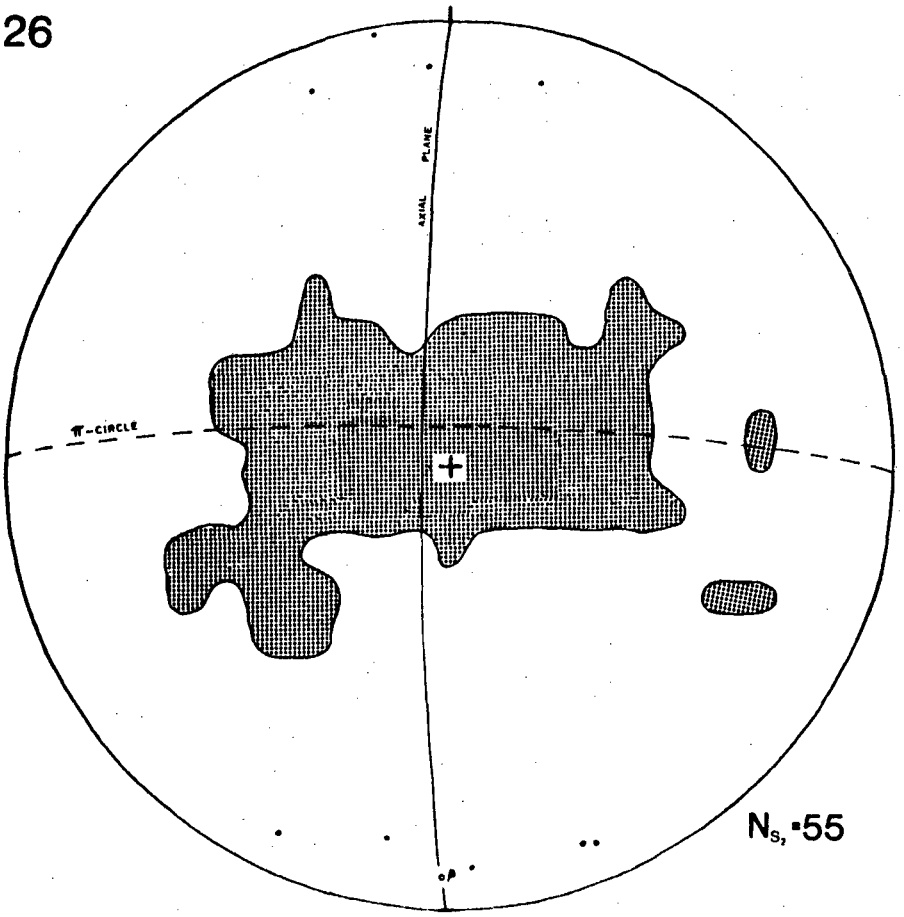

Compilation of subfabrics (S_2-poles and mesoscopic fold axes), domain 1 (Map 3, De Trap). Contour at 0%.

COMPASS DIAGRAMS

(Long axis orientation of quartz grains)

1. The three-dimensional configuration of the compass diagrams (co.dgms.) is depicted by similarly numbered diagrams 1 to 16.

2. Where grain sizes are differentiated, the coarse fraction (A' larger than 1 mm) is represented by co.dgms. D, the fine fraction (A' smaller than 0.4 mm) by co.dgms. E and the composite by co.dgms. A.

3. The proportion measurements per class interval can be read with reference to the broken circle.

4. The orientation data (modulo π) are grouped in 20^{o} classes.

COMPASS DIAGRAMS

(Long axis orientation of quartz grains)

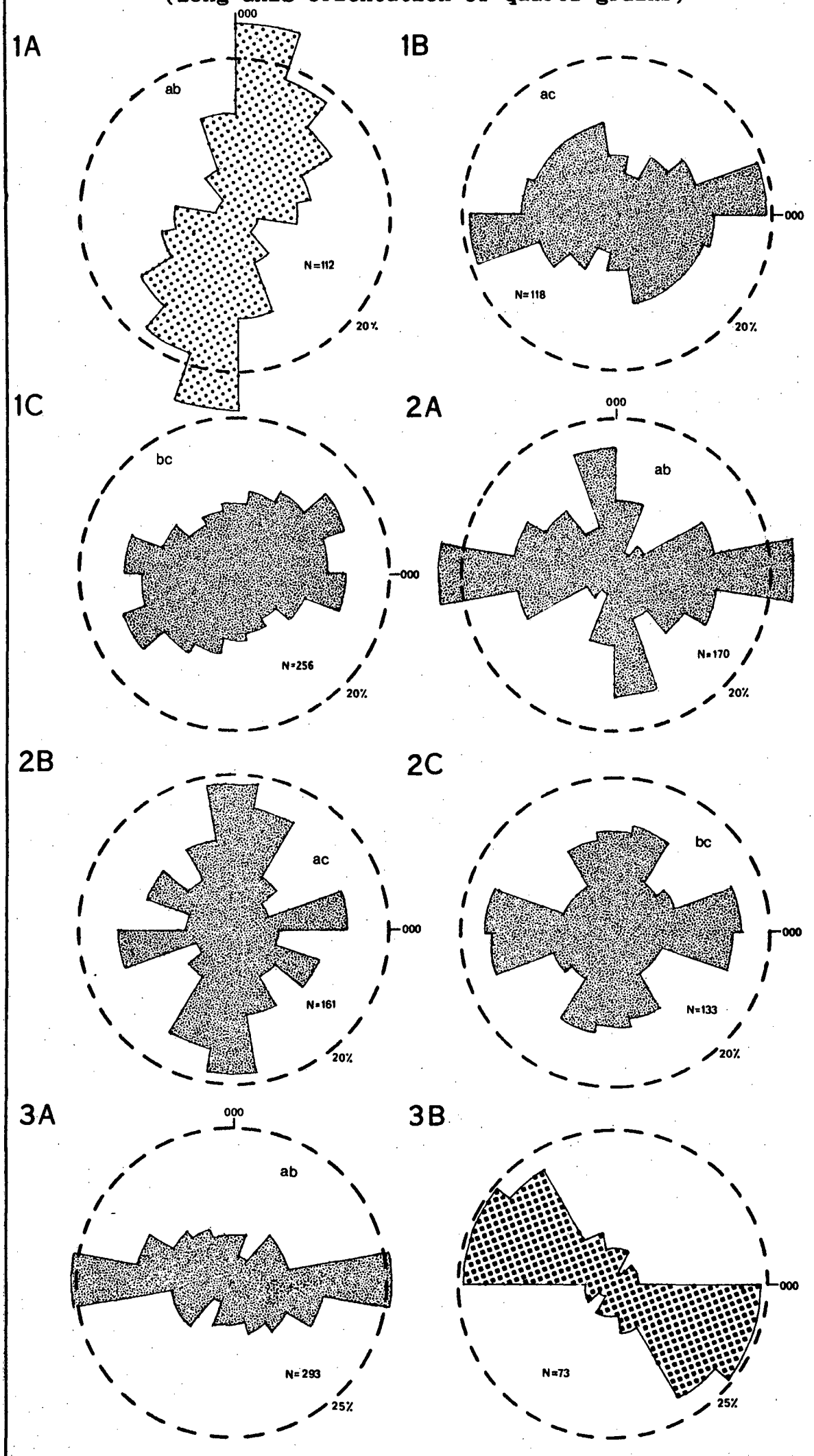

COMPASS DIAGRAMS

(Long axis orientation of quartz grains)

3C

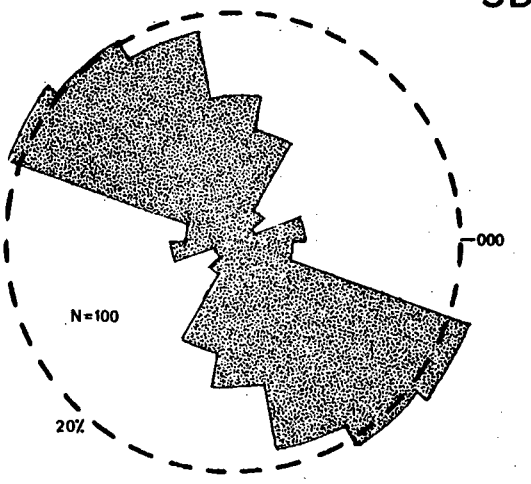

3D

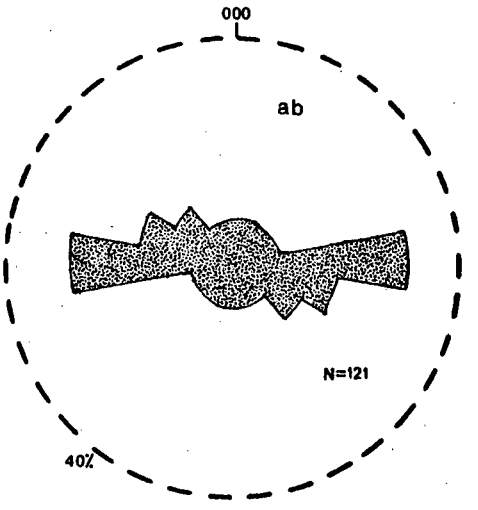

3E

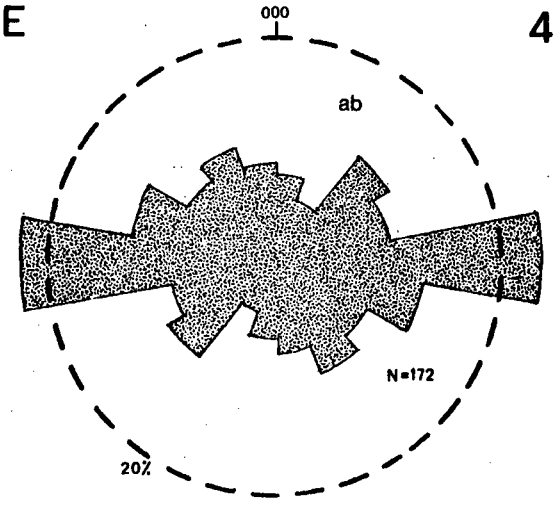

4A

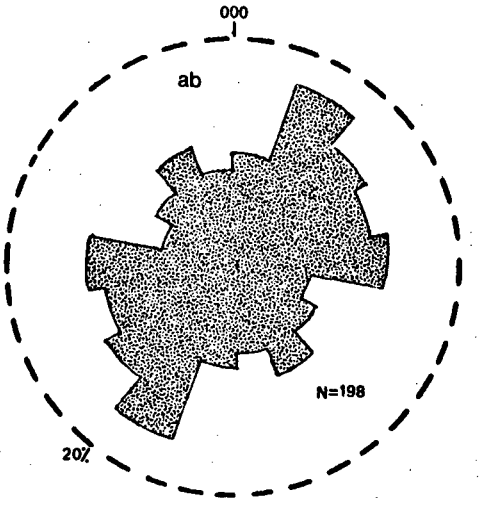

4B

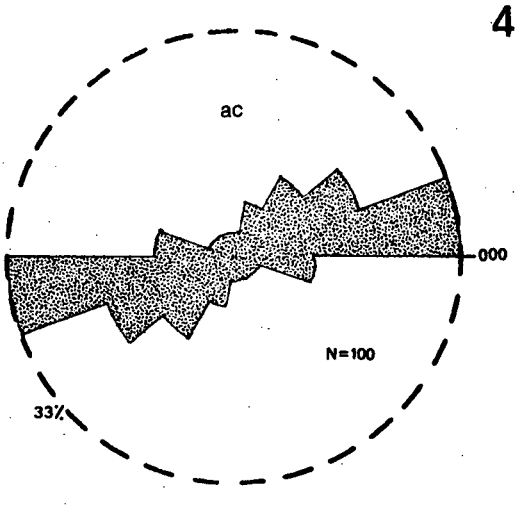

4C

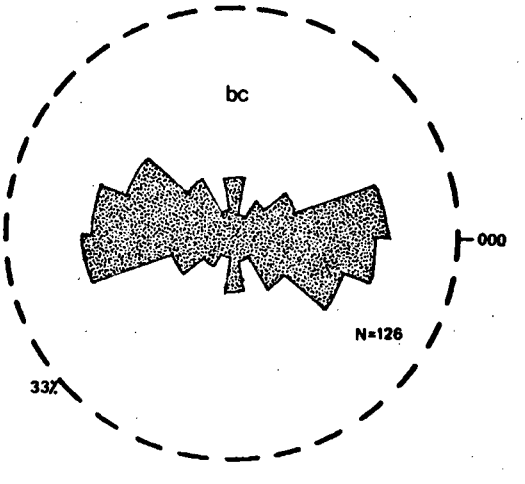

5A

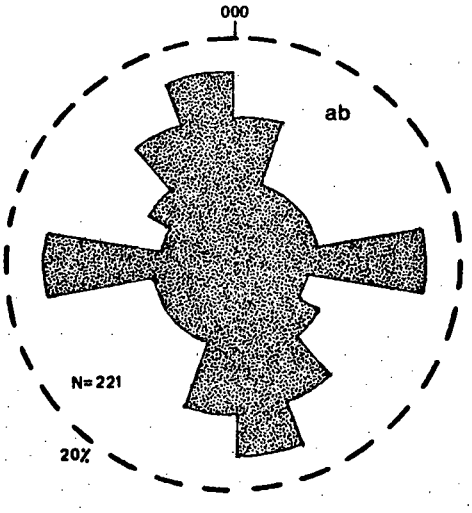

5B

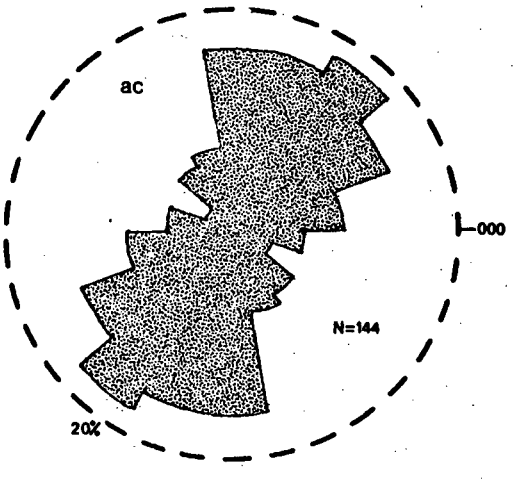

COMPASS DIAGRAMS

(Long axis orientation of quartz grains)

5C

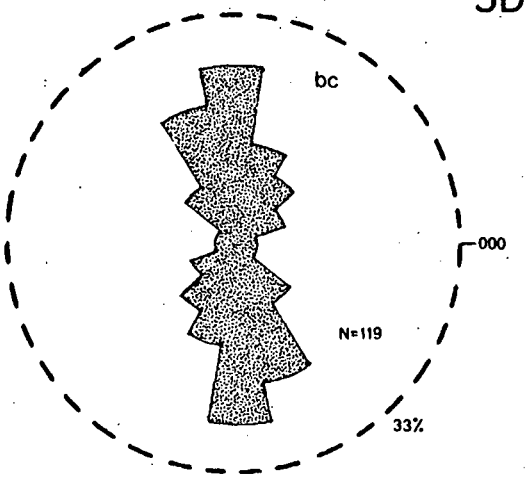

5D

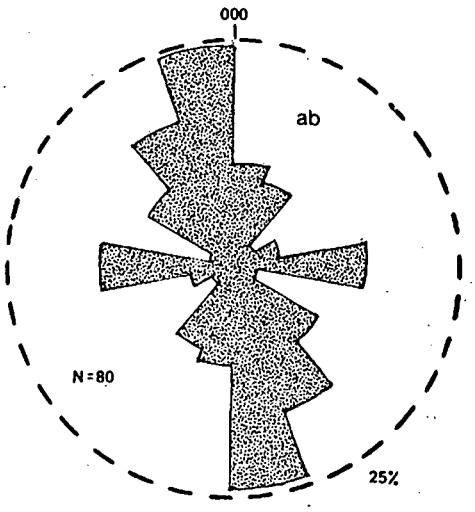

5E

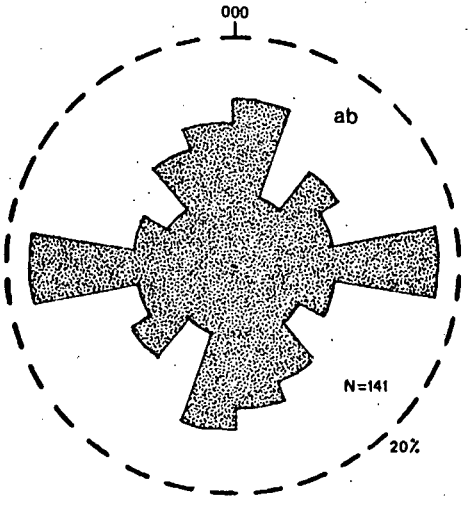

6A

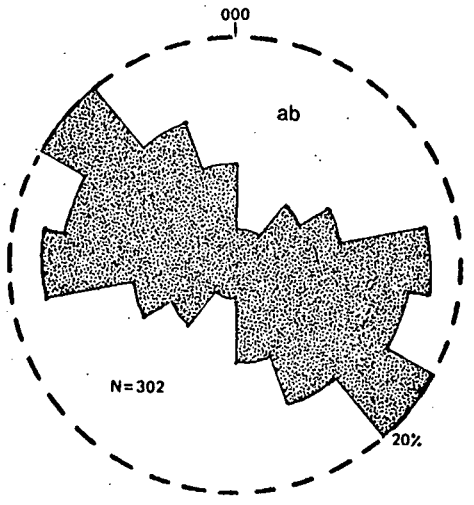

6B

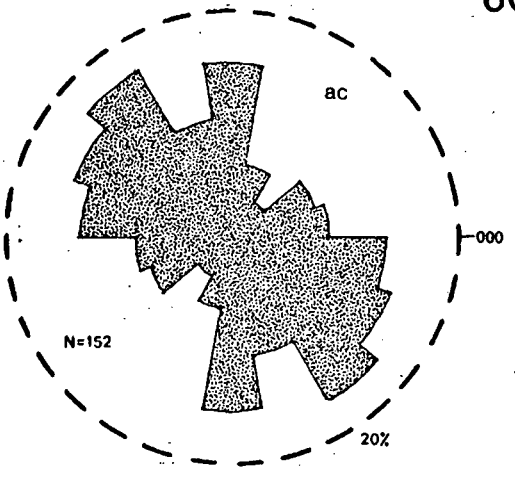

6C

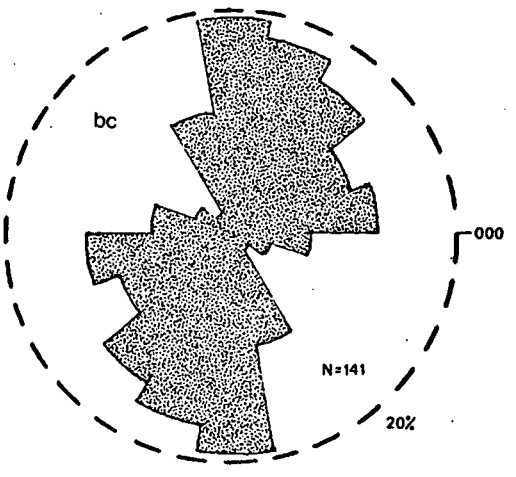

6D

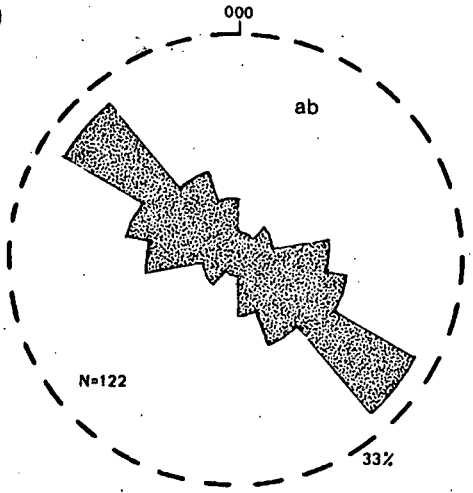

6E

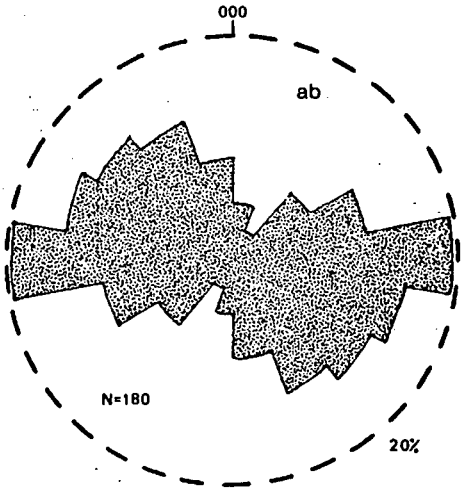

COMPASS DIAGRAMS

(Long axis orientation of quartz grains)

7A

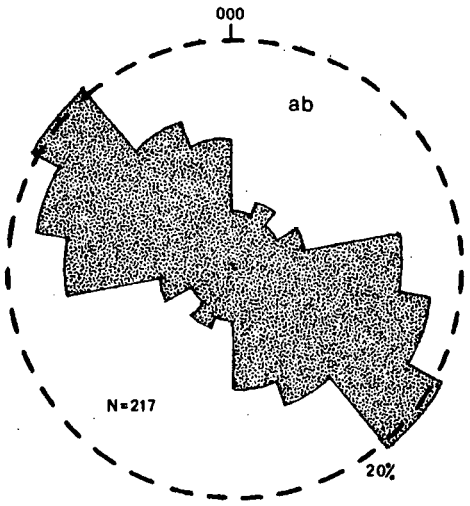

7B

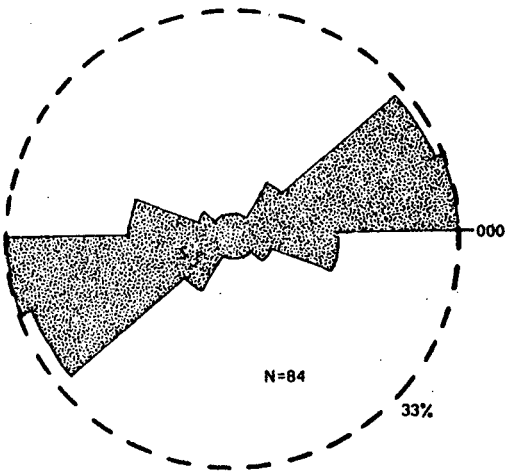

7C

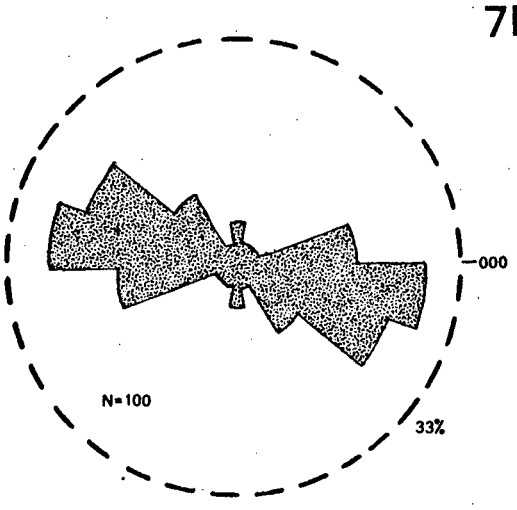

7D

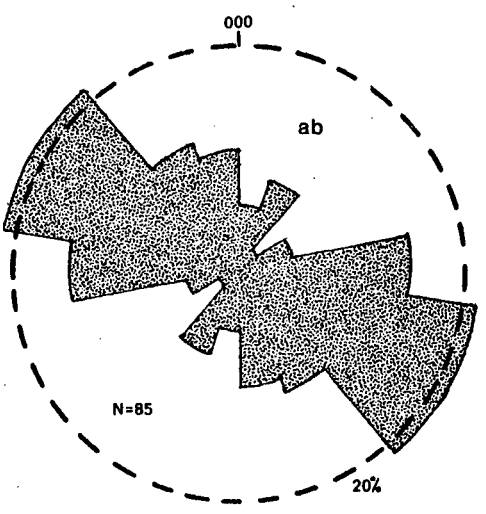

7E

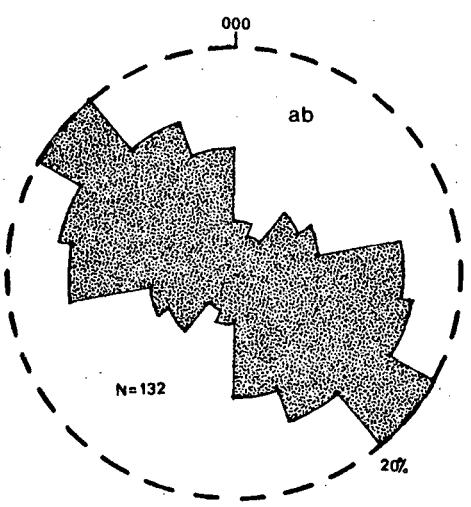

8A

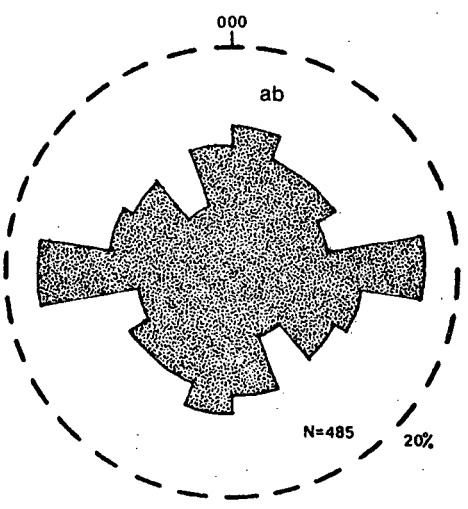

8B

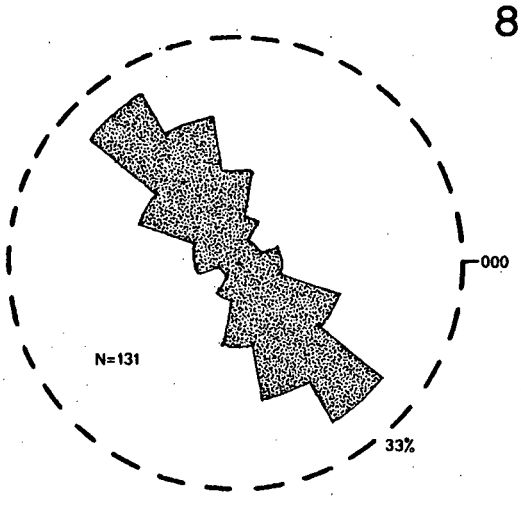

8C

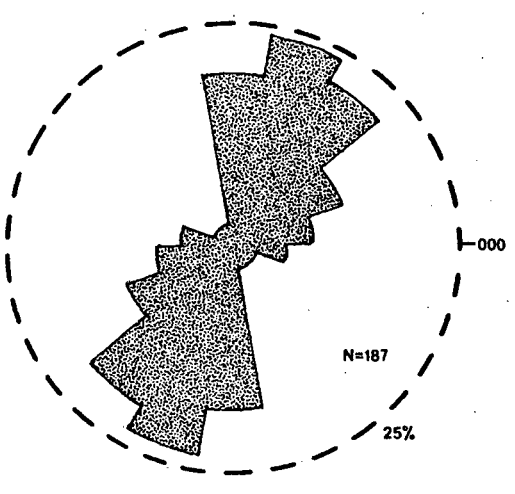

COMPASS DIAGRAMS

(Long axis orientation of quartz grains)

8D

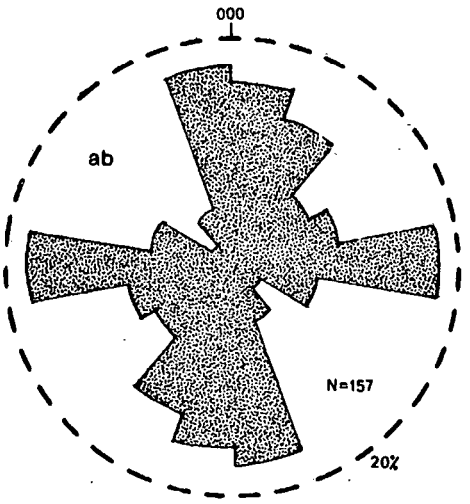

8E

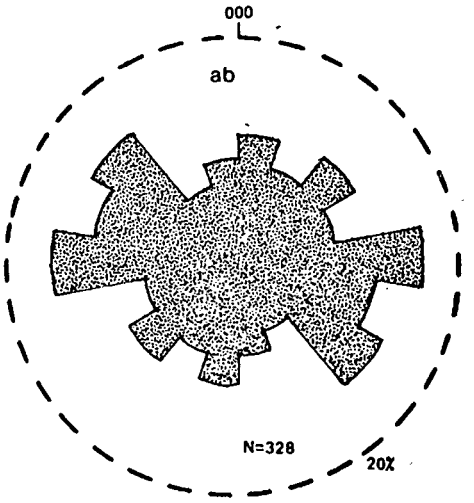

9A

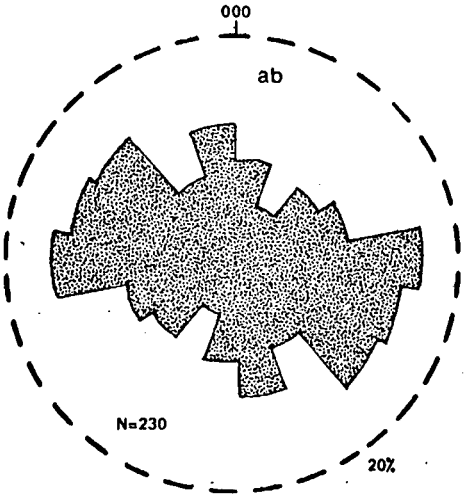

9B

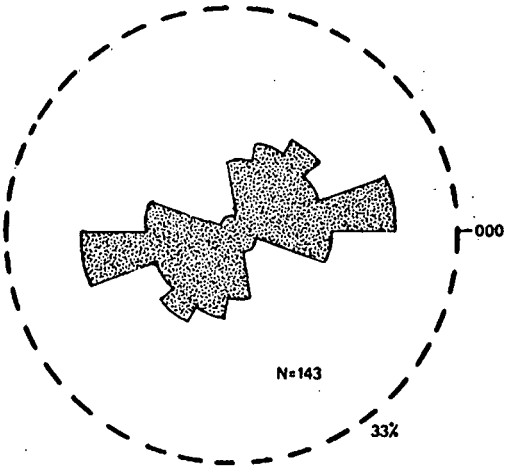

9C

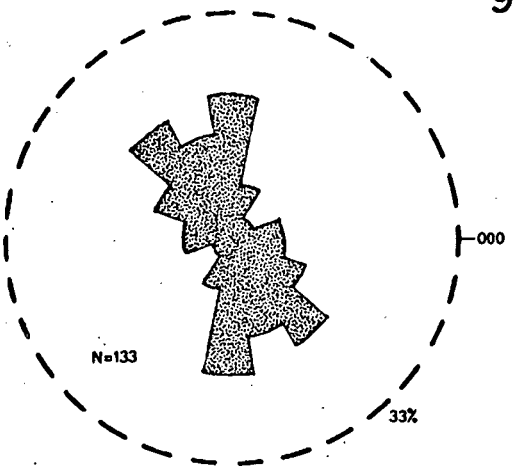

9D

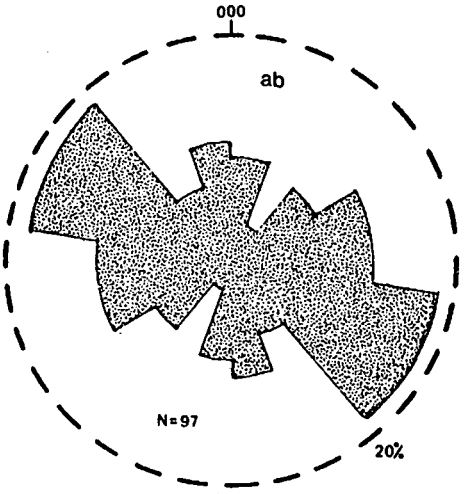

9E

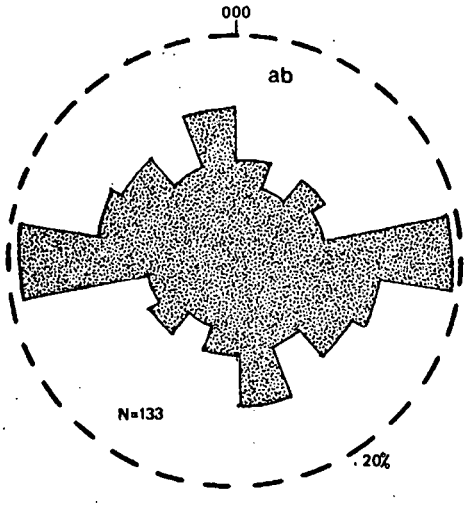

10A

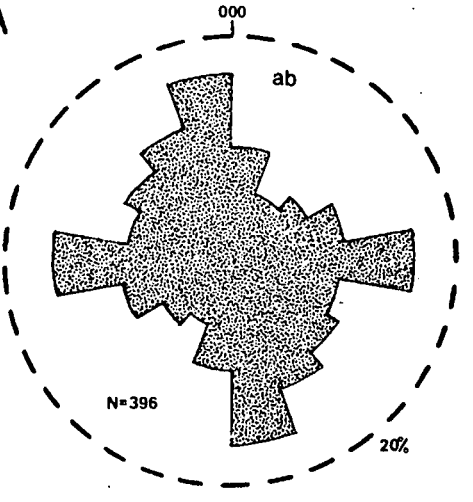

COMPASS DIAGRAMS

(Long axis orientation of quartz grains)

10B

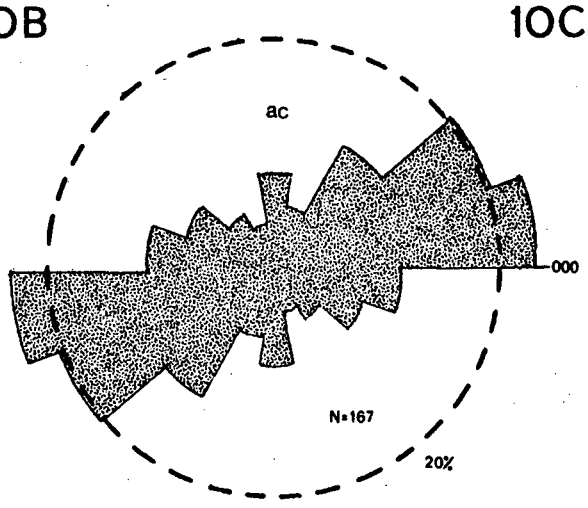

10C

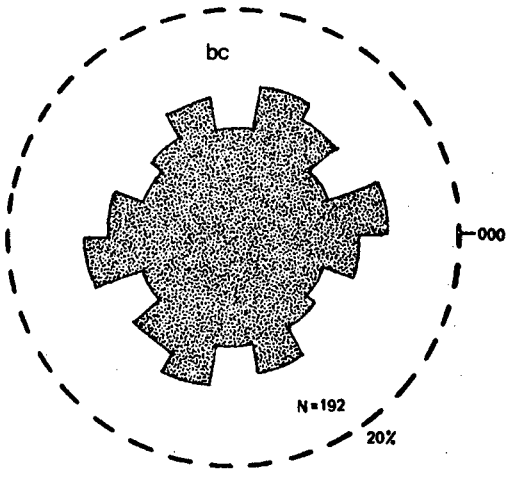

10D

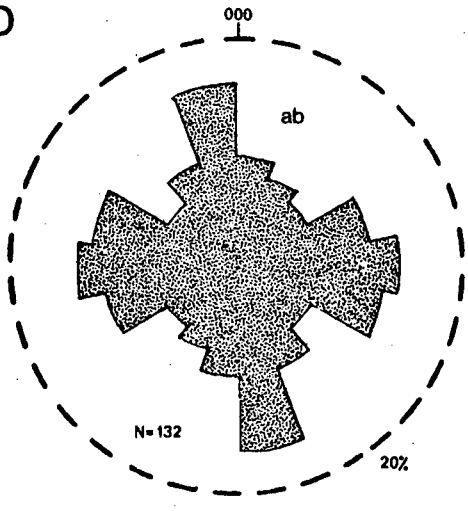

10E

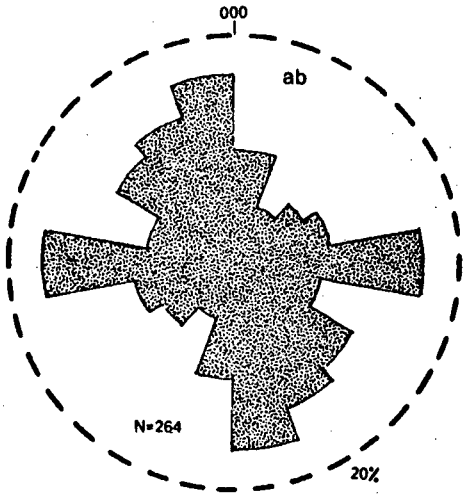

11A

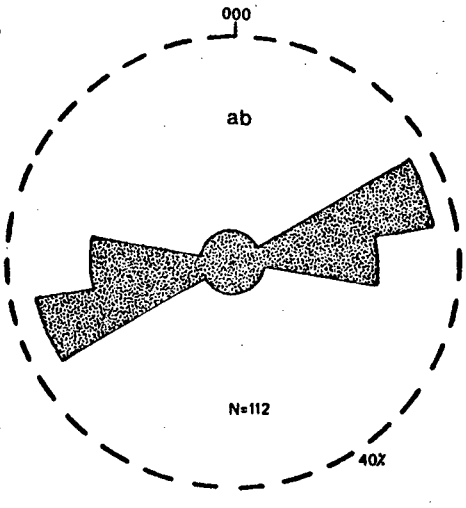

11B

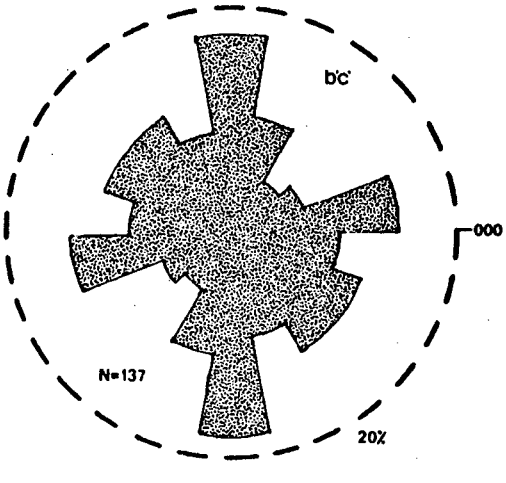

11C

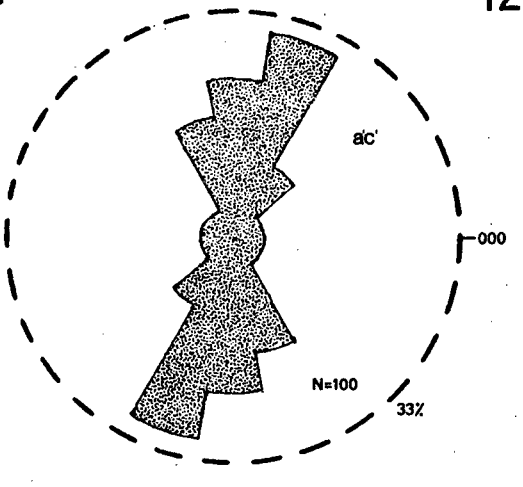

12A

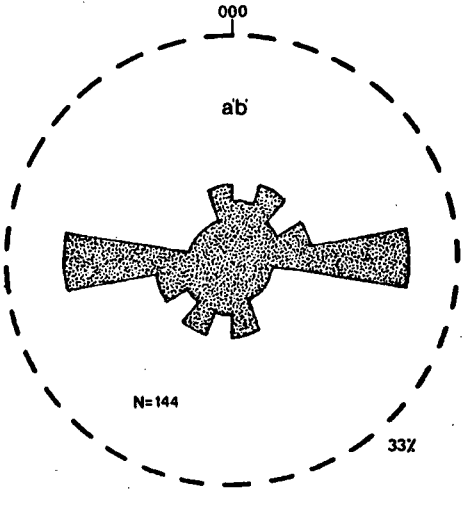

COMPASS DIAGRAMS

(Long axis orientation of quartz grains)

12B

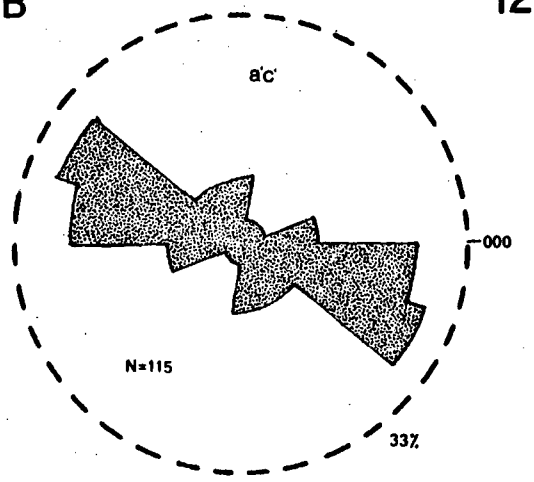

12C

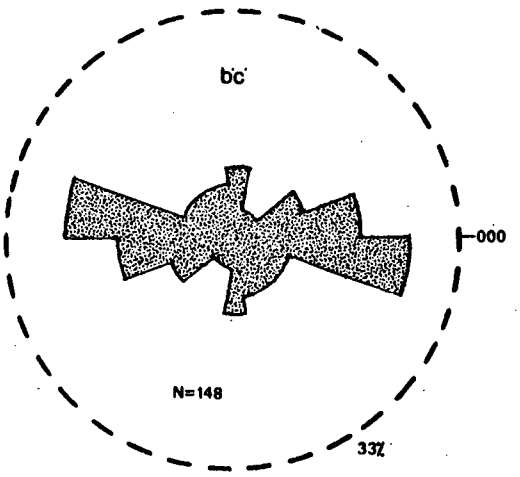

13A

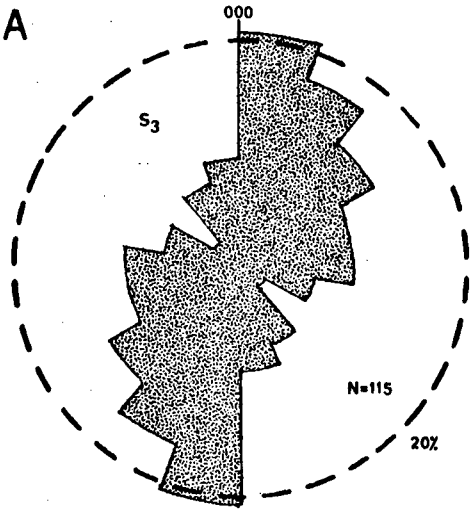

13B

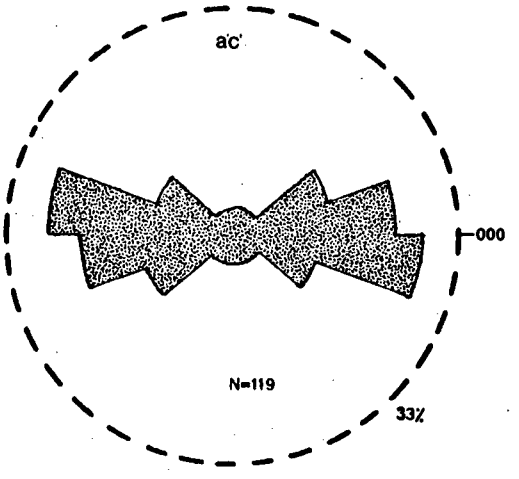

13C

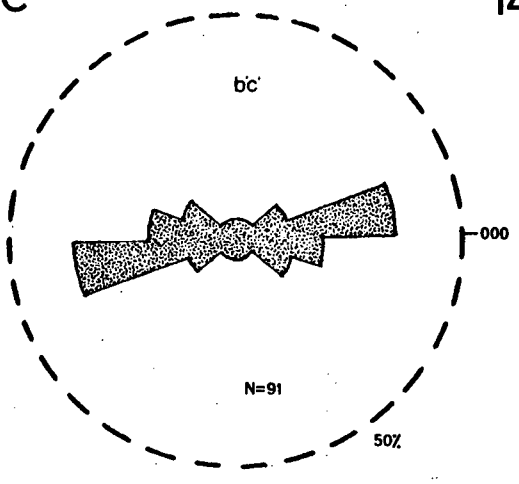

14A

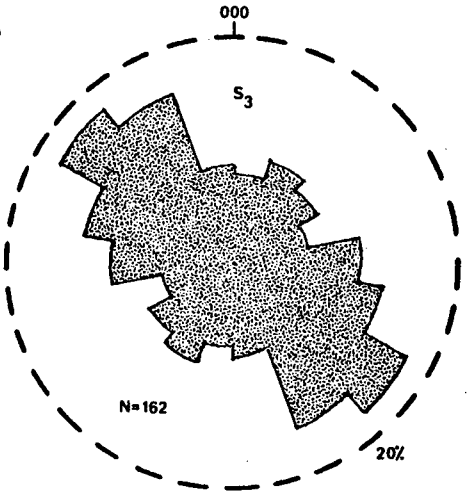

14B

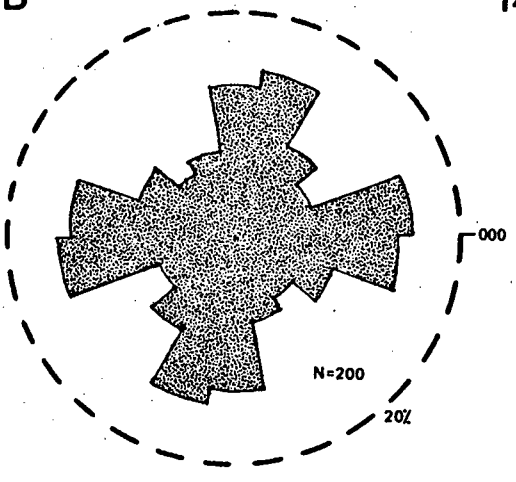

14C

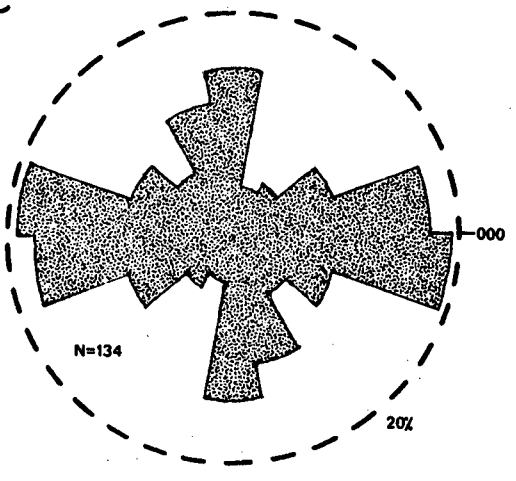

COMPASS DIAGRAMS

(Long axis orientation of quartz grains)

15A

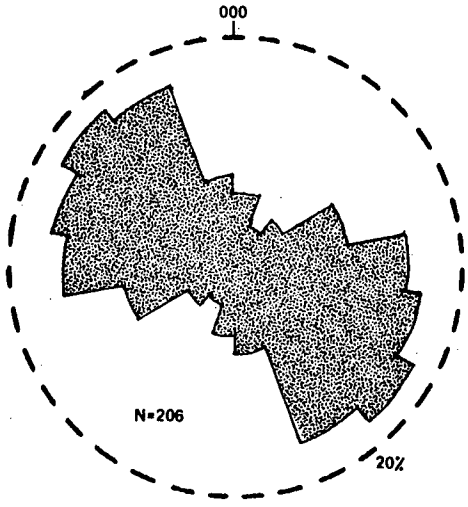

15B

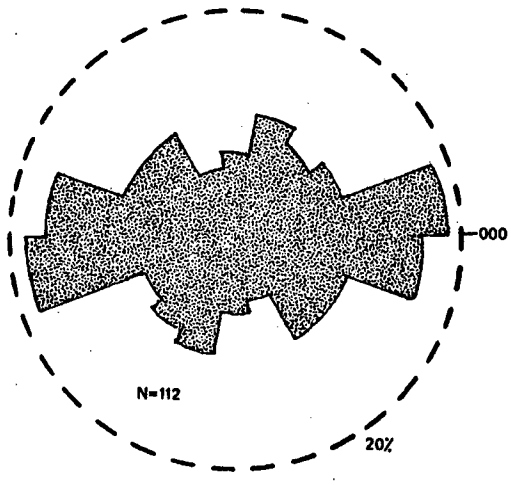

15C

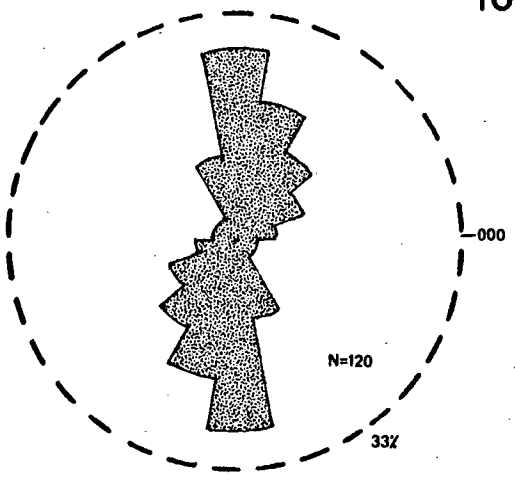

16A

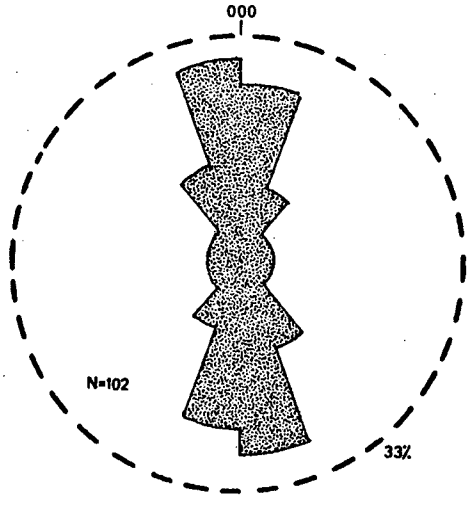

16B

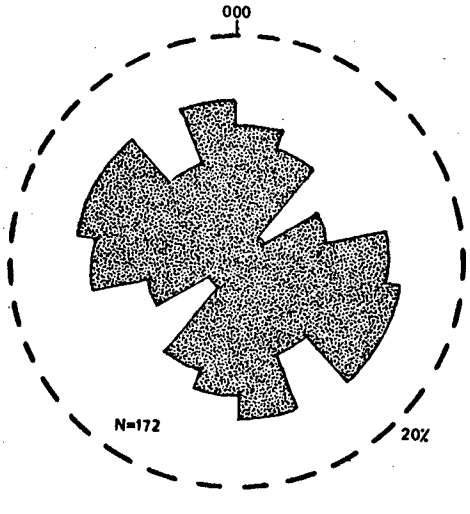

16C

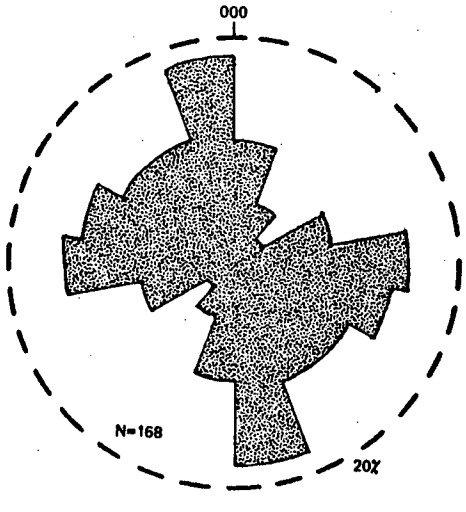

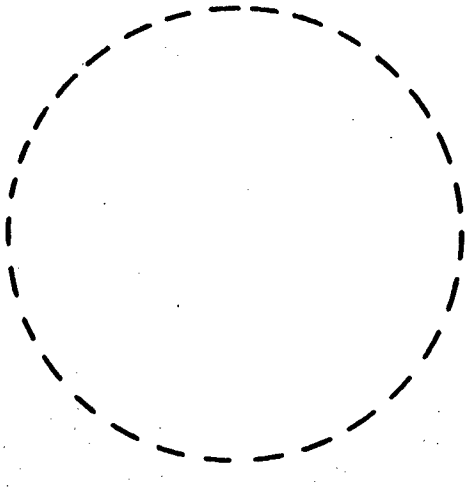

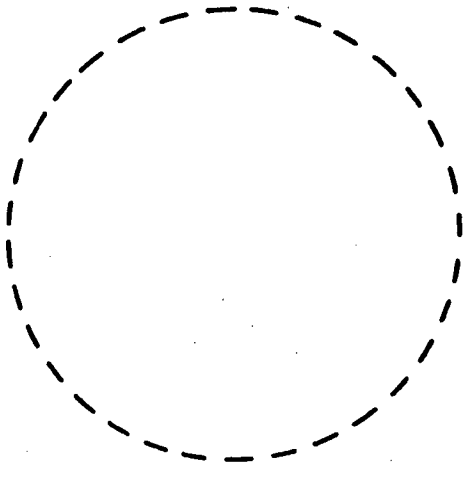

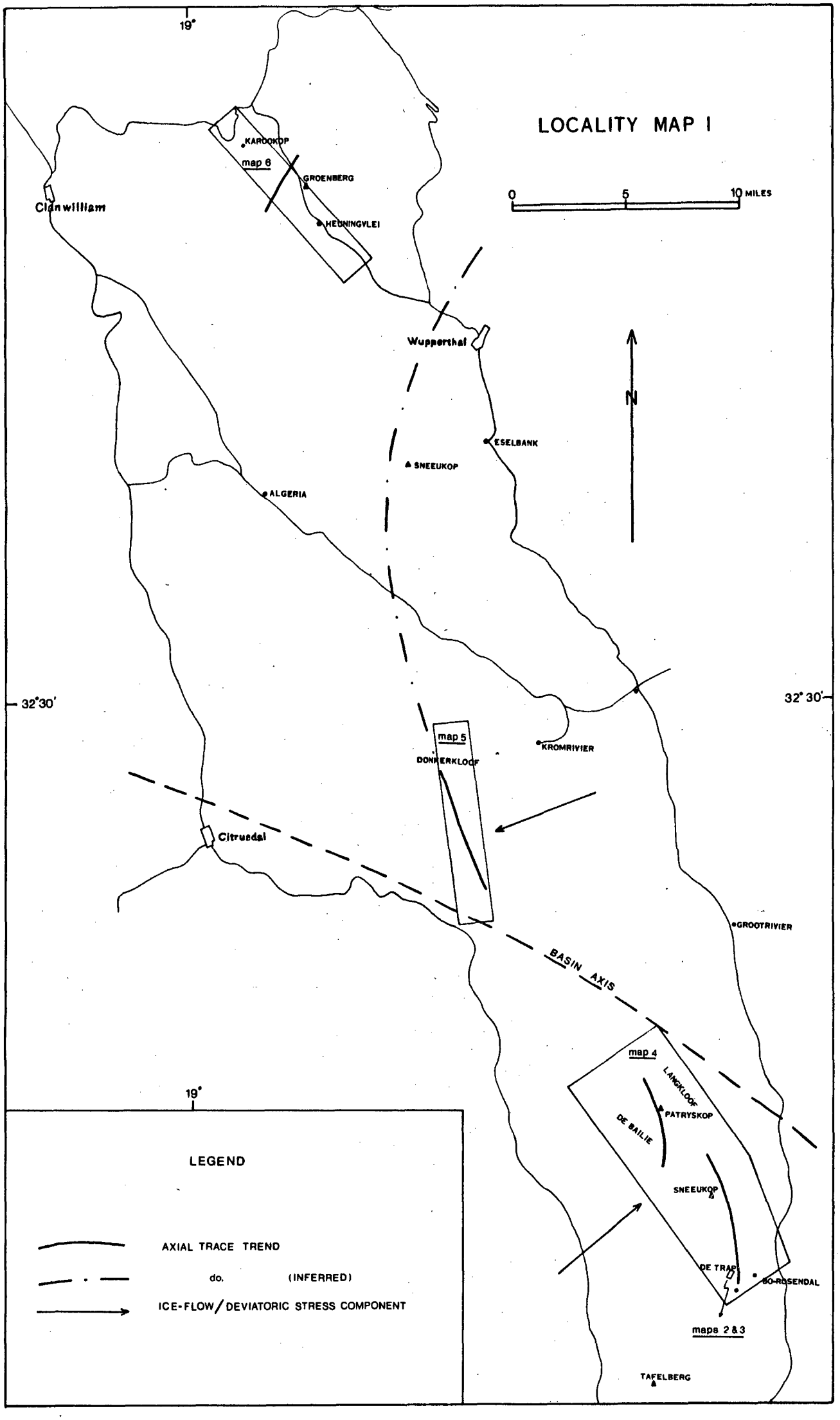

MAP 4

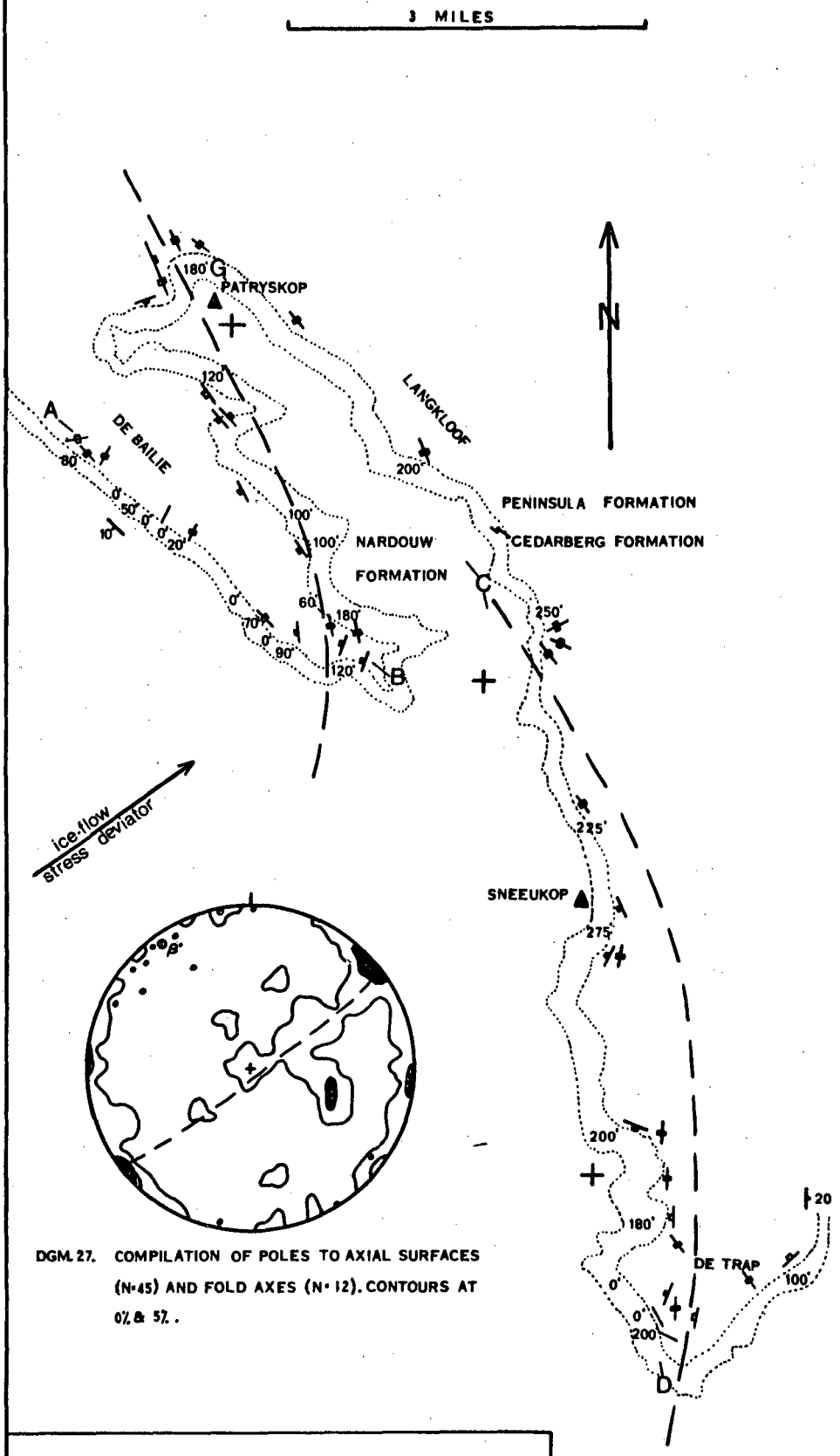

DGM. 27. COMPILATION OF POLES TO AXIAL SURFACES (N=45) AND FOLD AXES (N=12). CONTOURS AT 0% & 5%.

LEGEND

- REGIONAL ATTITUDE OF STRATIFICATION
- ATTITUDE OF FOLD AXIAL SURFACES
- TREND OF AXIAL TRACES
- 200' STRATIGRAPHIC THICKNESS OF FOLD ZONE
- ABGCD SECTION (SEE FIG. 2)

MAP 5

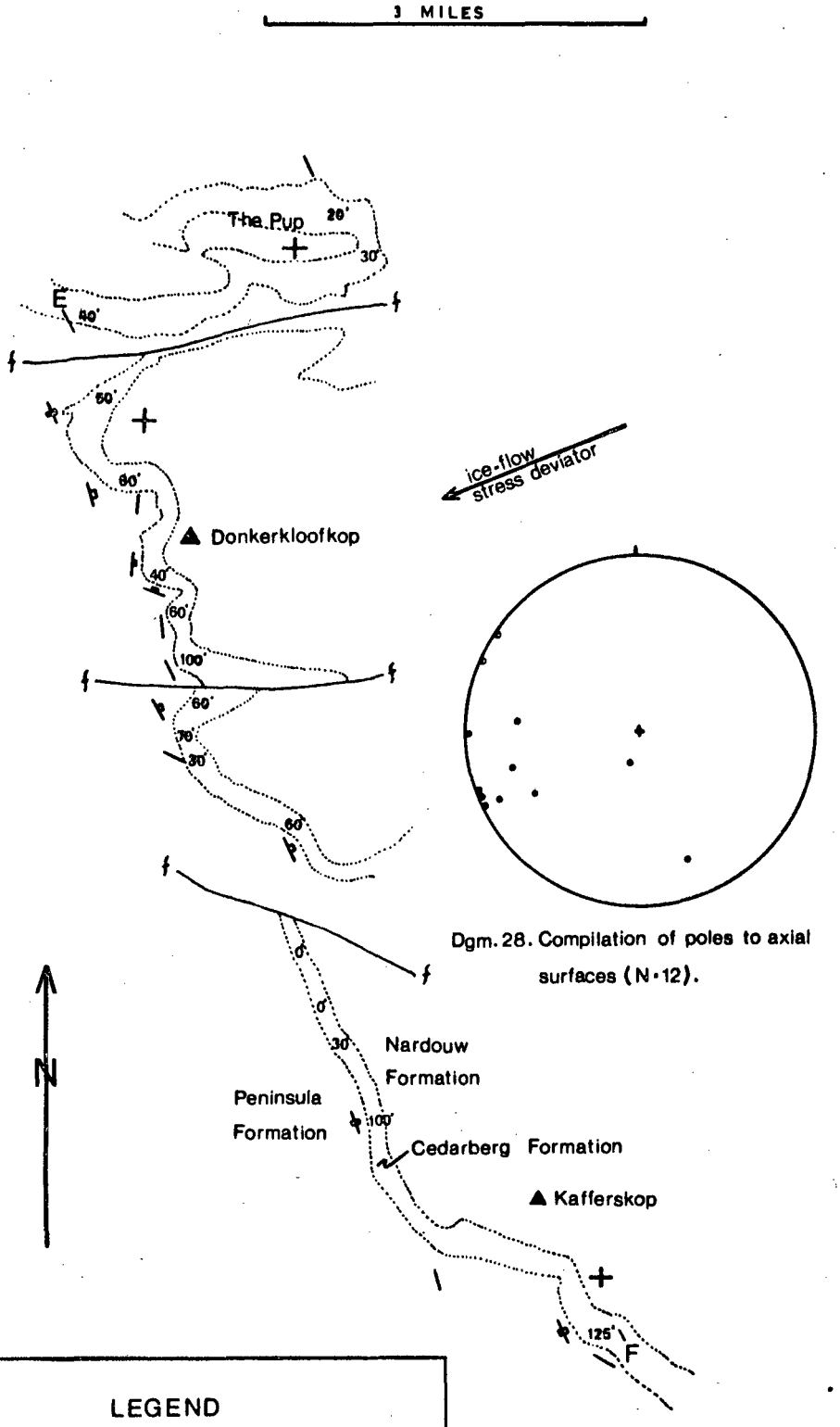

Dgm. 28. Compilation of poles to axial surfaces (N·12).

LEGEND

— attitude of fold axial traces and surfaces

125' stratigraphic thickness of Fold Zone

EF section (see fig. 2)

MAP 6

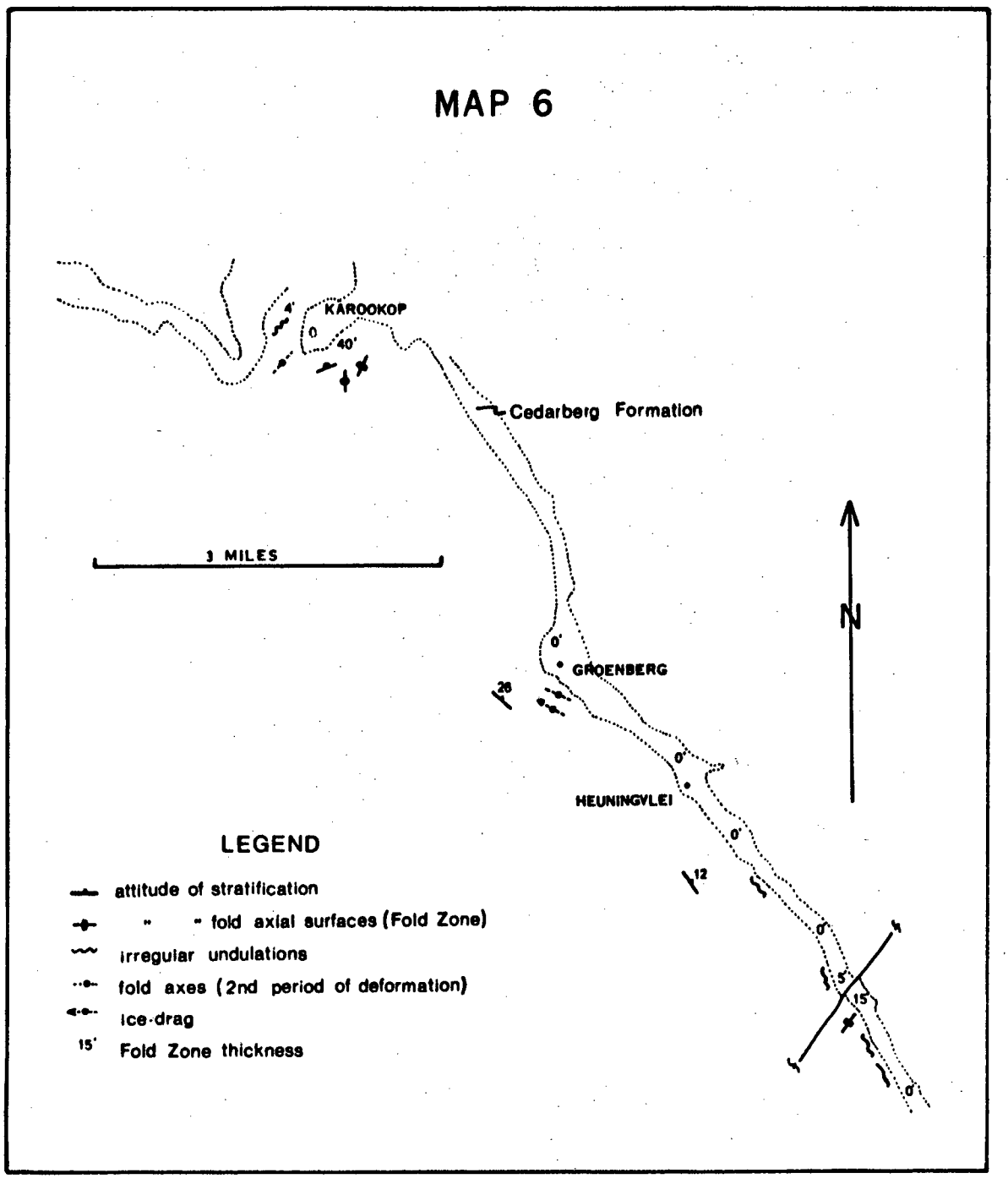

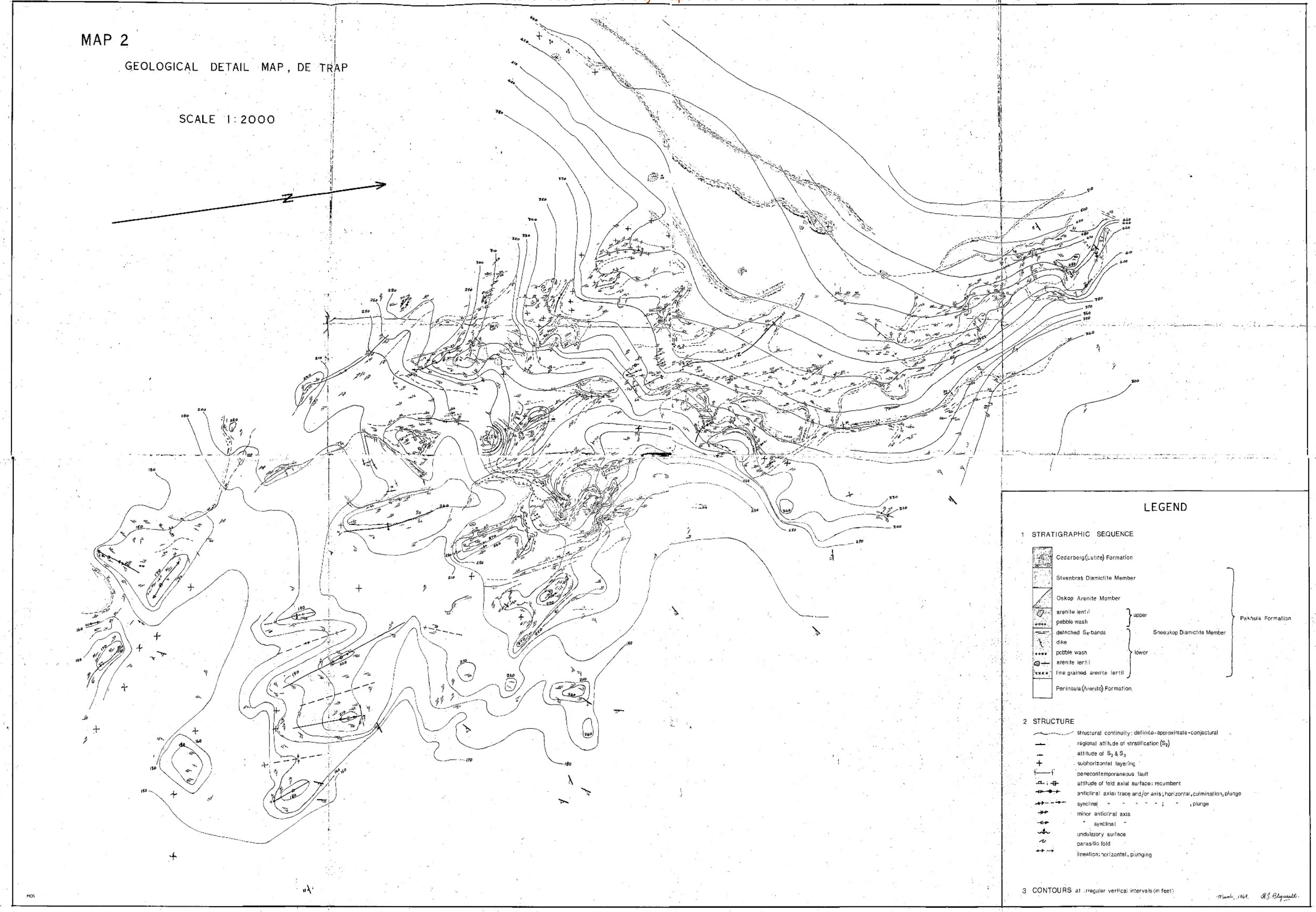

MAP 3

GEOLOGICAL INTERPRETATION MAP, DE TRAP

SCALE 1:2000

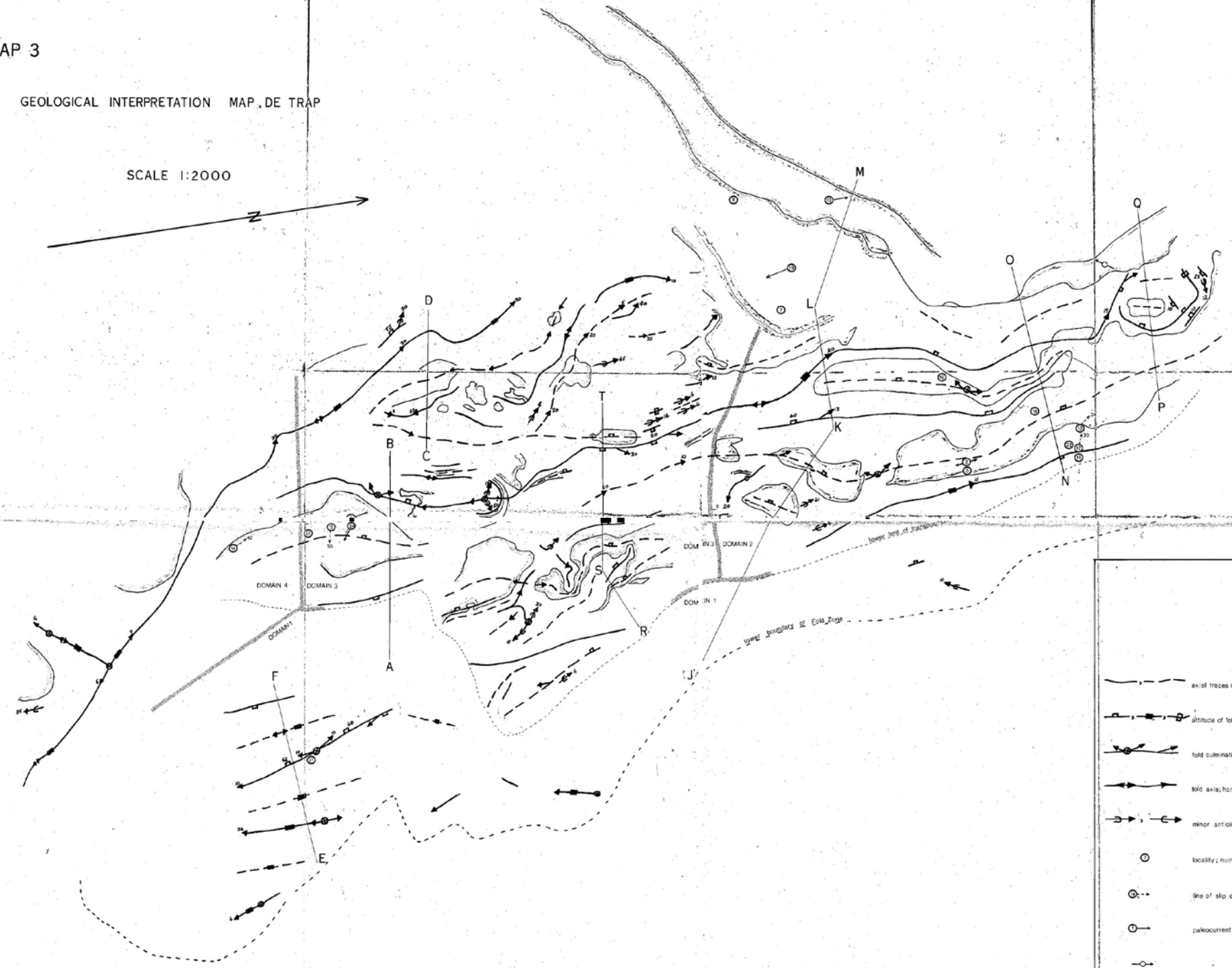

LEGEND

(for lithology see Map 2)

- axial traces or axes of anticlines and synclines
- attitude of fold axial surface; vertical, recumbent
- fold culmination with attitude of axes relative to axial trace
- fold axis; horizontal, plunging
- minor anticline and syncline
- locality; number corresponds with diagram no.
- line of slip or flow; a (kinematic)
- paleocurrent inferred from fabric analysis
- cross-stratification

Sections are shown in figs. 11-15

Nov., 1968 G.J. Klopper

HOS